Amy Steiner

The influence of freeze-thaw cycles on the shear strength of Illite clay

The influence of freeze-thaw cycles on the shear strength of Illite clay

By

Amy Steiner

in partial fulfilment of the requirements for the degree of

Master of Science
in Geo-Engineering

at the Delft University of Technology,
to be defended publicly on Friday June 24, 2016 at 16:30

Supervisor:	Dr. ir. W. Broere	TU Delft
Thesis committee:	Dr. P.J. Vardon	TU Delft
	Prof. Dr. C. Jommi	TU Delft
	Dr. A. Barnhoorn	TU Delft

This thesis is confidential and cannot be made public until December 31, 2016.

An electronic version of this thesis is available at http://repository.tudelft.nl/.

TU Delft

Preface

No decision to return to school after working as a consultant is simple, or, especially in my case, an easy one. Obtaining a master's degree, which would allow me to stand out from my peers, seemed like a very effective way to pursue my interests in geotechnical and arctic engineering while improving on my experience in consulting. Ultimately, this journey would not have been possible without help looking into research done at different universities and graduate programs in Europe. TU Delft has one of the best geotechnical engineering programs in the world, and cutting-edge research and facilities, as well as quality of the staff and students made attending a no-brainer.

Needless to say, my committee provided much-appreciated guidance. My chairman, Dr. Wout Broere, was never far away and offered insight into the experimental aspects of this research. His willingness to help as problems with the lab setup arose again and again was very much appreciated. Dr. Auke Barnhoorn gave suggestions and assistance in processing and interpreting the CT data, and his feedback helped improve the quality of this thesis substantially. Research into frozen soil is important to me, and Dr. Phil Vardon was willing to accommodate that. For that, and his day-to day-assistance, I am eternally grateful.

Everyone should have an advocate, and I am grateful to have many people who helped fill that role. You are too numerous to list in full, but I would like to thank some of the most important people, who often were unaware of how much their actions, big and small, meant to me. The shared experiences and uplifting words of my fellow graduate students added colour to long days in a cold lab and geo-corner. My understanding friends, climbing, and running partners helped keep me sane and made sure I took breaks. Paul Perreault, who has been an inspiration and mentor to me over the years, and is living proof that nothing is impossible, was willing to act as a sounding board, and his advice and insight has meant everything to me. His unwavering support and belief in me has helped me made this experience all the more valuable.

Even from another continent, advice from my long-time friend and yet another incredible mentor, John Ryer, kept me from forgetting about the light at the end of the tunnel. Long days, broken lab equipment, gallons of coffee, and the occasional fire kept me on my toes and ensured there will be stories to tell on future river trips.

Next, my parents and sisters helped keep me sane and were willing to commiserate with me about the never-ending work that goes along with school. The late-night phone calls and Skype dates were a huge factor in my continued sanity and success. I am lucky to have your support and love.

Last but not least, my incredible partner Everet made this adventure possible. From moving from Alaska to Europe, tolerating my long hours and chronic stress, and lending a supportive ear, I cannot express how thankful I am for your understanding and insight as I talked incessantly about frozen dirt. Even though you don't know much about soil, your support means more to me than you know.

One cannot forget the laboratory staff at TUD, who helped keep my tests going and deal with the many unexpected problems with the systems. Kees van Beek and Marten van der Meer were especially amazing. During the hectic 5 months of lab work, my lab mates were incredibly understanding of the time constraints of my tests and made sure the shared supplies were available and stocked.

Without all this support, this Master's degree would not have been possible. Because of all of you, this new chapter of my life has been absolutely fantastic.

A. Steiner
Delft, 24 June 2016

Table of Contents

List of Figures

List of Tables

Abstract

Thermo-active structures, such as energy piles, are used to store and extract heat energy from soil. In areas with seasonal freezing and thawing, such infrastructure is subjected to changes in the soil structure and, consequently, the soil strength. This research investigated the influence of repeated freeze-thaw (FT) cycles and different freezing rates on the shear strength of a frost susceptible Illite clay. Samples of saturated clay were subjected to between 1 and 20 FT cycles, and the shear strength was determined using undrained unconsolidated triaxial tests on the thawed samples. Soil subjected to freezing exhibited a reduction in shear strength compared to never-frozen soil. Slower freezing rates (warmer surface temperatures) resulted in lower shear strength. Results indicated an inverse relationship between the number of FT cycles and the shear strength with a constant applied freezing temperature. Strength recovery occurred between 1 and 3 freezing cycles. Between 3 and 7 FT cycles, the shear strength decreased, after which it approached an equilibrium shear strength between 7 and 10 FT cycles. The increase in shear strength between 1 and 3 FT cycles at a high freezing rate was not identified in the literature reviewed, but coincides with a decrease in stiffness and ice lens thickness. The reduction in shear strength with increasing FT cycles was attributed to movement of pore water through the sample and formation of ice lenses, which damaged the soil microstructure. The ice lenses formed via cryogenic suction pulling unfrozen pore water towards the freezing front and layer where a new ice lens was growing. Macro-CT scans showed decreasing size of ice lenses with increasing FT cycles, and denser ice lens formation near the freezing surface. The largest change in shear strength and ice lens formation occurred between a surface temperature of -5 and -10°C. Ice lenses increased in size moving away from the freezing surface, and a saturated ‘slurry’ layer formed when the samples thawed. Samples failed along the plane of the largest ice lens. Slower freezing rates resulted in thicker ice lenses and slurry layers, which resulted in lower shear strength and stiffness. At high freezing rates, the soil stiffness was almost double that of the never-frozen clay due to local consolidation of clay fragments. With decreasing freezing rates, local consolidation was offset by formation of large horizontal ice lenses. CT scans indicated that after being exposed to multiple FT cycles, the microstructure of the clay was destroyed. The evolution of shear strength should be taken into account in geotechnical design, as a period of thermal consolidation may be required prior to full loading and the rate and number of times a soil is frozen significantly impacts its shear strength.

List of Symbols

Roman Symbols

c_u	Mobilised shear strength [kPa]
E	Elastic modulus (stiffness) [kPa]
e	Void ratio [-]
k	Hydraulic conductivity [m/s]
LL	Liquid limit [%]
p	Pore pressure [kPa]
p_{ob}	Overburden pressure [kPa]
p_{sep}	Separation pressure [kPa]
PI	Plasticity index [%]
PL	Plastic limit [%]
R	Thermal resistance [$m^2 \times K/W$]
T_{bf}	Freezing temperature applied at bottom of sample [°C]
T_{bt}	Heating temperature applied at bottom of sample [°C]
T_{tf}	Freezing temperature at top of sample [°C]
T_{tt}	Thawing temperature at top of sample [°C]
t_f	Sample freeze time [hr]
t_t	Sample thawing time [hr]
w	Water content [%]

Greek Symbols

γ_d	Dry unit weight [kN/m^3]
γ	Unit weight [kN/m^3]
ρ	Density [g/cm^3]
ρ_d	Dry density [g/cm^3]
σ	Shear stress [kPa]
σ_3	Confining pressure [kPa]
τ	Shear strength [kPa]

Definitions

Active ice lens – The warmest ice lens in a freezing soil that is increasing in size (growing).

Active layer – The top soil layer that undergoes freezing and thawing cycles over time (e.g., annually). Also referred to as seasonally frozen ground.

Applied surface temperature – Temperature applied at one side of the sample to freeze or thaw the soil. The applied surface temperature influences the rate the sample freezes at.

Bulk ice – A mass of ice that exceeds the volume of the pores (e.g., ice lenses).

Closed-system freezing – Freezing in a system where water can neither enter or leave the system. Also known as in-situ freezing.

Cryogenic suction – Suction developed by the attraction of unfrozen water to ice. This is the primary mechanism for water transport via capillary flow towards ice lenses.

Freezing front – the boundary between frozen and unfrozen ground advancing through the soil.

Freezing pressure – the heaving pressure that occurs from the volumetric expansion of water as it freezes.

Freezing rate – The speed that the temperature penetrates the soil column

Frozen fringe –The zone between the warmest (active) ice lens and 0° isotherm where ice is present in the pores.

Frost susceptible soil – Soil where ice segregation occurs during freezing. Frost susceptible soils are categorized by the U.S. Army Corps of Engineers Frost Susceptibility Criteria F1 through F4. Silts and clays are considered highly frost susceptible soils.

Hydrodynamic forces – Forces caused by the formation of ice that act on ice and soil particles.

Ice lens – A primarily horizontal lens-shaped body of ice of any size. Ice lenses range in size from extremely small (hairline) to several meters thick.

Mechanical properties – Properties that govern strength and deformation (e.g., creep, consolidation, hydrodynamic consolidation).

Overburden pressure – The pressure exerted on a soil by a surface load.

Periodic lensing –Horizontal layers of ice in the frozen portion of a soil.

Pressure melting – Melting of ice caused by application of pressure.

Separation strength – The stress required to separate soil particles from each other or a bonding agent.

Thaw consolidation – Time-dependent compression caused by the drainage of pore water from thawing soil.

Thaw weakening – The reduction in shear strength due to the dissipation of excess pore pressure during thawing of ice in a frost susceptible soil.

Thermal gradient – The change in soil temperature with depth.

Thermo-active structure – A structural element (e.g., pile) designed to store and extract heat from the ground.

Thermosiphon – A passive or active heat transfer device installed in a frozen soil to extract heat from the ground.

1. Introduction

Engineering in cold regions presents many difficulties, especially in seasonally frozen ground when frost susceptible soils, namely silts and clays, are present. The presence of such soils results in challenges for foundation designs, as the structures tend to experience differential settlement and creep. Frost susceptible soils are defined as a soil where 'significant ice segregation [lensing] will occur when the requisite moisture and freezing conditions are present' [1]. They are often associated with permafrost areas and 'active' soil layers that experience seasonal freezing and thawing. Permanent changes in soil structure as a result of freezing are not well understood, despite the implications for long-term soil strength development. Formation of ice within soil accounts for vertical displacement, known as frost heaving, that can damage infrastructure, and the soils subjected to freezing and thawing cycles experience a reduction in shear strength. Adding to the challenges of designing in frozen ground, residents in these areas tend to have higher energy costs associated with heating their homes during colder winters. The use of energy-storage devices, such as thermo-active structures that add or extract energy from the ground, could reduce heating costs and provide some degree of soil improvement by accelerating consolidation, depending on the soil properties and ground temperature. Thermo-active structures can double as structural elements, such as thermal piles, where a heat extraction measure is installed in conjunction with the pile. However, research into geo-energy infrastructure in seasonally frozen soils is limited, and the evolution of shear strength over time should be taken into account, as a period of thermal consolidation may be required prior to full loading, to allow the soil to stabilise.

1.1. Background

Seasonally frozen soils present challenges for geotechnical design and construction, as they are subject to frost heave, settlement, and changes in shear strength. In northern latitudes, the top of the active layer can reach temperatures of -30°C in winter and warm to only 10°C during summer months. This is due in part to the temperature gradient induced by underlying permafrost, which results in soil temperature being slightly cooler than ambient air temperature in summer, and slightly warmer in winter [2]. Different freezing surface temperatures are expected to cause a change in the shear strength, with stronger soils associated with colder surface temperatures. Furthermore, the influence of freezing rates on the long-term strength development of soil may become an important geotechnical design consideration in areas with seasonally frozen soils.

Geo-energy infrastructure, such as ground source heat systems, induce thermal cycles in the ground, which may cross the freeze/thaw boundary. These thermo-active structures result in changes to the soil structure that affect the bearing capacity [3]. As the active layer thickness increases, the feasibility of energy storage and extraction from the soil should be evaluated, as thermal piles may be able to reduce the temperature variation in the active layer and reduce surface displacement.

Soil freezing is influenced by the temperature at the ground surface, soil type, availability of water, and overburden pressure. These factors control the speed the freezing front, defined as the advancing boundary between frozen and unfrozen soil [4-6], penetrates the soil. It should be noted that as long as the temperature of the soil is below 0°C , it can be considered frozen, even if the soil is dry (e.g., there is no ice present). The freezing rate describes the time required for the soil column to freeze. Actual freezing occurs

instantaneously at the 0°C isotherm, and heat energy is released at this interface. This results in different temperatures at different depths of the soil, which is known as a thermal gradient.

The freezing rate will influence the development of shear strength by changing the soil structure. This strength development can be evaluated using mobilised shear strength. Mobilised strength is defined as the shear stress in a medium subjected to compression before failure [7]. It is developed by normalising the shear strength to a reference strain, often 0% (e.g., no applied load). The mobilised strength can be used to investigate the development of the shear strength of a soil before failure as a load is applied. The strain at which the material fails is known as the mobilisation strain.

In practice, undrained shear strength is often chosen as the key soil parameter when designing with clays [8]. Mobilisation of shear strength with axial strain can be used to evaluate factors of safety for service and limit-state designs by tracking the changes in shear strength. The behaviour of seasonally frozen ground has significant implications for engineering design and construction. Current design practices in frost susceptible soils focus on surface deformation caused by frost heaving. Changing soil structure due to repeated freezing cycles may be a factor deserving greater consideration, as long-term changes in soil strength occur. Understanding the development of soil properties would allow engineers to adjust their designs to account for the strength development of clay in seasonally frozen areas, as well as determine the length of time needed for thermal consolidation and soil stabilisation prior to full loading.

1.2. Research question

Based on gaps found in existing research into the influences of freezing cycles and surface temperature on soil strength, the following research question was developed:

What is the influence of cyclic freezing and different ground temperatures on the shear strength of an Illite clay?

This question was investigated by breaking it into the following sub-questions:

1. *What is the influence of repeated freeze-thaw (FT) cycles on shear strength?*

   This research attempted to identify a relationship between the number of FT cycles and shear strength in order to estimate the change in soil shear strength over time.

2. *What is the influence of the surface temperature (which controls the freezing rate) on shear strength after 1 FT cycle?*

   Different surface temperatures cause the soil to freeze or thaw at different rates. This research attempted to identify the influence of different surface temperatures and how they affect the shear strength.

3. *What is the influence of freezing rate and number of FT cycles on soil structure and ice lens formation?*

Different freezing surface temperatures will result in different ice lens formations, which in turn will change the soil structure and, by extension, the shear strength. The relationship between structural changes, number of FT cycles, and freezing rate was evaluated by measuring the shear strength and changes in soil structure due to freezing.

1.3. Limitations

Previous research has indicated that soil experiences a reduction in deformation and volume changes with increasing FT cycles. Deformation and volumetric changes have not been considered in this research. A freezing apparatus developed by van den Bosch [9] was used for this research. Modification of this apparatus to handle drained conditions would provide information pertaining to long-term, in-situ (consolidated, drained) conditions, but was not feasible in the available time and without considerable effort. Due to the amount of time required for each freeze-thaw cycle and other time constraints, strength recovery with time was not evaluated. Because undrained conditions were used, changes of the cohesion and angle of internal friction could not be evaluated. Additionally, movement of pore water through the sample between freezing and thawing cycles may be different than in-situ conditions, as temperature is being applied from the bottom of the sample, rather than the top as would occur in-situ.

1.4. Report outline

The second chapter of this report discusses the existing literature on freezing and thawing in soils, including physical properties, strength, and soil structure. Then, two conceptual models are considered, the first for un-disturbed conditions and the second for thermo-active structures and a hypothesis on the results of this research was formed. A physical model to answer the research question was developed and is described Chapter 4, along with the laboratory setup and sample preparation. The laboratory tests are discussed in Chapter 5. An in-depth analysis of the results from these tests is found in Chapter 6, and Chapter 7 presents a discussion of the findings. Finally, Chapter 8 presents the conclusions and makes recommendations for future study. Additionally, possible applications in engineering design are described.

2. Literature Review

Research on frozen and seasonally frozen soils primarily focuses on frost heaving and permafrost. Most geotechnical textbooks discuss engineering considerations for these conditions, emphasizing the calculation of active layer thickness and frost heave deformation. Physical properties, shear strength, and soil structure as they pertain to freezing and thawing cycles have been investigated independently, but very little research was found that relates all three aspects. This chapter discusses the findings of existing literature as it pertains to freezing soils and strength development, starting with soil properties and strength, and followed by soil structure and ice lens formation.

2.1. Influence of freezing on soil properties

This section will discuss the changes and interrelationships between physical properties (void ratio, density, and hydraulic conductivity) and mechanical properties (strength) of a soil after freezing.

The physical properties of soils (i.e., water content, hydraulic conductivity, permeability, and volume) stabilize between 3 and 9 FT cycles [3, 10]. The presence of some minerals, such as chlorides, will impact the freezing point of pore water and thus the ice lens formation within the soil [9], but because the influence is generally very small, it is often ignored. Research by Czurda [11] and Liu and Peng [12] noted that compressive strength reduces with increasing salt content due to the decreasing freezing temperature of water and films of unfrozen water forming around the soil grains. However, these films are considered to have a negligible impact on soil strength development under freeze-thaw cycles.

The freeze-thaw history of over-consolidated clay can result in an increased void ratio *e*, while normally consolidated clay experiences a decreased *e*. The void ratio can be linked to increased pore water and a lower tensile strength in a saturated soil [13]. Sensitive clays tend to exhibit remoulding effects from displacement and stresses during freeze-thaw cycles [11]. Soils that have never been exposed to freezing exhibit a higher stiffness E at the beginning of shearing. Clays subjected to freezing exhibit lower stiffness, which is attributed in part to a decrease in cohesion with increasing FT cycles [13].

Lai, et al [14] and Qi, et al [15] assert that the relationship between the thermal gradient (cooling rate), suction, and overburden pressure is not well understood. There seems to be general agreement that higher overburden pressures result in smaller ice lenses, faster consolidation, and fewer changes in the soil structure.

The majority of the research reviewed for this paper is within the context of frost heave (deformation) after a low number of FT cycles with a single applied surface freezing temperature. An increased hydraulic conductivity is expected with increasing FT cycles, which causes consolidation in the soil below the frozen fringe. The corresponding changes in void ratio will have the greatest influence on the shear strength.

2.2. Soil strength

Shear strength under undrained conditions is often used as the primary soil parameter in geotechnical design, since it will result in a weaker soil than under drained conditions. The stress conditions imposed on the soil, including confining and overburden pressures, will greatly impact the strength behaviour of the soil [3, 6, 10, 13, 16]. Unconfined soils subject to frost heave and thaw settlement have a characteristic change in strength, with the stress effects and displacement causing a change in soil structure and reduction in strength [12, 16]. As a soil is subjected to freeze-thaw cycles, it experiences settlement due to decreased pore space. The greatest change in shear strength is expected to occur within the first 3 to 10 cycles and approach an equilibrium state as the pore space reduces [11, 12, 15, 17-19]. After a large number of FT cycles, the shear strength of clays has been observed to increase slightly [10]. The change in void ratio from the formation of ice lenses has been linked to a change in the soil structure as soil particles are displaced, which in turn disrupts the particle interlocking and decreases cohesion [10, 13]. This results in a reduction in the strength of the clay [10, 18, 20]. Ice bonding during freezing can reduce the bearing capacity of the thawed soil by increasing the void ratio [12, 16, 18].

Triaxial tests on samples undergoing a series of freeze-thaw cycles showed a decrease in strength with an increasing number of cycles. In these tests, the lowest failure strength occurred between 3 and 7 cycles for all freeze-thaw series [10]. However, after approximately 10 cycles at constant confining pressure, the soil exhibited some strength recovery, especially under high confining pressures (>800 kPa), and approached the strength of a never-frozen soil after a large number of cycles [10]. Wang [18] also noted that thawed clay exhibits a transition from strain-softening to strain-hardening as the confining pressure is increased. Under a surface load, the volume change of the soil by frost heave forces is reduced, resulting in compressive subsidence at the beginning of freezing and decreasing frost heave deformation with increasing cycles [11, 21]. In other words, a surface load causes the soil to behave in a semi-confined way during freeze-thaw cycles, and increasing overburden pressures will increase soil strength by inducing consolidation and higher confining pressures [3, 17, 22].

In the long-term, the soil consolidates with increasing FT cycles, with a net increase of shear strength [11]. Multiple studies have identified consolidation and an increased hydraulic permeability k after repeated freezing cycles [15, 21]. Chamberlain and Gow [21] suggested that the increased k is due to microcracking caused by water expansion during freezing, resulting in a net increased flow resistance. This has been linked to an increased shear strength and stiffness in clays subjected to 1 freezing cycle [16, 17]. The increased k is attributed to the formation of vertical cracks through the soil, while the rest of the material consolidates.

Laboratory FT testing is usually carried out on cylindrical soil samples in a temperature controlled setting. Liquid coolant can be used to control the freezing and thawing temperatures, and freezing samples can be installed in a material testing cell to allow multi-axial mechanical tests [15, 23]. Heating plates like Peltier elements are also used [9]. Freezing apparatuses apply either one-dimensional freezing from a cap on one side of the sample, freezing from two caps, or all-around freezing of the entire sample [10, 12, 18, 21].

Long-term consolidation due to cryogenic suction and overburden pressure can result in strength recovery, but is likely only applicable under high confining pressures and drained conditions. Because most literature focuses on relatively few (3 to 5) FT cycles, conclusions regarding long-term behaviour due to changes in the soil structure are limited.

2.3. Changes in soil structure and ice lens formation

2.3.1. Ice lens formation

Qi [19] observed expansion of drained, overconsolidated soils at the beginning of thawing, attributed to the release of the suction-induced restraining forces between the particles. At the start of thawing, this force suddenly deceased, releasing stress and causing sudden expansion of the soil. Normally consolidated soils tended to settle during the first freezing cycle due to suction beneath the freezing front, which is prevented by formation of ice lenses. These observations were supported by lab tests by Volokhov [24].

As the freezing front progresses, the temperature, pore pressure, and cryogenic suction in the soil change. Figure 1 shows the development of these properties with depth. The soil profile consists of 3 zones: (a) the frozen zone, (b) frozen fringe, and (c) unfrozen zone. Ice lenses form above the freezing front (0° isotherm) [3, 25, 26]. Pore water is pulled towards the ice lens boundary via cryogenic suction until the available pore space is full, at which point a new lens is initiated at a warmer temperature closer to the edge of the frozen fringe [5, 6, 25]. These horizontal layers of ice are known as periodic ice lenses. Faster freezing fronts (e.g., higher freezing rates caused by lower applied surface temperatures) cause a decreased permeability in the frozen fringe, which leads to less flow of water to the ice lenses. This results in smaller ice lenses near the freezing side that increase in size with depth [3]. The size of ice lenses are limited by the available water in the soil [3, 6, 25].

The temperature profile in Figure 1(B) assumes one-dimensional freezing, uniform properties of the frozen and unfrozen soil, and neglects the ice lenses in the frozen zone. The thermal gradient with depth is assumed to be constant through each zone and increases when the soil is frozen due to the freezing pressure from the water-ice phase change. Because the phase change between water and ice occurs in the frozen fringe, it has a smaller thermal gradient than the frozen zone. Heat energy is released during the phase change that occurs in zone (b).

The water-ice phase change at the ‘frozen fringe’, defined as the zone between the warmest (‘active’) ice lens and 0° isotherm, has several significant impacts. The increase in pore pressure within the frozen fringe (Figure 1(C)) is largely due to the volumetric expansion of the water-ice phase change [6, 27]. Cryogenic suction draws unfrozen water towards the freezing front, growing the ice lenses and further increasing the pore pressure [26]. This induces some consolidation and pushes the water away from the freezing front, resulting in vertical cracks.

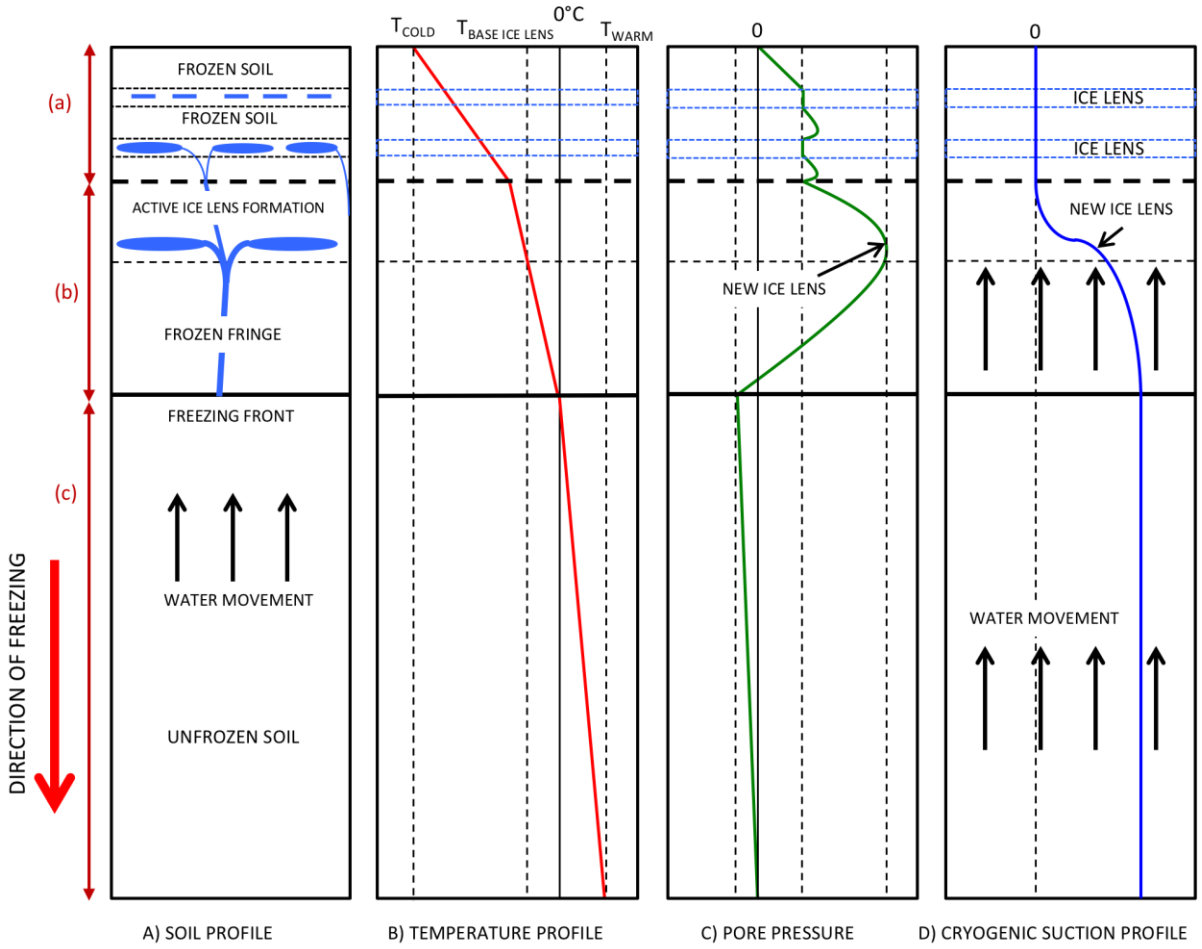

Figure 1: A) Schematisation of soil; B) Temperature profile; C) Pore pressure profile; D) Cryogenic suction profile (for one-dimensional freezing) (based on Andersland and Ladanyi [3] and Arenson [5])

The increase in pore pressure in the frozen fringe where active ice lenses form (zone (b)) can be attributed to the 9% volumetric expansion due to phase change. Cryogenic suction accounts for the movement of water towards ice during freezing and is the primary mechanism for water transport towards an ice lens. It can be described by Darcy's Law assuming an effective permeability that is a known function of the ice saturation level [25]. Cryogenic suction occurs primarily in the frozen fringe (zone (b), profile D), where both ice and water are present. The suction within the frozen fringe causes the pore pressure to decrease below the active ice lenses as water is pulled out of the pores below. During freezing, the lower (unfrozen) part of the soil consolidates as water moves towards the ice lenses. Lenses will continue to form until the lower part of the soil has been reduced to its shrinkage limit [3]. The soil will continue to freeze even after the soil has reached its shrinkage limit, and as long as the temperature of the soil is below 0°C, it can be considered frozen [28].

The thermo-hydro-mechanical interactions during soil freezing are shown in Figure 2. These interactions influence the size and orientation of ice lenses, largely due to the movement of pore water within the sample. An additional hydro-mechanical relationship, not shown on this figure, involves cryogenic suction, which increases the overall hydraulic conductivity and simultaneously consolidates the underlying soils. The

freezing front penetration is independent of the overburden pressure and separation strength and thus is not sensitive to ice lenses.

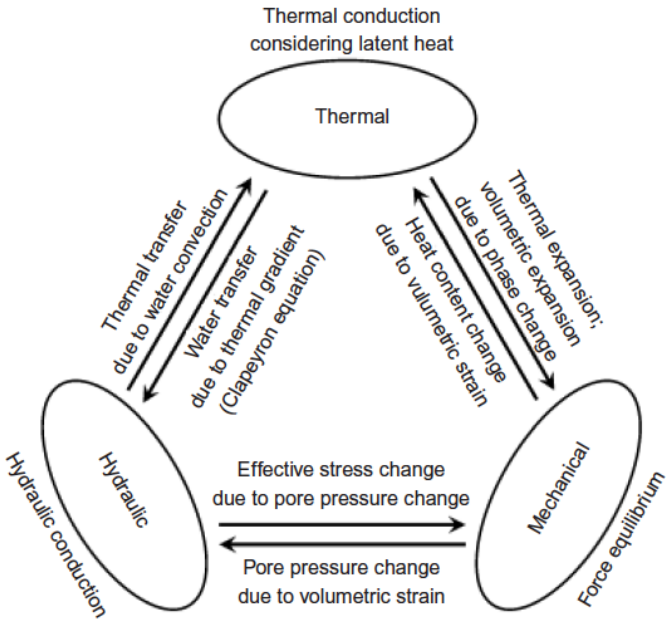

Figure 2: Thermo-hydro-mechanical interaction mechanism in freezing soils from Thomas [26]

2.3.2. Formation of cracks

Chamberlain and Gow [21] suggested that the vertical cracks seen in frozen soils are the result of shrinkage caused by negative pore water pressure during freezing. Arenson [5] identified them as tension cracks formed as the soil reaches its tensile strength, while Chen [4], Harris [27] and Harris [27] postulated that vertical cracking is a result of dilation from surface deformation (frost heave) and temperature. Lai [14] proposed that because thermal gradient varies within the soil column, uneven shrinkage deformation causes vertical cracks. They labelled this cracking mechanism 'temperature (thermal) cracking'.

Horizontal cracking occurs when the tensile strength is exceeded by the stress of the soil. Water migrates towards the horizontal ice lenses along vertical cracks [5], which form before the horizontal lenses. The thickness of the vertical cracks has been shown to remain constant with time and number of FT cycles. Arenson [5] reported that 'Because water flow along vertical ice lenses controls the amount of water that migrates through the frozen fringe, it is basically the tensile strength of the soil at a certain stress state that governs ice lens growth'. The ice lenses intersect the vertical cracks and deflect in the direction of freezing, causing increased vertical cracking, decreased flow resistance, and increased permeability in the thawed soil [21]. It follows that vertical cracks will be thinner for lower surface temperatures and faster freezing rates, since water will not have time to move through the sample.

Arenson [5] also noted that increasing overburden pressure resulted in larger spacing between the vertical cracks, while the size of the horizontal ice lenses decreased. Alley [2] determined that overburden pressure lowers the melting temperature of ice by increasing the unfrozen water content, thus reducing the volume of bulk ice and size of the ice lenses.

2.3.3. Stresses due to ice lens formation

There is not a consensus on the cause of these vertical cracks. Since it is accepted that in order for ice lenses to form, the overburden pressure and separation strength of the soil must be overcome, and that ice lensing is a non-homogenous process resulting in an increased volume and known to create vertical cracks, it is reasonable to conclude that these vertical cracks are caused by a combination of tension and thermal cracking. Several stresses are exerted on the soil during freezing and directly influence the formation of ice lenses and soil strength. Figure 1(C) shows the increase in pore pressure in the frozen soil between the ice lenses. The pore pressure through the ice lenses is constant, since there is no change in the water content, consolidation, or overburden pressure once the pore water has frozen. The suction is overcome by the increasing pore pressure from ice formation pushing the water away, causing consolidation that in turn increases the effective stresses directly below the freezing front.

The water movement due to cryogenic suction and the hydrodynamic force acting on the ice and soil particles below the frozen layer elongate the ice lenses in the direction of heat flow during freezing [3, 5, 25, 27]. As the freezing front penetrates the soil, positive pressure develops at the water-ice interfaces. This is known as 'freezing pressure' [27] and accounts for vertical displacement, or heaving, of a frozen soil.

As can be seen in Figure 2, water movement through a soil is coupled to the thermal gradient. A higher water content creates in a larger thermal gradient, which in turn causes the pore pressure and effective stress of the soil to increase due to volumetric expansion due to the phase change. Thomas [26] noted that ice lenses form when the pore pressure is equal to the overburden pressure p_{ob} plus the separation strength p_{sep} of the soil ($p > p_{ob} + p_{sep}$). It follows that lower overburden pressures and separation strength result in more ice lenses.

2.3.4. Influence of freezing rate on ice lens formation

The rate of freezing, defined as the speed that the sample freezes along its height, will affect the formation of ice lenses, which in turn influence the soil structure [3, 28]. With slower freezing, larger ice lenses form, and pore water may end up on the surface before freezing completely [12, 25]. High thermal gradients and faster freezing rates result in a smaller change in grain structure, as the pore water will freeze in the available pore space before suction can have a significant influence. However, some grain realignment is expected, regardless of applied freezing temperature, to accommodate the expansion of pore water as it freezes [11, 12, 25]. The extent of the structural changes are dependent on the water content, freezing rate, thermal gradient, and applied surface temperature that result in ice lensing [20].

Frozen soils often contain some unfrozen water at temperatures below 0°C. However, Putkonen [29] noted that the most of the pore water is frozen around -1°C, and by -3°C the amount of unfrozen water can be considered negligible. Ground surface temperature is heavily influenced by the amount of snow cover and exposure to direct sunlight, which can warm the air directly above the ground where measurements are typically taken [1, 2, 29]. Areas with high snow cover are more likely to have ground surface temperatures between 0°C and -5°C, while areas with very little or no snow but cold winters can have ground surface temperatures between -10°C and -20°C [2, 4, 30]. Warmer surface temperatures result in slower penetration of the freezing front in to the soil, and thus require more time to freeze to the same depth.

In undrained conditions, soil will freeze but no ice lensing will occur after some depth because the available water has been sucked towards the freezing front and the underlying soil has reached its shrinkage limit. Cryogenic suction along vertical cracks in frozen clay is widely agreed to account for the growth of horizontal ice lenses within the frozen fringe.

2.4. Thaw weakening

Changes in the grain structure occur as the pore water freezes, causing particle realignment along the plane of ice lensing. This realignment will be maintained after thawing, and 'thaw weakening' caused by the melting of ice and frozen soil can create a saturated region that results in a loss of bearing capacity [3, 21, 31]. This layer persists until the water can be reabsorbed into the aggregates [1]. With time and drainage, soil has been seen to recover much of its strength. In compressible, frost susceptible soils, such as clays and silts, thaw weakening can occur without the presence of frost heaving.

While the existence of thaw weakening is well established, documentation of the saturated 'slurry' layers described by Andersland and Ladanyi [3] and Ghazavi and Roustaei [32] after thawing of ice lenses is limited. Clays are known to exhibit undrained behaviour in the short and mid-term, and it follows that melted ice will take time to redistribute through the sample. The existence of a very weak layer where the ice lenses were located could explain the temporary loss of strength.

2.5. Summary and conclusions of literature review

Most changes to the shear strength of soil will occur within the first 7 FT cycles. The formation of horizontal ice lenses perpendicular to the direction of freezing causes rearrangement of the soil particles and results in lower shear strength. With increasing FT cycles, the reduced void ratio will result in consolidation and shear strength stabilisation. Vertical cracking in frozen soil results in a net increase in hydraulic conductivity, but local decreases in permeability as soil blocks consolidate and vertical cracks grow. The hydraulic conductivity of the frozen soil is expected to increase with increasing FT cycles, which in turn causes consolidation in the unfrozen soil below the frozen fringe. This reduces the ability of water to move through the soil itself, and the vertical cracks create channels for water to move through.

3. Conceptual models

This chapter will discuss two conceptual models relevant for the application of this research. The first model represents undisturbed conditions found in-situ, and examines the shear strength and ice lens formation. The physical model developed in Chapter 4 will evaluate the undisturbed scenario. The second model looks at the influence of an energy pile on strength development in seasonally frozen soils, focusing on long-term behaviour, neglecting changes to the soil structure and shear strength due to installation effects. The second scenario serves as an application of the first when thermo-active structures are present. The relationship between these models and this research is defined, and a hypothesis developed to answer the research question '*What is the influence of cyclic freezing and different ground temperatures on the shear strength of an Illite clay?'*.

3.1. Model 1: Undisturbed conditions

Model 1 describes undisturbed conditions prior to any change in the soil or thermal regime due to site clearing or construction. The physical model developed in Chapter 4 represents the undisturbed conditions described in this section.

Ice lenses tend to form parallel to the plane of shearing (e.g., perpendicular to loading). Cracking due to volume changes during the FT process result in vertical ice lens formation, which allows water to flow through the soil and form horizontal ice lenses. Changes in volume and grain structure are expected to stabilise after some number of FT cycles as the depth of the active layer equilibrates and the soil consolidates. Under these conditions, some shear strength recovery in the long-term is expected, influenced in part by consolidation from settlement. This phenomenon is known as 'thaw consolidation'. Thaw consolidation is defined as 'time-dependent compression resulting from thawing of frozen ground and subsequent drainage of pore water' [27]. This settlement will continue to occur as long as the thawing front is advancing and until the pore pressure is dissipated.

Figure 3 shows the development of horizontal and vertical ice lenses over time with a constant applied freezing surface temperature. During freezing, pore water will attempt to move across the freezing front, resulting in ice lens formation, as discussed in 2.3.1. Ice lens formation and frost heave. The periodic lensing is a result of the water migration along the vertical cracks towards lower temperatures (ice) until the available pore space is full. Once the pore space is full, a new ice lens initiates at a warmer temperature near the freezing front. The size of both the horizontal and vertical lenses increases as the freezing front penetrates the soil. Pore water is sucked from the underlying unfrozen soil towards the frozen fringe, contributing to the increased size of the lenses. When water is available within the system, vertical cracks may form that allow water to escape to the surface. In clayey soils, escaping water can push clumps of soil up to the surface to form lumpy formations known as hummocks.

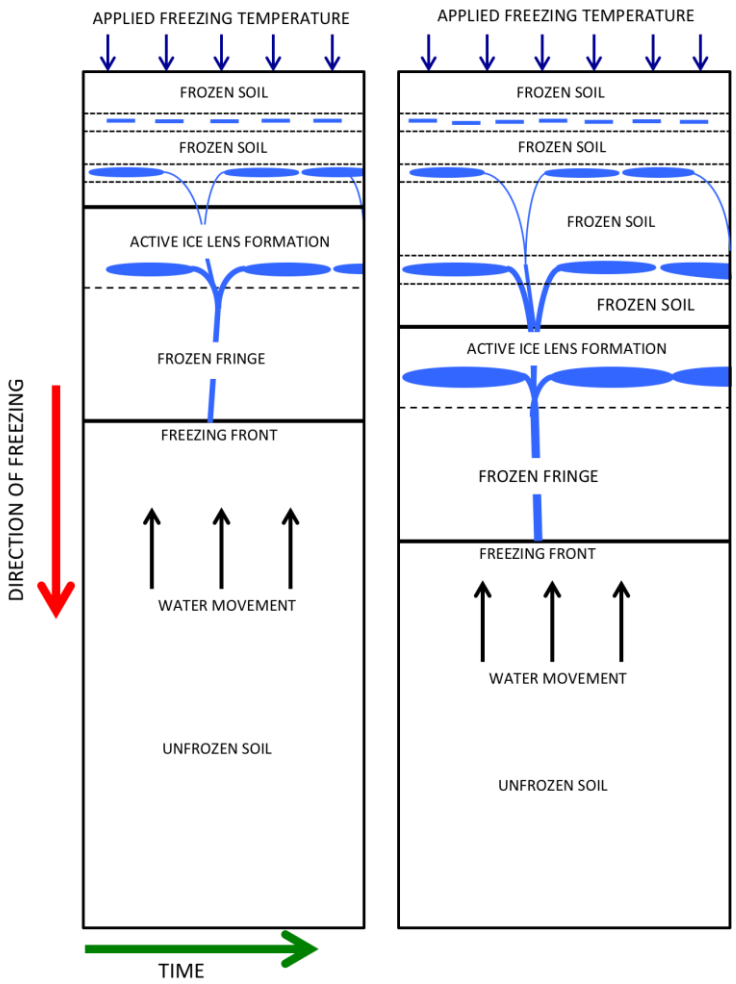

Figure 3: Development of ice lenses over time for undisturbed conditions as described in Model 1.

At colder surface temperatures, heat is removed more rapidly from the soil and more, smaller ice lenses form. Warmer surface temperatures and slower freezing rates result in fewer lenses, which are larger than those formed at faster freezing rates [25].

As the soil is subjected to multiple freezing and thawing cycles, the size and location of the ice lenses stabilises. This is caused by the hydraulic conductivity *k*, which increases after 1 FT cycle. With additional freezing cycles, *k* continues to increase, but at an increasingly lower rate, until reaching a new balance state after approximately 7 FT cycles [10]. After 7 FT cycles, the number of cycles no longer influences the soil properties. Increasing FT cycles result in more vertical cracks and horizontal ice lenses throughout the soil. This means that the soil structure undergoes changes due to the ice lens formation that translates to changes in shear strength and physical properties, such as void ratio.

The volume change resulting from pore water freezing causes an increase in horizontal stress, as the soil is confined in that direction. A significant increase in vertical stress occurs, and the soil will 'heave' in order to relieve it [25, 33]. After many freezing cycles, consolidation ends and the soil strength stabilises. The equilibrium state extends to both the physical and mechanical properties of the clay. However, any changes

at the ground surface (clearing, construction, etc.) disrupt the thermal equilibrium, and the soil properties begin to change until equilibrium is re-established.

3.2. Model 2: Thermo-active structure

The second conceptual model looks at the influence of thermo-active structures on a soil profile. This model is intended to represent potential applications of this research and is not part of the physical model.

The purpose of a thermo-active structure is to store heat energy in the ground for extraction at a later time. In permafrost regions, surfaces are often cleared and allowed to sit to allow the active layer and soil to settle and re-establish thermal equilibrium. Thermosiphons can be used to prevent soil from thawing or freezing (the mantra in cold regions is, 'if it's frozen keep it frozen; if it's thawed keep it thawed'.). A thermosiphon relies on either passive heat transfer (natural convection) or forced circulation systems to remove or add heat to the ground when the air temperature is lower than the ground temperature to maintain the soil state [3]. Generally, thermal piles are cast in place with the heat transfer element (thermosiphon) installed within the rebar cage prior to placement of the concrete.

Figure 4 shows the thermal footprints of a traditional pile and an energy pile. In this scenario, the frozen soil is thawing as a result of energy flux. Recall that installation of any structural element on or in the soil will alter the thermal properties of the soil, resulting in surface settlement and consolidation. In areas subject to seasonal freezing, the difficulty becomes controlling the size of the thermal footprint ('thaw bulb'). The multi-directional heating from the surface and thermal pile will result in a larger thermal footprint and increased rate of consolidation around the pile. This causes the surrounding soil to reach equilibrium more rapidly and accelerates strength recovery due to consolidation, similar to the undisturbed conditions described in Model 1 with increasing FT cycles.

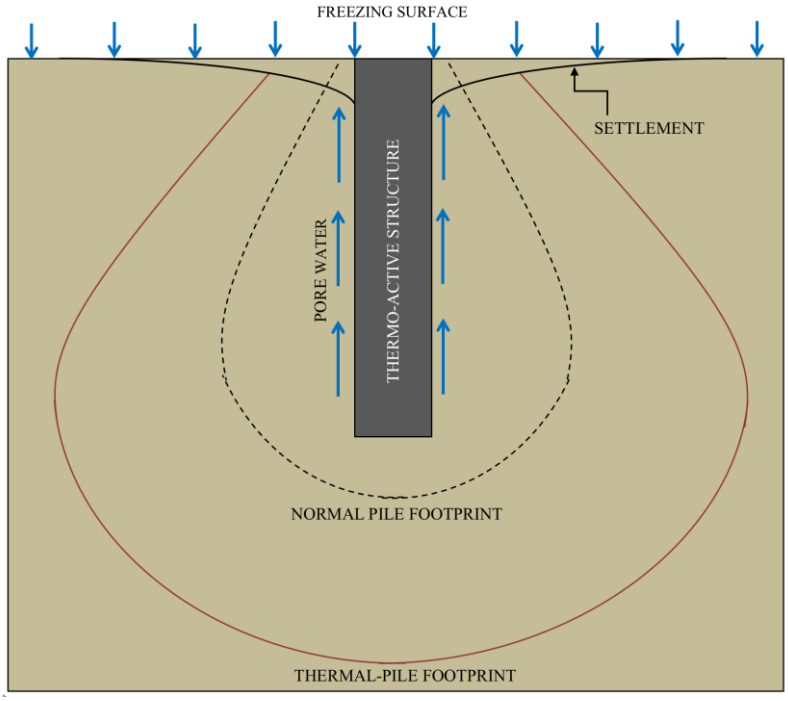

Figure 4: Thermal footprint with thermo-active structure using the soil as a heat sink vs. normal pile

Recall that soil exposed to freezing cycles will experience a 9% volume increase from the water-ice phase change, while the pile volume and location will remain constant. The structure itself acts as a 'drain' that accelerates the flow of pore water to the surface, resulting in fewer ice lenses and a more stable condition over time around the pile itself. As pore water moves out of the soil, the water content, and by extension the heat storage capacity, decreases, resulting in diminishing returns. Minimizing changes to pore pressure and water flow by maintaining a single soil state would improve the efficiency and life-span of a thermal pile by stabilizing the soil properties.

Figure 5 shows the development of ice lenses with increasing overburden pressure from a structure, neglecting installation effects. As loads are applied to the soil, the increasing pressure decreases the distance between the vertical cracks. Stress concentrations at the intergranular contacts allow the ice to melt more easily. This phenomenon is known as 'pressure melting'. The influence of pressures from surface loads translates to smaller ice lenses and reduced displacement during freezing [6, 25]. Vertical ice lenses form along the sides of the structure, resulting in increased lateral pressures [3]. In the case of thermal piles where the soil is prevented from freezing (Figure 4), the adfreeze bond between the ice and structure, which can generate shear stresses up to 150 kPa [33], is replaced with lateral stresses from pressure melting. Pressure melting can prevent ice lenses from forming along the side of the pile and allow water that would freeze in undisturbed conditions to flow up the side of the structure and out of the soil.

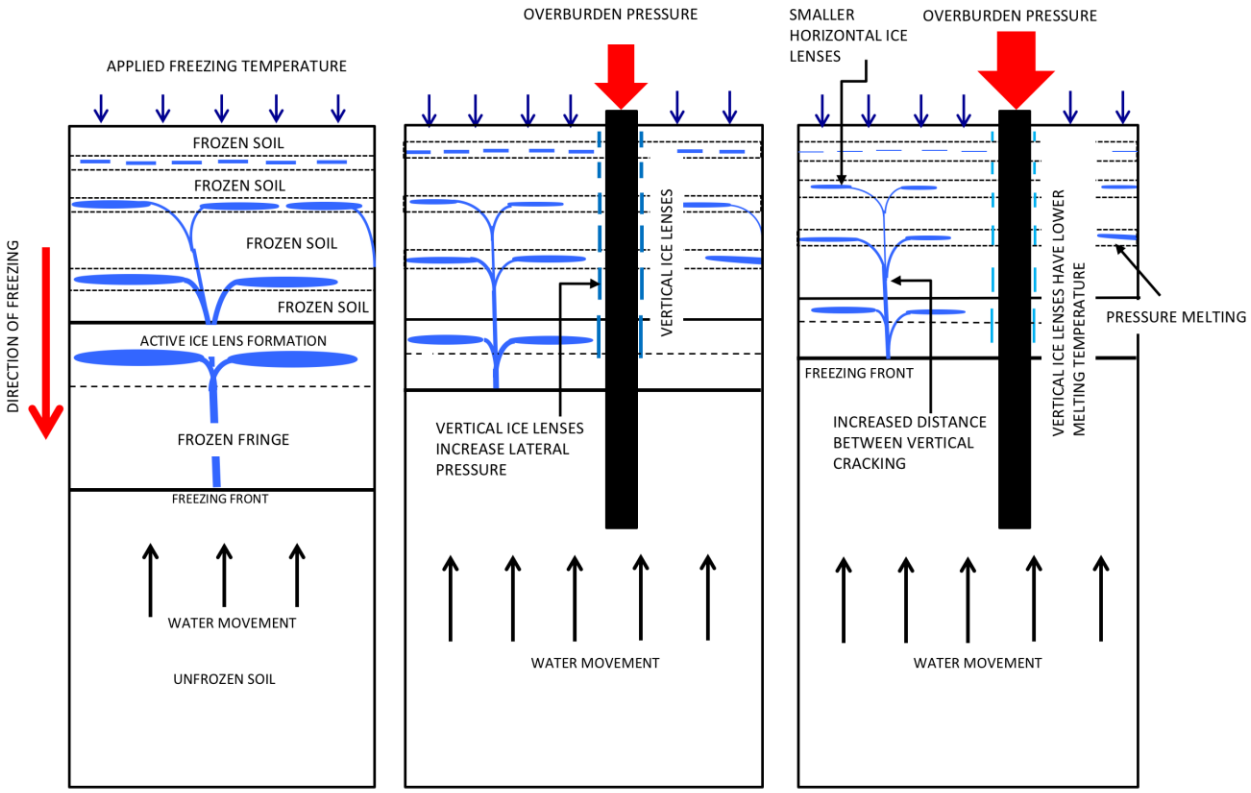

Figure 5: Influence of overburden pressure acting on a structure in frozen ground as described by Model 2. From left to right: In-situ conditions; Pile with overburden pressure resulting in smaller ice lenses and formation of vertical lenses along the side of the pile; Increased overburden pressure resulting in pressure melting, fewer ice lenses, and less displacement during freezing (based on Alley [2] and [3]).

3.3. Application of conceptual models to research

The models described above assume one-dimensional heat flow in an open system, where water can enter and leave the soil. One-dimensional heat flow describes an element with temperature applied at one side and assumes a linear temperature gradient with depth in the different areas of soil, as shown in Figure 1(B). The one-dimensional heat flow and undrained conditions tested in this research correlate to the side of a pile within the frozen layer and frozen fringe perpendicular to the pile. Figure 6 shows the location of the sample elements analysed in this research as they pertain to the in-situ conditions and thermo-active structure.

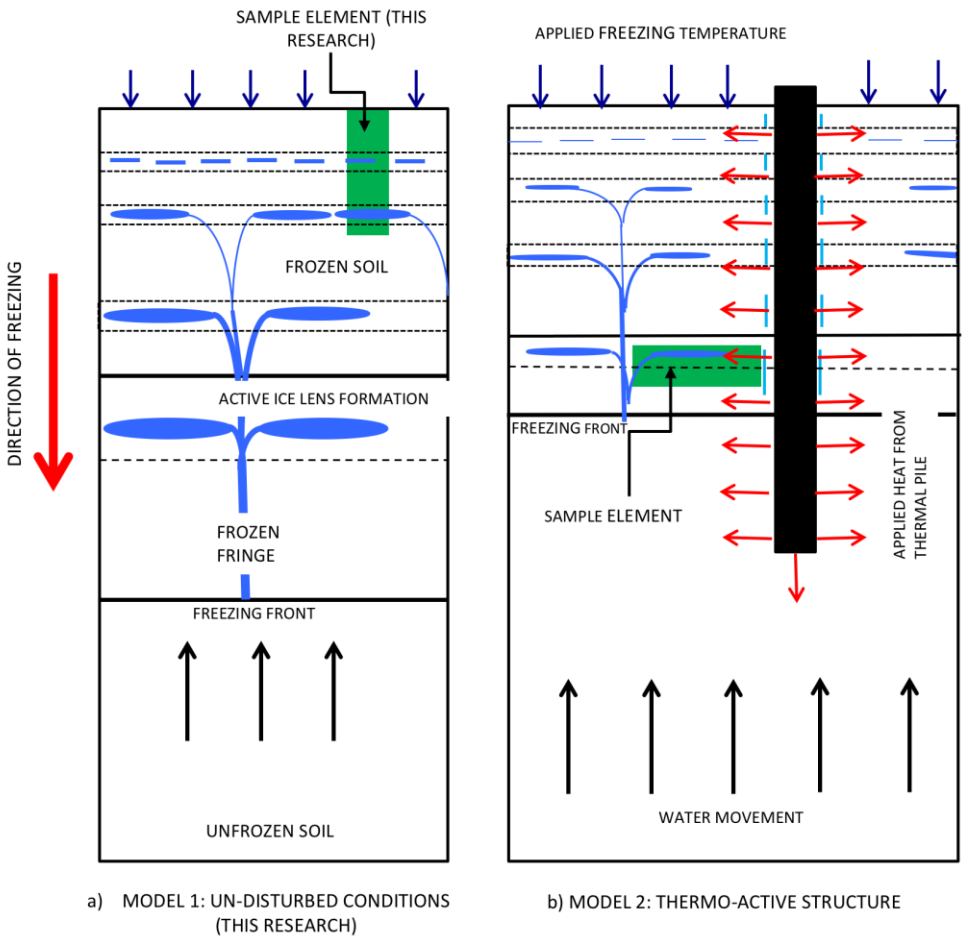

Figure 6: Location of sample tests in this research in conceptual models. LEFT: Element location for undisturbed conditions (Model 1); RIGHT: Element location with a thermo-active structure (Model 2).

This research focuses on the undisturbed conditions shown in part a) of Figure 6 and described by Model 1. The results for in-situ conditions can be extrapolated to the element shown in part b), which is subjected to two-dimensional heating due to the heat injection/extraction by the energy pile. With enough depth, the influence of the surface temperature will be negligible and only the heat transfer from the thermal pile will influence the soil element, allowing it to be modelled with one-dimensional heat transfer.

3.4. Hypothesis

Based on the conceptual models discussed in this chapter and the literature review (Chapter 2), hypotheses have been developed to answer the research question '*What is the influence of cyclic freezing and different ground temperatures on the shear strength of an Illite clay?*'. The sub-questions and associated predictions are as follows:

1. *What is the influence of repeated FT cycles on shear strength?*

The shear strength of the clay will decrease with increasing FT cycles. Most of the changes in shear strength will occur within the first 7 cycles, after which the strength will continue to decrease, but at a very low rate approaching an equilibrium strength.

2. *What is the influence of the surface temperature on shear strength after 1 FT cycle?*

The shear strength will increase with colder applied surface temperatures (higher freezing rates) and decrease at warmer temperatures.

3. *What is the influence of freezing rate and number of FT cycles on grain structure and ice lens formation?*

Ice lenses will form in horizontal (periodic) layers of increasing size moving away from the freezing side. Larger ice lenses will occur at lower freezing rates, which will result in lower shear strength. The size and distribution of the ice lenses will become more uniform with increasing FT cycles. After 7 cycles, the ice lens distribution and soil structure changes will stabilize.

4. Physical modelling

A physical model was developed to answer the research question '*What is the influence of cyclic freezing and different ground temperatures on the shear strength of an Illite clay?*'. An experiment was designed to evaluate the shear strength development of clay with increasing number of FT cycles and different freezing rates under in-situ conditions. This experiment represents the first model (undisturbed conditions) described in Chapter 3. The experimental approach is given in Section 4.1. A detailed description of the laboratory setup and freezing apparatus is given in Section 4.2. The steps for sample preparation are discussed in Section 4.3, and the considerations for choosing the number of freezing cycles and applied surface temperatures are elaborated in Section 4.4. The boundary conditions for the physical model are then defined in Section 4.5., and conclusions are stated in Section 4.6.

4.1. Experimental approach

Based on the literature review and standard geotechnical design approaches, undrained conditions were modelled, as they will result in lower shear strengths than drained materials. The apparatus used in this research is a closed-system that simulates confined, undrained conditions with a freezing front penetrating from the surface (one-dimensional heat transfer). Water can move through the sample but cannot leave the system. In reality, although clay often exhibits undrained behaviour, it is semi-confined and experiences volume changes, especially during freeze and thaw.

Samples were mixed in batches and a triaxial test was performed on a never-frozen sample from each batch. Unit weights were taken from every sample, and the prepared samples were placed in an insulated container and subjected to FT cycles. The samples were allowed to freeze from the bottom until the top of the sample reached -2.5°C for at least 1 hour to ensure the pore water was completely frozen. The samples were allowed to thaw until the temperature at the top exceeded 3°C for at least 1 hour to ensure all the ice had melted. After the specified number of FT cycles was reached, the still-frozen samples were placed in a triaxial machine, and the load piston was lowered (docked) to prevent collapse during thawing. An unconsolidated undrained (UU) triaxial test was performed to determine the shear strength of the thawed samples. Macro-CT scans were performed on some of the frozen samples to evaluate the changes in soil structure. The samples chosen for CT scanning were designed to track the expected shear strength development with number of FT cycles, in order to relate changes in the soil structure to the mobilised shear strength.

4.2. Lab setup and apparatus

A setup located in the TU Delft climate lab was used to apply freeze-thaw cycles to the samples. The apparatus was designed by van den Bosch [9] to analyse the formation of ice lenses in silty soils and Illite clay. This setup is capable of running up to six (6) samples simultaneously, with independent temperature controls for each sample. During this research, no more than 4 units were operational at any given time. Samples were set on a heating plate located on the bottom of the freezing apparatus, and temperature readings at the top and bottom of the sample were recorded by the computer controlling the heating plate. The samples were frozen or thawed from the bottom using a copper plug to inject or extract heat from a Peltier module into the sample. This one-dimensional freezing simulated in-situ conditions.

The FT apparatus is made up of 10 main components, as indicated in Figure 7. The three cooling components, (1), (5) and (6), prevent the setup from overheating. The Nepton heat sink (6) removes heat from the hot side of the Peltier element (2), which is responsible for applying temperature to the bottom of the sample and is connected to the power box at (3). The applied freezing temperature at the bottom of the sample T_{bf} is set using the MP3 software on the computer and controls the temperature of the Peltier element. The temperature readings at the bottom of the samples are taken by a sensor in the copper plug (4). A silica heat transfer compound is applied to the Peltier module (2) before the copper plug (4) and sample box are placed on top of the heating element. The plug is then connected to a power box (10) at connection (8). The top temperature sensors (7) are tied in to the controller box (9) and then the power box (10), where the data is fed in to the laptop. The top temperature sensors (7) are fed through a hole in the insulation insert in the sample and pushed approximately 2 mm into the top of the sample.

The apparatus components, as labelled in Figure 7, are described as follows:

(1) Cooling transformer and power for Peltier module;
(2) Peltier module (heating element);
(3) Connection between Peltier module and power box;
(4) Copper plug;
(5) Cooling fan;
(6) Nepton 280L extra-large 280 mm radiator, duel JetFlo 140 fans liquid CPU coolers;
(7) Temperature sensor;
(8) Connection between copper plug (4) and controller box (9);
(9) Controller box where temperature sensors (7) connect and tie in to power box (10);
(10) Power box (connects to laptop).

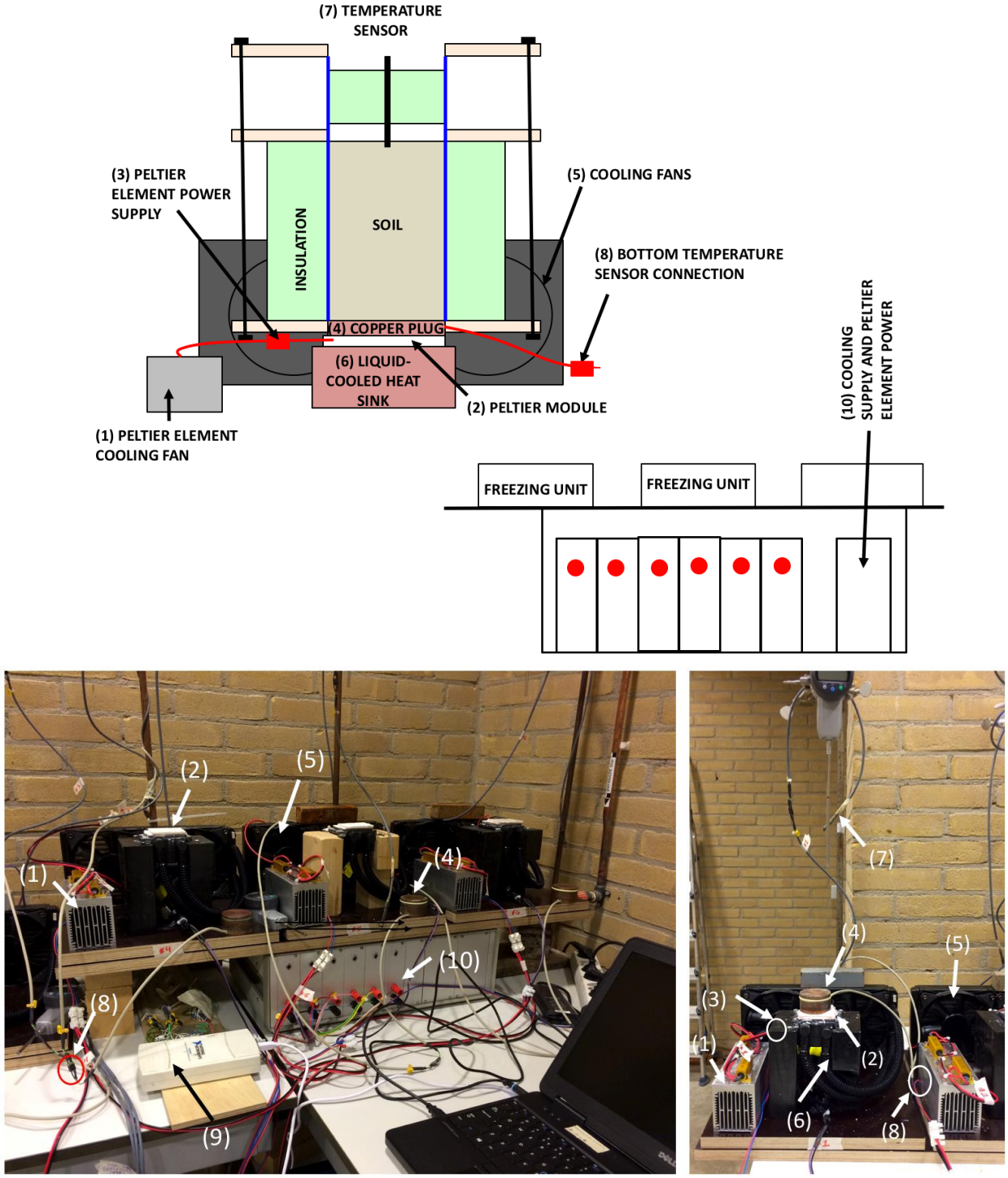

Figure 7: TOP: Schematic of FT apparatus; BOTTOM: Actual apparatus

4.2.1. Sample casing

The soil samples were built into a cylindrical Perspex casing with a latex membrane to prevent water flowing out of the sample. The casing dimensions were 50 mm inner diameter and 200 mm high. For ease of removing the sample, the casing was cut in half lengthwise. The bottom of the membrane was connected

to a cylindrical copper plug using gaskets to make the sample watertight and improve heat transport to the sample. A cylindrical insulation insert was placed on top of the sample and secured with the rubber membrane.

Figure 8 shows the disassembled sample casing, consisting of (from left to right) the Perspex cylinder, rubber membrane, gaskets to secure the sample and hold the Perspex cylinder closed, insulation insert, and copper plug. The centre image shows an assembled sample prior to being placed into the Perspex cylinder, and the right image shows the fully assembled sample casing.

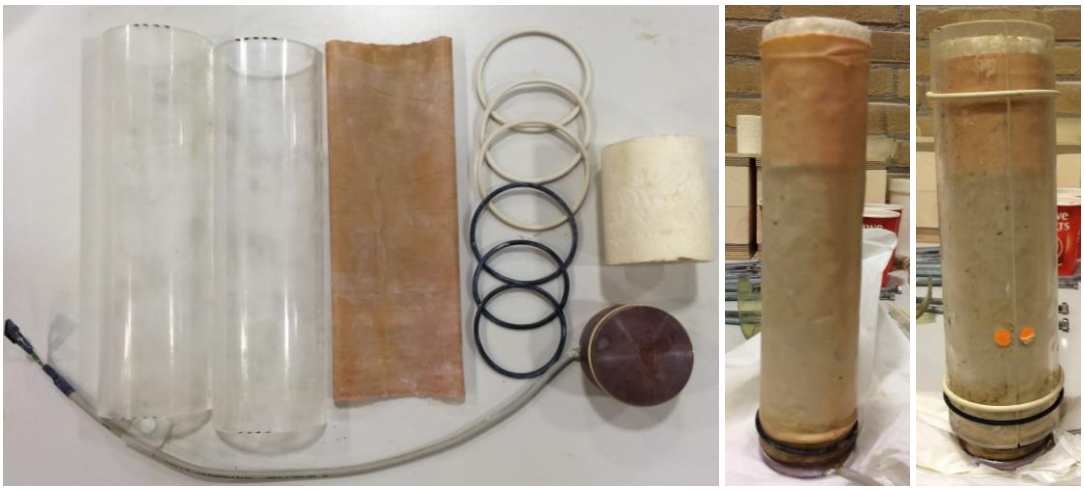

Figure 8: LEFT: Disassembled sample casing; CENTRE: Assembled sample without Perspex cylinder; RIGHT: Assembled sample in Perspex cylinder

4.2.2. Sample container

The sample container was designed to create a thermal envelope to prevent heat transfer to the atmosphere during freezing and thawing. This was achieved using two layers of URSA XPS insulation with a minimum thermal resistance *R* of 2.00 m^2×K/W, and thermal conductivity of 0.034 W/m×K. The total dimensions of the sample box were 194 mm x 194 mm x 120 mm (l x w x h). The insulation was placed between a plywood bottom, middle, and top plate to hold it in place. The bottom plate was constructed of three plates with dimensions of 194 mm x 194 mm x 30 mm and a circular opening in the centre for the copper plug. The sample casing was seated in this hole and the insulation placed around it. The two plywood plates at the top of the insulation and sample casing held the insulation in place and prevent axial movement of the casing. The plates were fixed together with four M6 stud bolds. The total dimensions of the assembled sample container were 194 mm x 194 mm x 245 mm (l x w x h). Figure 9 shows the completely disassembled sample container and casing components.

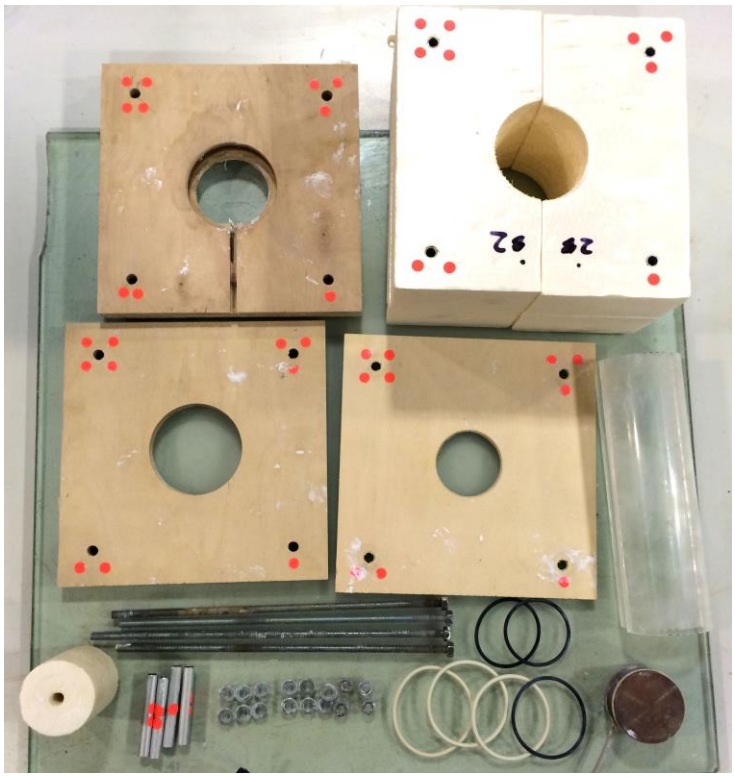

Figure 9: Disassembled sample casing and container

Figure 10 shows a schematic of the freezing apparatus and sample box, as well as a cross section of an actual sample unit.

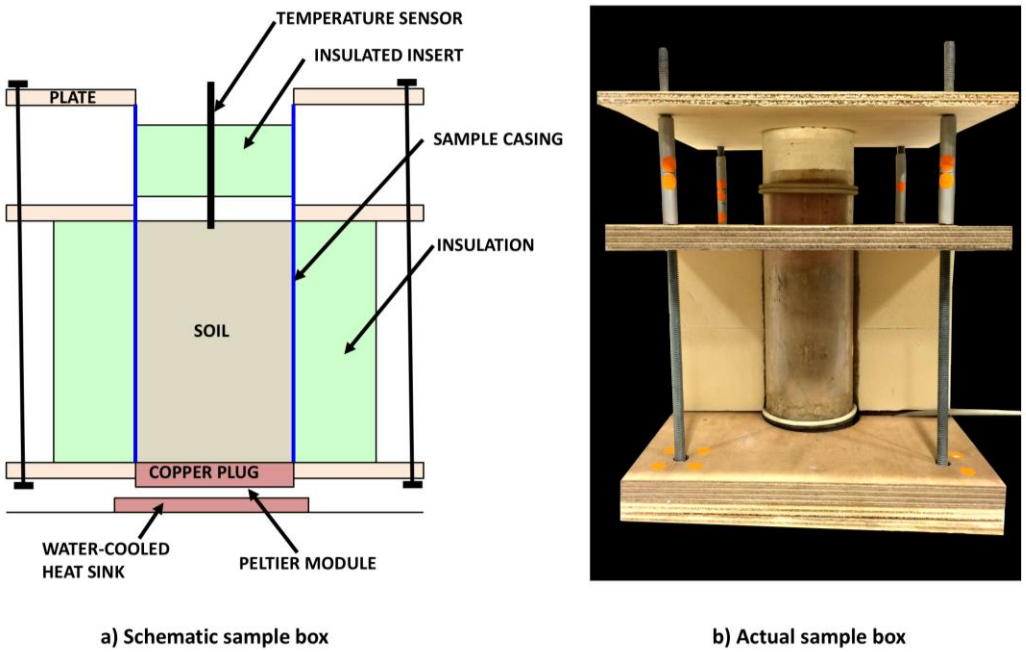

Figure 10: LEFT: One-dimensional sample container schematic; RIGHT: Actual sample container

4.3. Sample preparation

The USACE Frost Susceptibility Criteria defines the tendency of a soil to experience deformation (frost heave) during freezing. For example, gravel, considered a non-frost-susceptible soil, falls under frost group 1 (designated F1), while saturated, fine-grained soils, such as clays, fall under frost groups F3 or F4, depending on level of saturation and plasticity index [1]. A plasticity index $PI < 12\%$ is required to fall into F4 (highly frost susceptible). F3 or F4 soils will be significantly affected by FT cycles. Determination of the *PI* for the commercially available, overconsolidated Illite clay used in this research gave a $PI = 34\%$. This classifies the material as F3. While a slurry is ideal for uniform sample preparation, triaxial tests to determine the initial strength cannot be done on a slurry, so this option was discarded. Instead, the clay was prepared so it was soft enough to be handled while remaining stiff enough to hold its shape after cutting. The samples were prepared with a target water content of 18% and dry unit weight $\gamma_d = 18.9\ \frac{kN}{m^3} \pm 4.2\%$ ($\rho_d = 1.9 \frac{g}{cm^3}$). A summary of the sample preparation is as follows:

1. Water was added to Illite clay and mixed until the desired workability was obtained. This was checked by rolling a small amount of material into a 3 mm thick string, similar to the method for determining the plastic limit. The clay was then kneaded to remove air and shaped into long rolls, which were cut into approximately 130 mm by 70 mm sections. The clay rolls were stored in airtight plastic bags for no more than 4 days;

2. The rolls were placed in a frame and cut to approximately 50 mm by 120 mm After removal from the frame, the ends of the samples were trimmed flat;

3. The samples were measured using callipers and cut to 100 mm. The final sample height and diameter were measured at 3 separate locations. A rubber membrane was placed over the cut sample using a hollow plastic cylinder. The sample was then placed inside the sample container and box (Figure 10);

4. The height and diameter of the remaining sample section (approximately 20 mm tall) were measured in 3 places and the wet weights were taken. This was placed in an oven at 105°C and used to determine the unit weight and water content of the sample;

5. A silica heat transfer compound was applied to the heating plate at the bottom of the freezing apparatus, and the sample was set onto it. The top temperature sensor was then pushed through a pre-cut hole in the insulation insert approximately 3 mm into the top of the sample.

Figure 11 shows the equipment used to cut and measure the samples, as described in step 2. A cut sample with the rubber membrane installed can be seen to the left of the cutting frame.

Figure 11: Sample cutting equipment (clockwise from top left): cut sample with membrane, cutting frame, plastic cylinder for installing membrane, callipers, wire cutter

The naming convention used for the samples was 'TX-#'. The 'T' stands for 'test batch' number 'X', followed by the sample number within that batch. For example, the second sample prepared from test batch 3 would be named 'T3-2'.

4.4. Freeze-thaw cycles

The long-term shear strength development of Illite clay with increasing freeze-thaw cycles and different freezing rates were evaluated during this research. Because of time constraints, the applied surface temperature T_{bf} = -20°C was the primary testing temperature, and lower freezing rates were used for comparison of strength development and ice lens formation. To evaluate the influence of freezing rate on soil strength, the samples were frozen with different surface temperatures and thawed at +20°C for the duration determined in Section 5.2. Sample freeze and thaw time. Two categories of thermal cycles were run: short-term (1 cycle) for T_{bf} = [-5, -10, -15, -20] °C, and long-term (3, 5, 7, 10, and 20 cycles) for T_{bf} = -20°C.

4.4.1. Number of cycles

The distribution the FT cycles evaluated was based on the expected strength development of the soil. The literature indicated that the largest change in soil properties would occur within the first 7 cycles. Long-term scenarios, using a typical design life of 30 years for a thermal pile and assuming 1 freezing cycle per year, would require approximately 30 FT cycles. Due to the time required for a complete FT cycle, it was not practical to apply this many cycles in this research. Based on the literature review, soil was expected to reach an equilibrium condition well before 20 cycles.

4.4.2. Sample freezing and thawing

A freezing temperature T_{bf} was applied at the bottom of the sample via the Peltier element. The phase change can be observed in the temperature vs. time graphs at approximately 0°C. The temperature was maintained until the top of the sample reached a temperature below -2°C for 1 hour. This was designed to compensate for potentially lower freezing temperatures of pore water as a result of salts in the soil and

incomplete freezing due to absence of ice nucleation [18]. As previously discussed, the chemical composition of the soil can impact the freezing temperature of the pore water, and since this was not being investigated in this research, a lower temperature was used to ensure the sample was frozen. The amount of time required for the entire sample to reach freeze at different surface temperatures was determined as described in Section 5.2. Sample freeze and thaw time.

After ensuring the entire sample was frozen, a thawing temperature of T_{bt} = +20°C was applied until the top of the sample exceeded +3°C for 1 hour. Maintaining the thawing temperature at the bottom of the sample for an additional hour ensured that all of the ice had melted. Note that the top of the sample continues to warm after the thawing temperature is no longer applied, as the thawing front takes time to penetrate the soil and melt the pore water. After all FT cycles were completed, the frozen samples were thawed in a triaxial cell filled with 17°C water for at least 6 hours. When time allowed, samples were allowed to thaw overnight.

4.5 Boundary conditions

The thermal envelope created by the insulation box and insert was assumed to allow negligible heat loss via radiation and one-dimensional heat transfer. Samples were assumed to have uniform properties before freezing.

The samples were frozen under confined, undrained conditions in a closed system. Saturated, dense clays generally exhibit short and mid-term undrained behaviour. Because of this, undrained tests on the selected clay were considered reasonable. Furthermore, modification of the apparatus for testing in drained conditions may result in a less efficient thermal envelope because space would be required between the insulation and copper plug at the top and bottom of the sample to accommodate an external water supply.

Evaporation at the top of the sample was limited by the USRA XPS insulation insert placed on the sample top, and was considered negligible.

4.6. Summary

The physical model used in this research was designed to evaluate undisturbed conditions, as described in 3.1. Model 1: Undisturbed conditions. The apparatus applied temperatures at the bottom of the sample. The sample was insulated on the top and sides and assumed to have negligible heat loss to the atmosphere. The cut soil sample was encased in a rubber membrane and Perspex casing with a copper plug at the bottom to facilitate heat transfer from the Peltier element. The temperature at the top and bottom of the sample were measured and each sample was assumed to be confined and undrained. The number of FT cycles and applied freezing surface temperatures T_{bf} were based on the expected strength development with number of freezing cycles and surface temperatures experienced in cold regions based on the literature review.

5. Lab tests

This chapter describes the tests performed to realize the physical model described in Chapter 4. Tests done in accordance with a standard testing method are briefly described and the reader is referred to the relevant standard. The data processing needed to obtain results from the laboratory tests are discussed in Section 5.6. Data processing. The following parameters were required for the analysis of this research:

- Plasticity index *PI*
- Freeze and thaw times t_f and t_t
- Water content w
- Unit weight γ
- Shear strength τ
- Mobilised shear strength c_u

5.1. Atterburg limits (*PI*)

The plasticity index of the clay was determined using ASTM D4318-10e1 Standard Test Methods for Liquid Limit, Plastic Limit, and Plasticity Index of Soils [34]. The plasticity index *PI* of the saturated sample dictates the Frost Susceptibility Category of the clay as described by the US Army Corps of Engineers [1]. A *PI* < 12% is required to fall into Frost Susceptibility Category 4 (highly frost susceptible). Determination of the *PI* for this material (Illite clay) gave a *PI* = 32%. This classifies the clay in Frost Susceptibility Category F3. The *PI* was determined using the average of 3 Atterburg limits. The values from these tests are shown in Table 1.

Table 1: Atterburg limit test results

	Sample 1	**Sample 2**	**Sample 3**	**Average**
Plastic limit *PL* [%]	23.42	22.50	22.98	22.97
Liquid limit *LL* [%]	49.21	53.68	59.66	54.18
***PI* = *LL* – *PL* [%]**	25.79	31.18	36.68	31.22

5.2. Sample freeze and thaw time

Prior to beginning the FT cycles, the actual time required to freeze a clay sample at different surface temperatures was determined. Samples were placed in the apparatus, and the time required for the top of the sample to reach -2.5°C for 1 hour was determined for different T_{bf}. After ensuring the entire sample was frozen, a thawing temperature of T_{bt} = 20°C was applied, and the time required for the entire sample to exceed 3°C for 1 hour was measured. The phase change can be seen on the temperature vs. time graphs generated by the MP3 program and was used to confirm the samples had frozen/thawed. Samples subjected to only 1 FT cycle were frozen until they reached an 'equilibrium' temperature, where the reading at the top of the sample (furthest from the freezing side) stabilised. The minimum freezing time for each T_{bf} are given in Table 2.

Table 2: Experimentally determined sample freezing and thawing time for different applied temperatures

T_{bf} [°C]	t_f [hr]	t_t [hr]
-5	96	-
-10	48	-
-15	22	-
-20	15.5	5.5

To confirm that the thawing time was sufficient and check the effectiveness of the insulation envelope, a sample was completely frozen and allowed to thaw 'naturally', e.g., with the Peltier element turned off, so the thawing temperature at the bottom of the sample was equal to ambient air (approximately 14.5°C). Once the top of the sample exceeded 3°C for 1 hour, it was removed from the insulation and cut in half.

Figure 12 shows the naturally thawed sample. It can be seen that water moved through the sample via vertical cracks, and the sample fell apart as soon as it was cut in half longitudinally. Free water was observed at the top of the sample when the insulation insert was removed, and water seeped out of the sample when it was cut.

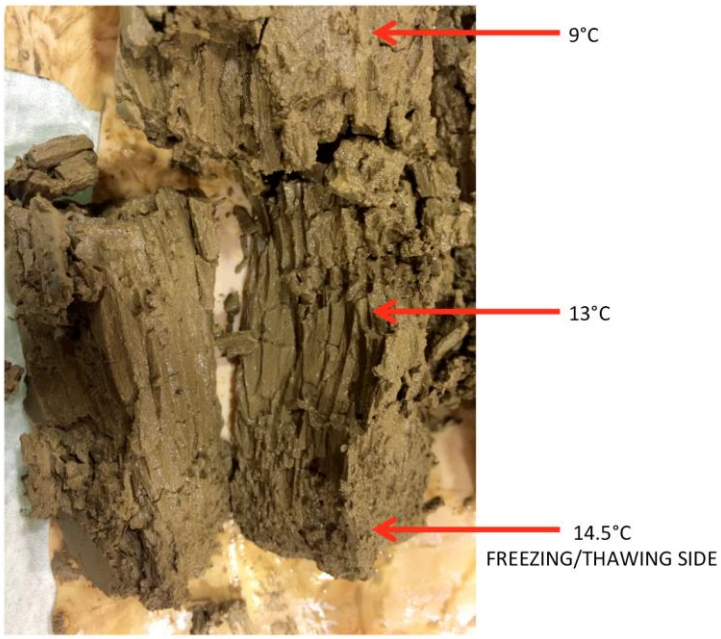

Figure 12: Grain structure of 'naturally thawed' sample with temperature readings and locations

A hand-held thermometer was used to take temperature readings in the thawed sample. The temperature in the middle of the sample was measured at approximately 13°C, when the bottom side of the sample (where temperature was applied) was room temperature (~14.5°C) and the top was approximately 9°C. This test confirmed that the insulation around the top and sides of the sample box provided a sufficient heat envelope.

5.3. Unit weight and water content (γ and *w*)

The unit weight of the soil was determined per ASTM D7263 Standard Test Methods for Laboratory Determination of Density (Unit Weight) of Soil Specimens [35]. The samples were obtained by cutting a section from each cut sample prior to freezing and measuring the height and diameter in three places. To ensure the results of the FT tests could be compared, efforts were made to ensure the wet and dry unit weights of all sample batches were within 4% of each other, with target $\gamma_d = 18.9 \frac{kN}{m^3}$ and moisture content w = 18%. Table 3 gives the average dry unit weight and water content for each test batch of clay.

Table 3: Material properties for each test batch of Illite clay

Batch	γ_d [kN/m^3]	w [%]
1	18.46	16.3%
2	19.15	15.4%
3	19.22	17.2%
4	18.27	19.5%
5	18.41	18.9%
6	20.26	18.2%
7	18.33	19.0%
8	18.11	20.3%
9	18.67	18.3%
10	20.38	16.0%
11	18.11	20.3%
12	19.65	19.0%

The water content of the prepared samples was less than the plastic limit of the clay. This was done to maintain the workability of the material, so the samples maintained their shape after cutting. Data sheets for the unit weights are located in A2.2. Unit weights.

5.4. Shear strength: Triaxial tests (τ)

Triaxial tests were chosen to determine the shear strength, rather than shear box tests, for several reasons. Shear box tests are used to test the interface shear strength and friction angle by applying a normal load. There is no confining pressure or deviator stress, and a shear box apparatus would have to be modified to prevent water and material loss from a thawing sample. Triaxial tests are better suited to characterising the deviator stress and failure behaviour of material, and using water to apply confining pressure kept the thawed sample from collapsing or buckling prior to loading. More importantly, it was possible to prevent water and material loss from the thawed samples using triaxial tests. Unconsolidated undrained (UU) triaxial tests were used to measure the shear strength of the thawed clay after the FT cycles were complete. The GDS triaxial machine used for this research is shown in Figure 13. GDS software was used to control the triaxial machine and controllers and record the test results.

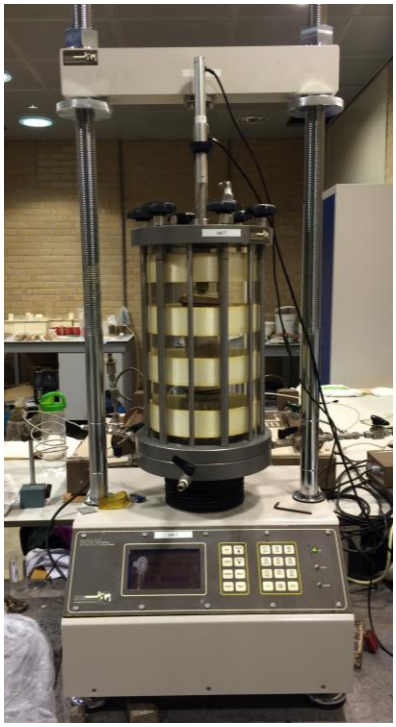

Figure 13: Triaxial apparatus

The test conditions for the triaxial tests were as follows:

- Axial load rate: 0.1 mm/min;
- Sample height: average height measured prior to beginning any freezing cycles;
- Sample diameter: average diameter measured prior to beginning any freezing cycles;
- Confining pressure: 400 kPa;
- Maximum load cell: 0.9 kN (stop condition);
- Maximum axial strain: 20% (stop condition).

These parameters were chosen because the physical model assumed a constant load from self-weight and undrained behaviour. This allowed a single confining pressure to be used. The loading rate was chosen to be small enough so as not to influence the stress development in the sample, without being so low as to push water out of the sample and trap it between the clay and the membrane, which would effectively allow the sample to consolidate. Results of the triaxial tests are located in A2.3. Triaxial Results.

5.4.1. 'Never frozen' triaxial tests

Using ASTM D4767-1: Standard Test Method for Unconsolidated Undrained Triaxial Compression Test for Cohesive Soils [36], one triaxial test was performed on a never-frozen sample from each test batch of clay.

5.4.2. Previously frozen (thawed) soil triaxial tests

After removal from the freezing unit, the frozen sample was taken out of from the casing and placed into the triaxial machine. The load piston was lowered onto the cap until the load sensor read 0 kN, and the triaxial cell was filled with 17°C water until the sample was completely covered. The sample was allowed

to thaw in the water for at least 6.5 hours. After thawing, the water in the cell was replaced with de-aired, de-mineralised, room temperature (14.5°C) water prior to starting the UU triaxial test in accordance with ASTM D4767-1: Standard Test Method for Unconsolidated Undrained Triaxial Compression Test for Cohesive Soils [36].

5.5. CT Scans

A macro-CT scan was performed after 1 freezing cycle for samples with T_{bf} = [-5, -10, -15, -20] °C. The frozen samples were removed from their frames and carried to the CT scanner in their insulation. The samples were scanned while still inside the insulation and Perspex cylinder. The CT scans took 0.6 mm slices, obtaining 206 images over the length of the sample. Approximately 15 minutes passed between removing the sample from the freezing unit, scanning, and loading into the triaxial cell. To evaluate the development of ice lenses with repeated FT cycles, CT scans were done on samples frozen at T_{bf} = -20°C after 1, 3, 7, and 10 cycles. A Siemens SOMATOM Definition macro-CT scanner was used (shown in Figure 14). The CT images were processed using Avizo 9.0.1 software.

Figure 14: Siemens SOMATOM Definition macro-CT scanner used for CT scans on frozen samples

5.6. Data processing

After completing the FT cycles, the raw temperature data for each sample was exported from the MP3 program used by the freezing units and inspected to confirm a phase change occurred at the top of the sample (furthest from the freezing surface).

After completion of the UU triaxial tests, negative trends after reaching local peak strengths were removed. These peaks were due to the inability of the GDS software to accurately measure the low confining pressure and small axial load used. The controller for the confining pressure has some variation that becomes more noticeable at low deviator stresses, and, while the load piston was one of the most accurate available, the very small loads applied by the piston (in the order of 0.02 kN) were too small to be measured accurately by the GDS software. At loads exceeding 0.1 kN, and confining pressures above 600 kPa, the software is very accurate. Using larger time steps between measurements (30 second intervals, rather than 10 seconds)

reduces these negative trends. Finally, the triaxial results were adjusted to report mobilised shear strength c_u by assuming no mobilised strength at 0% axial strain, thus shifting the x-y intercept of the mobilised shear strength vs. axial strain graphs to the origin.

5.7. Summary of lab tests

Atterburg limits were used to determine that the frost susceptibility criteria of the Illite clay used in this research was F3. The time required to freeze the samples at different applied surface temperatures was measured, and UU triaxial tests were done to measure the shear strength of never-frozen and thawed samples after completion of FT cycles. Macro-CT scans were used to track the ice lens development and changes in the soil structure. The results of the lab tests are discussed in the next chapter.

6. Results

The research question posed by this thesis could not be fully answered based on the existing literature. This chapter presents the results of the lab tests described in Chapter 5, and discusses their implications as it pertains to the research question, '*What is the influence of cyclic freezing and different ground temperatures on the shear strength of an Illite clay?*'. Variability within the system was addressed and suggestions for improvements to the test methods are made. Finally, the results are compared to the literature review and hypotheses developed in 3.4. Hypothesis.

6.1. Evolution of shear strength as a result of FT cycles

Previous research has suggested that a soil's shear strength decreases with increasing freeze-thaw (FT) cycles until it approaches an equilibrium strength after approximately 7 cycles. Based on this, each set of test conditions was designed to track the strength development of Illite clay and identify the number of cycles where the equilibrium strength was reached. Multiple tests under the same conditions were performed after 1, 3, and 7 FT cycles to help quantify the variability within the model. This is discussed in 6.7. Variability and reliability of results.

Figure 15 shows the shear strength development with different FT cycles. An asymptotic relationship between the shear strength and number of FT cycles was expected, with the strength reducing over time and levelling out after approximately 7 cycles. The rate of strength development and stiffness varied with the number of FT cycles, with the highest stiffness occurring after 1 cycle and the next-highest at 20 cycles. The influence of soil stiffness on shear strength is discussed in 6.6. Change in stiffness.

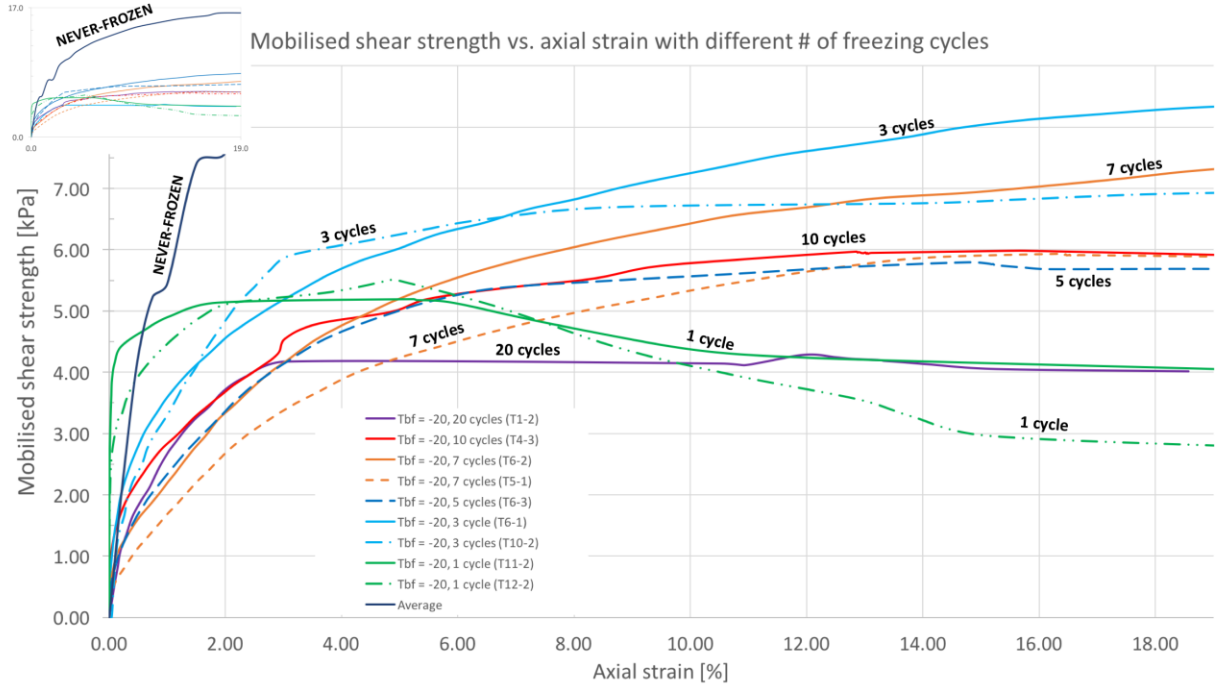

Figure 15: Mobilised shear strength vs. axial strain with different # of FT cycles at T_{bf} = -20°C

The development of mobilised shear strength can be used to identify the axial strains where the peak shear strength and strain hardening or softening occur. It is preferable that the shear strength of the load bearing soil is not reached at a site during construction. Table 4 gives the shear strength for samples with different number of FT cycles and freezing rates at different axial strains. CT scans were done on samples annotated with ^{CT} next to the number of cycles. These values are plotted in Figure 16 and Figure 17. As most of the samples exhibited strain hardening, there is no peak shear strength to plot. The values of axial strain shown in Table 4 were chosen to track the early strength development of the clay.

Table 4: Shear strength at different axial strains for various FT cycles at T_{bf} = -20°C and applied freezing temperatures

Sample #	T_{bf} [°C]	# FT cycles	Mobilised shear strength [kPa]			
			axial strain = 2%	axial strain = 4%	axial strain = 6%	axial strain = 10%
T11-2	-20	1^{CT}	5.13	5.24	5.13	4.35
T12-2	-20	1	5.13	5.51	5.14	4.00
T6-1	-20	3	4.59	5.70	6.35	7.30
T10-2	-20	3	5.14	6.11	6.48	6.72
T6-3	-20	5	3.50	4.72	5.25	5.55
T5-1	-20	7	2.71	3.96	4.52	5.32
T6-2	-20	7	3.46	4.72	5.50	6.45
T4-3	-20	10	3.79	4.89	5.29	5.78
T1-2	-20	20	3.71	4.20	4.18	4.15
T9-3	-15	1^{CT}	3.26	3.87	4.64	5.64
T5-2	-10	1^{CT}	2.43	3.42	4.00	4.88
T9-2	-10	1^{CT}	3.25	4.50	5.04	5.59
T7-1	-5	1^{CT}	1.10	1.75	1.98	2.25

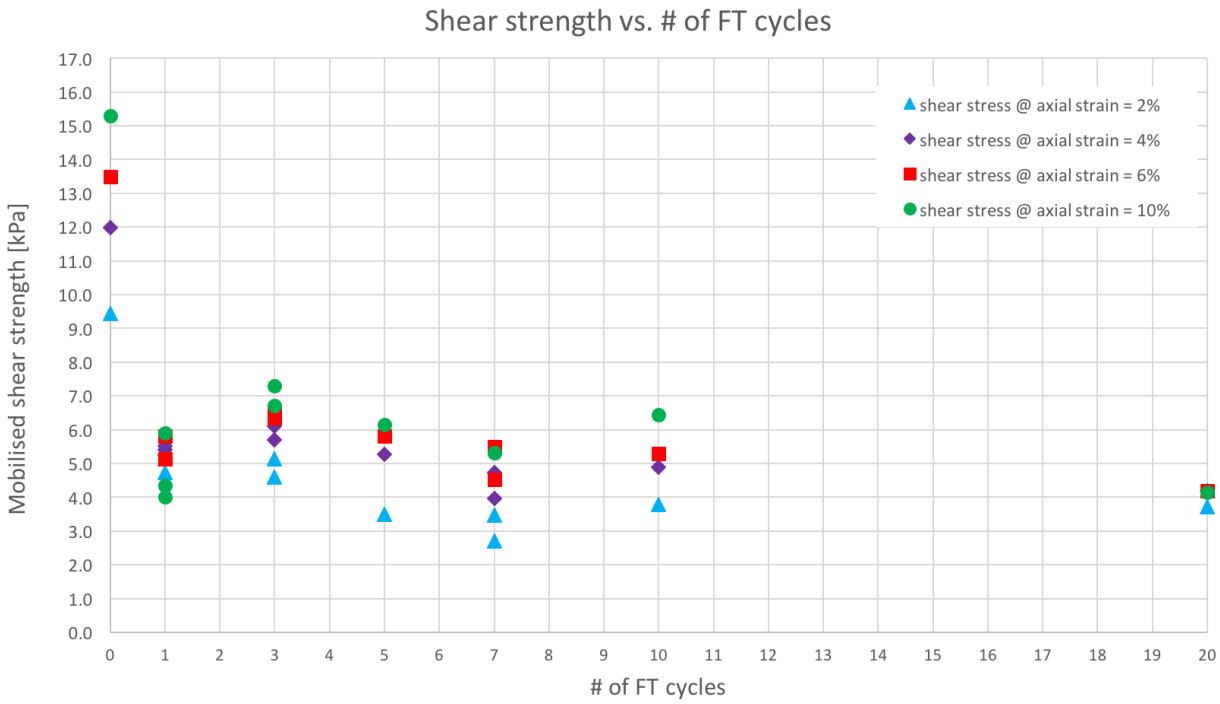

Figure 16: Mobilised shear strength vs. number of freeze-thaw cycles at different axial strains at T_{bf} = -20°C

A smaller spread between the shear strengths shown in Figure 16 indicates faster strength development, which can be seen in the steeper slopes shown in Figure 15. Looking at the sample subjected to 20 FT cycles at T_{bf} = -20°C, a high initial strength development is seen until 2% axial strain, after which the strength quickly stabilizes. The smaller changes in shear strength approaching 7 FT cycles are indicative of an equilibrium value for the shear strength with increasing FT cycles. Figure 17 presents the shear strength at each applied freezing temperature for different axial strains. This is simply a different representation of Figure 16, including both the number of FT cycles and different applied freezing temperatures.

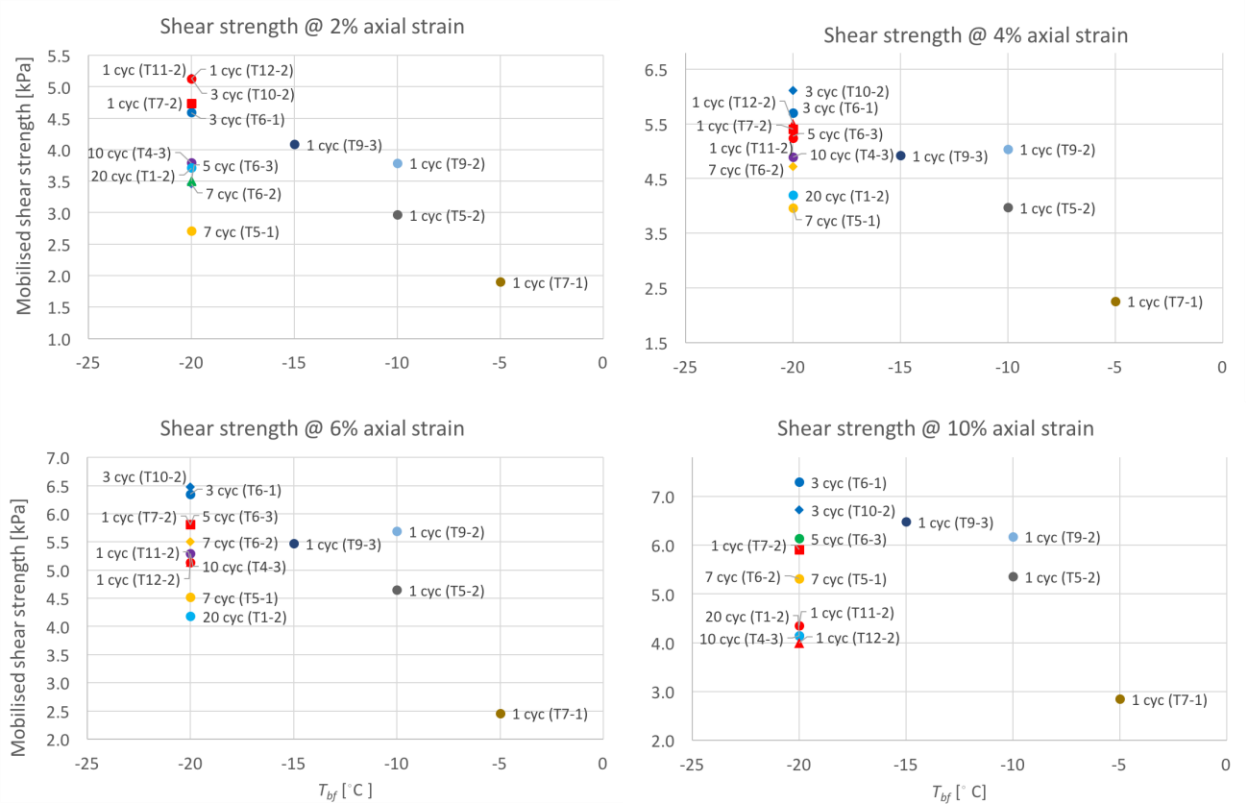

Figure 17: Mobilised shear strength vs. applied freezing temperature T_{bf} at different axial strains and number of FT cycles

Strain softening is seen after 1 freezing cycle (Figure 15). After 20 cycles, the shear strength stabilised and exhibited residual strength. For the intermediate cycles (3 through 10), strain hardening is seen. Mobilised shear strength at 2% axial strain for 3 freezing cycles was 19% larger than after 1 cycle, and at 10% axial strain the difference was 80%. After 3 cycles, the strength development began to decrease and approached an equilibrium strength after 7 cycles. The mobilised shear strengths for samples with T_{bf} = -20°C after 1 cycle (T7-2, T11-2, and T12-2) were smaller than expected, failing at lower axial strains than samples subjected to more cycles. Because the strength recovery between 1 and 3 FT cycles did not conform to expectations, additional tests were done. These tests confirmed the faster strength development, low mobilised strength, and failure at small axial strain under the boundary conditions used in this research.

6.2. Evolution of shear strength as a result of freezing rate

Samples with slower freezing rates were expected to have lower shear strengths. Several samples were prepared and tested at different applied freezing temperatures T_{bf}. Figure 18 shows the mobilised shear strength development for different freezing rates. As hypothesized, the shear strength increased with faster freezing rates. The largest difference occurred between T_{bf} = -5°C and -10°C, with T_{bf} = -15°C showing a slightly higher stiffness but similar strength to T_{bf} = -10°C. The variation between -10°C and -15°C can be explained by the non-homogenous nature of the Illite clay, and the values are effectively the same.

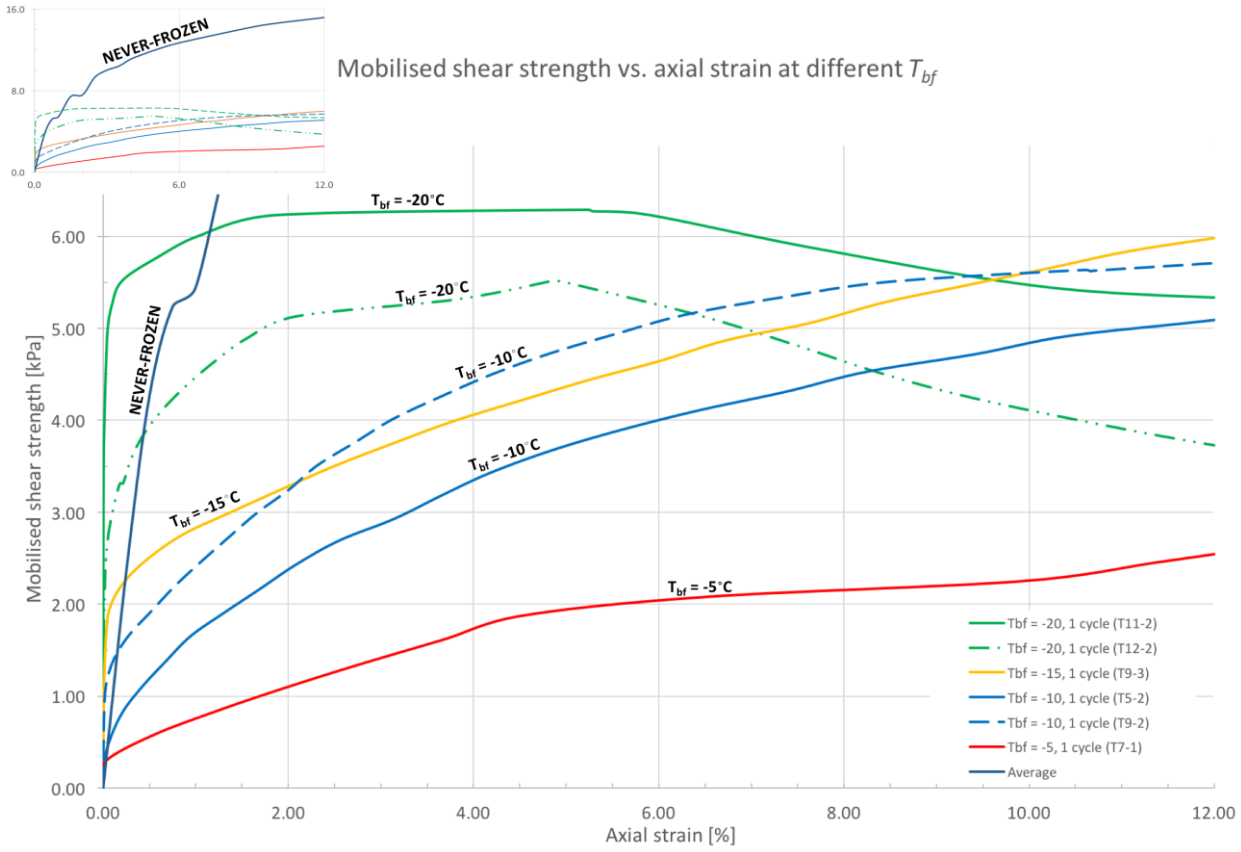

Figure 18: Mobilised shear strength vs. axial strain at different applied freezing temperatures after 1 FT cycle

After 1 freezing cycle, strain softening occurred at T_{bf} = -20°C. Samples frozen at lower freezing rates and warmer T_{bf} exhibited hardening.

6.3. Soil structure change with number of FT cycles

Horizontal ice lenses were expected to increase in size moving away from the freezing side. This was confirmed with the macro-CT scans, although it was difficult to identify horizontal lensing at faster freezing rates due to the small size of the ice lenses. The vertical cracks reduced in number and increased in size moving away from the freezing side. Figure 19 shows the cracking on the top of samples (furthest away from the applied temperature) subjected to an increasing number of FT cycles. Intact soil blocks occurred at fewer cycles, which can be seen by comparing the sample subjected to 1 cycle and the sample subjected to 3 cycles. The size of the soil blocks rapidly decreases with increasing FT cycles. Ice lenses decreased in size and filled the available pore space as the sample consolidated with increasing cycles, rather than allowing pore water to move through vertical cracks and displace soil for formation of large ice lenses. This indicates substantial degradation of the soil microstructure.

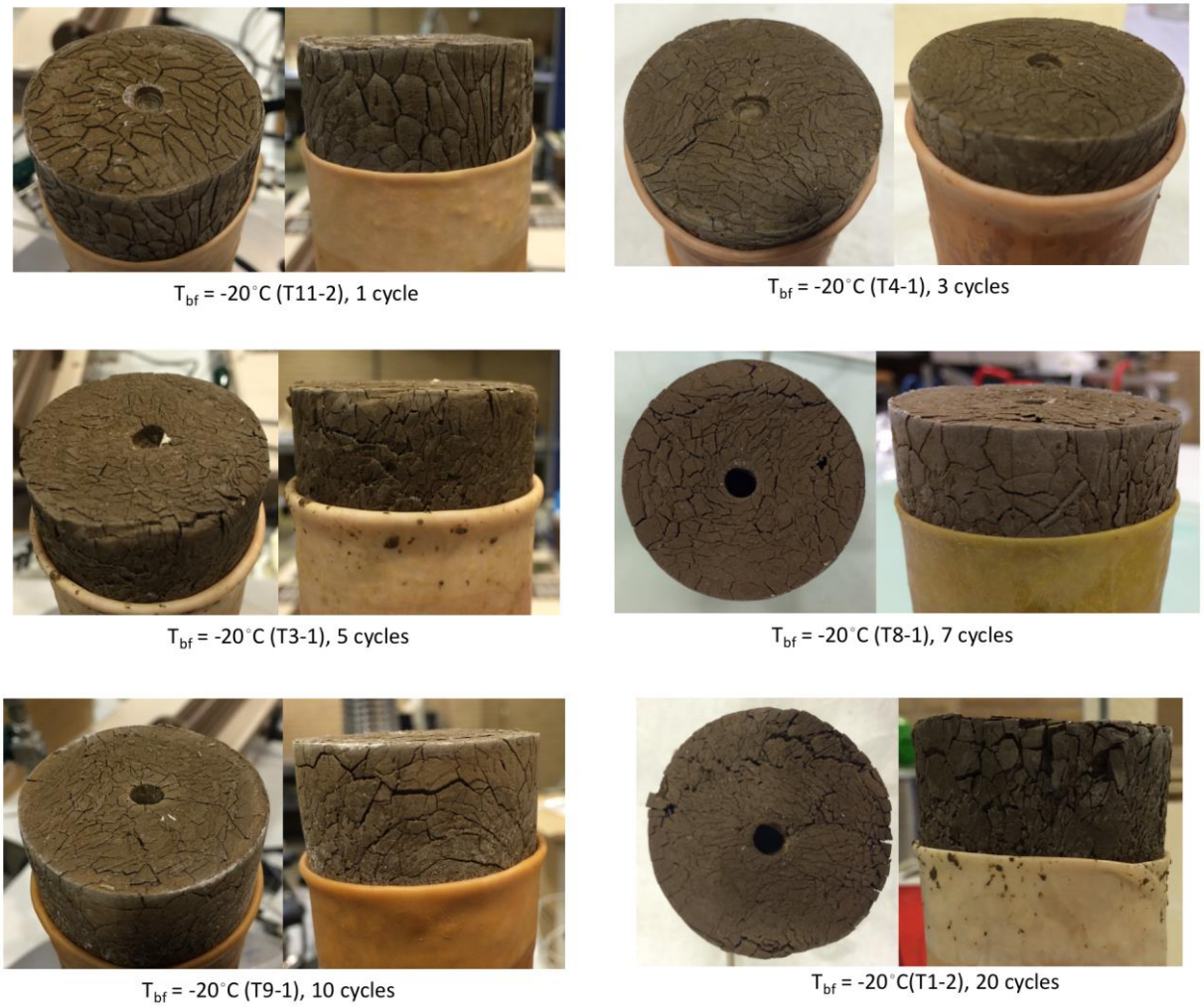

Figure 19: Cracking on frozen samples at T_{bf} = -20°C with different number of FT cycles

Figure 20 shows cracking at the top of a samples with T_{bf} = -20°C and increasing FT cycles, and CT scans with and without contrast on the ice lenses. The vertical cuts were taken through the centre of the sample and horizontal cross-sections at locations designed to show the ice lens and cracking development over the

height of the soil. The lens size decreased with increasing cycles in both the vertical and horizontal directions. Most changes in the soil structure occurred within the first 7 FT cycles, which coincided with the largest change in soil strength and stiffness. The frequency of very fine ice lenses near the freezing side increased, as did the thickness of the layer with very-fine ice lens distribution near the freezing surface. After 7 FT cycles, the ice distribution stabilised, as predicted in the conceptual models described in Chapter 3.

The decrease in the volume of bulk ice (ice lenses) with increasing FT cycles resulted in more, smaller ice lenses in both the vertical and horizontal directions. The more uniform ice distribution through the sample can be correlated to the reduction in shear strength seen in Figure 16. Recall that samples with slower freezing rates had lower shear strengths after 1 FT cycle. This suggests that the ice distribution through a sample directly influences the strength development over time. This is discussed in 6.5. Relationship between soil structure and failure location. The processed CT scans for all samples are located in A2.1. Macro-CT scans with different number of FT cycles.

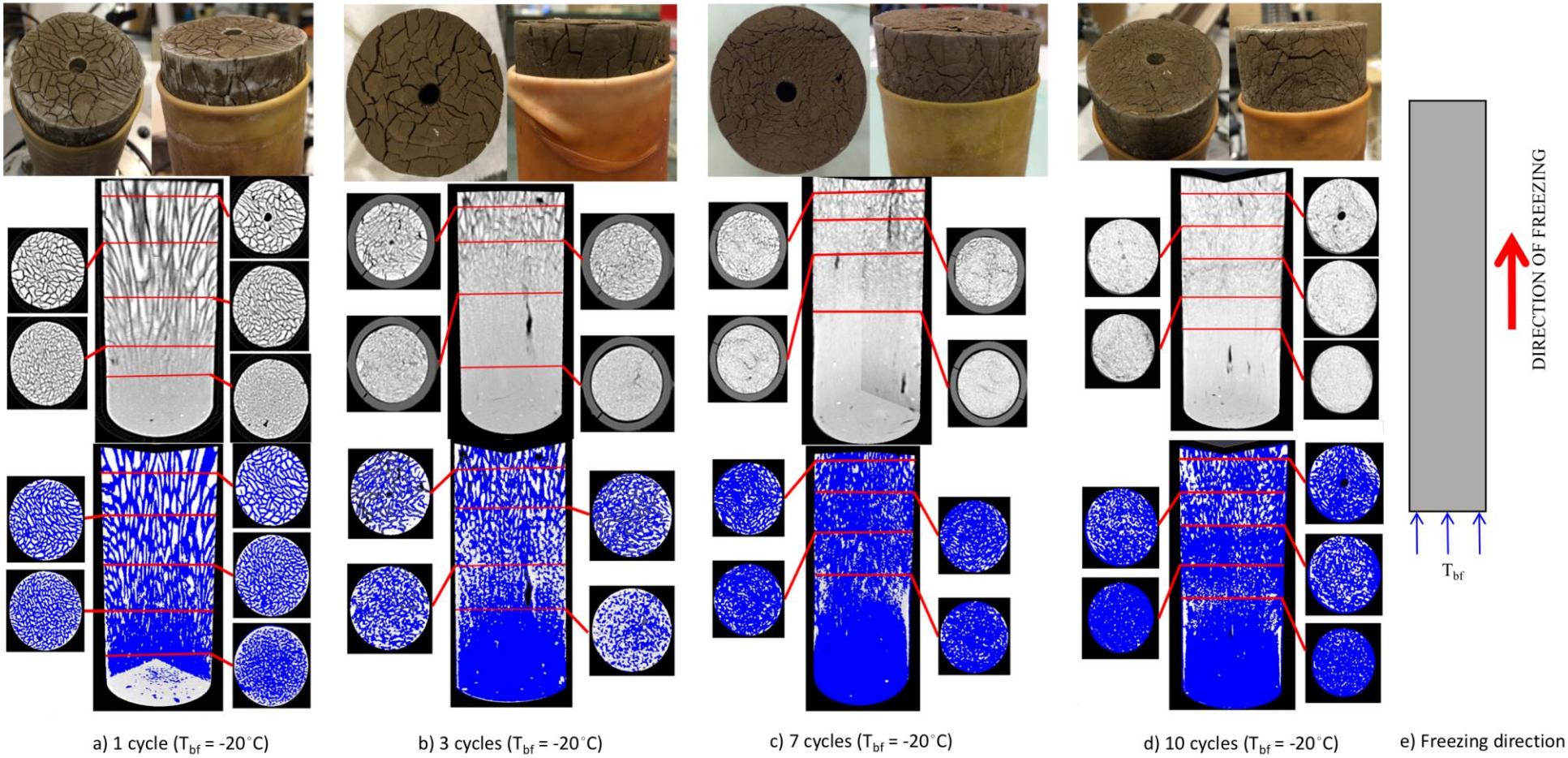

Figure 20: CT scans at increasing FT cycles for T_{bf} = -20°. TOP: Cracking on frozen sample before loading into triaxial cell; MIDDLE: CT scan of frozen sample. Pale grey is ice, white is soil, and black is voids; BOTTOM: Contrast CT showing ice distribution. White is solids, blue is ice, black is voids. (a) to (d) Increasing FT cycles: 1, 3, 7, 10. (e) Schematic showing freezing direction

6.4. Soil structure changes with freezing rate

The relationship between bulk ice and shear strength will be discussed in this section. Figure 21 shows cracking on the top and sides of samples on the 'free side' (farthest from the surface where temperature is applied) subjected to different freezing rates after 1 FT cycle. Both horizontal and vertical cracks increased in size moving away from the freezing surface. Cracking at the free side was documented prior to placing the frozen samples in the triaxial machine, e.g., the size of the cracks decreased with lower T_{bf}. Colder surface temperatures resulted in many, small cracks, while warmer surface temperatures resulted in larger vertical and horizontal cracking.

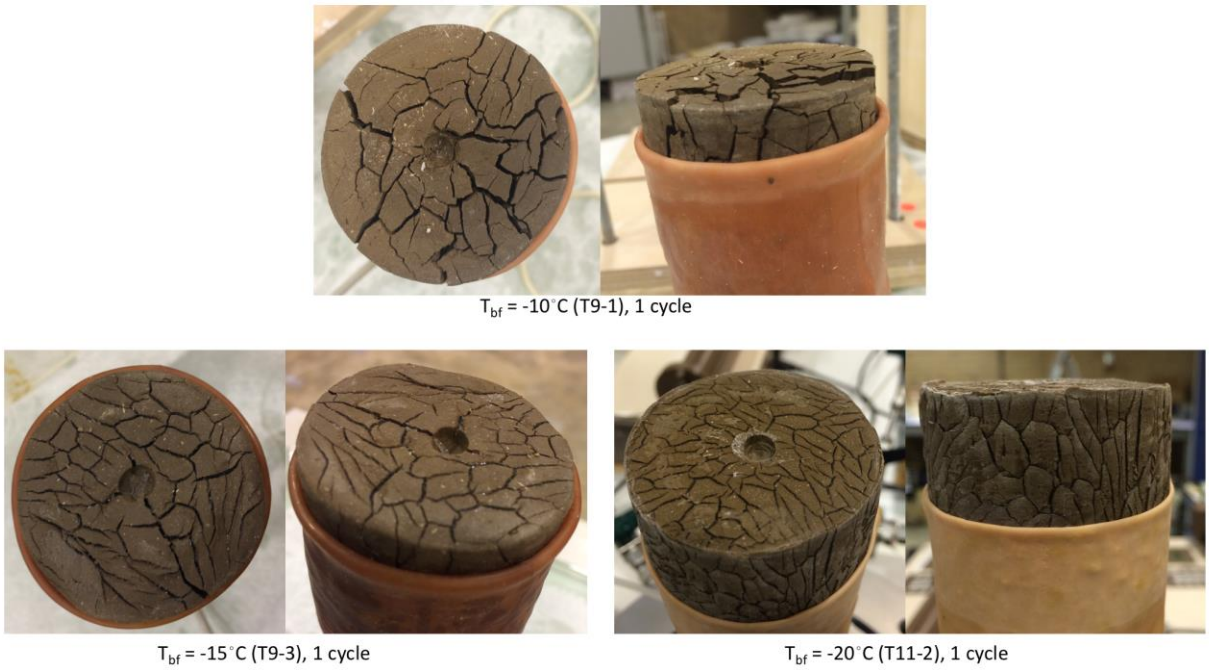

Figure 21: Cracking on frozen samples after 1 freezing cycle at different freezing rates

The ice lens development with different freezing rates is shown in Figure 22. The top image shows the cracking of the frozen sample at the free side of the sample, furthest from the applied surface temperature. The middle image is a vertical cut through the centre of the frozen sample from a CT scan, with cross sections showing the crack development over the height of the sample. In this image, the pale grey represents ice, voids are black, and white is soil. The bottom image is a contrast CT scan of the same cross sections with the ice highlighted in blue. Again, voids are shown in black and white represents solids.

Ice lenses were clearly visible from the macro-CT scans. The samples with slower freezing rates exhibited larger cracking and lensing in both the horizontal and vertical directions. With faster freezing rates, smaller cracks were observed. Both vertical and horizontal ice lenses increased in size moving away from the freezing side of the sample for all freezing rates. With lower T_{bf}, the ice lens and crack distribution through the sample became more uniform. This is attributed to the pore water freezing in place before moving through the sample via cryogenic suction, preventing large structural rearrangement due to formation of bulk ice.

Samples tested at T_{bf} = -5°C exhibited no ice lensing in the portion of the sample furthest from the applied surface temperature (see A2.2. Macro-CT scans after 1 FT cycle with different freezing rates). The ice lenses present in slowly frozen samples were significantly larger than those found with higher freezing rates. Vertical cracking ended shortly above the layer of horizontal ice lenses furthest from the freezing side. As expected from the literature review, slower freezing resulted in larger cracking in both the vertical and horizontal directions. The portion of the sample without ice lensing appears to have pulled away from the edges of the casing, creating a gap, which is indicative of a volume reduction due to consolidation. Recall that the material on the warm side of the freezing front experiences consolidation due to the cryogenic suction and hydrodynamic forces, which cause a reduction in hydraulic conductivity and ultimately causes the sample to reach its shrinkage limit. Because the amount of water available in a closed system is limited by the water content of the unfrozen soil, the lack of ice lensing after a certain depth can be explained by the movement of the available pore water towards the freezing front, resulting in the formation of larger and larger ice lenses until no water is available. Both samples with T_{bf} = -5°C showed similar ice lens development along the height of the sample, with reduced vertical lensing above the large ice lens.

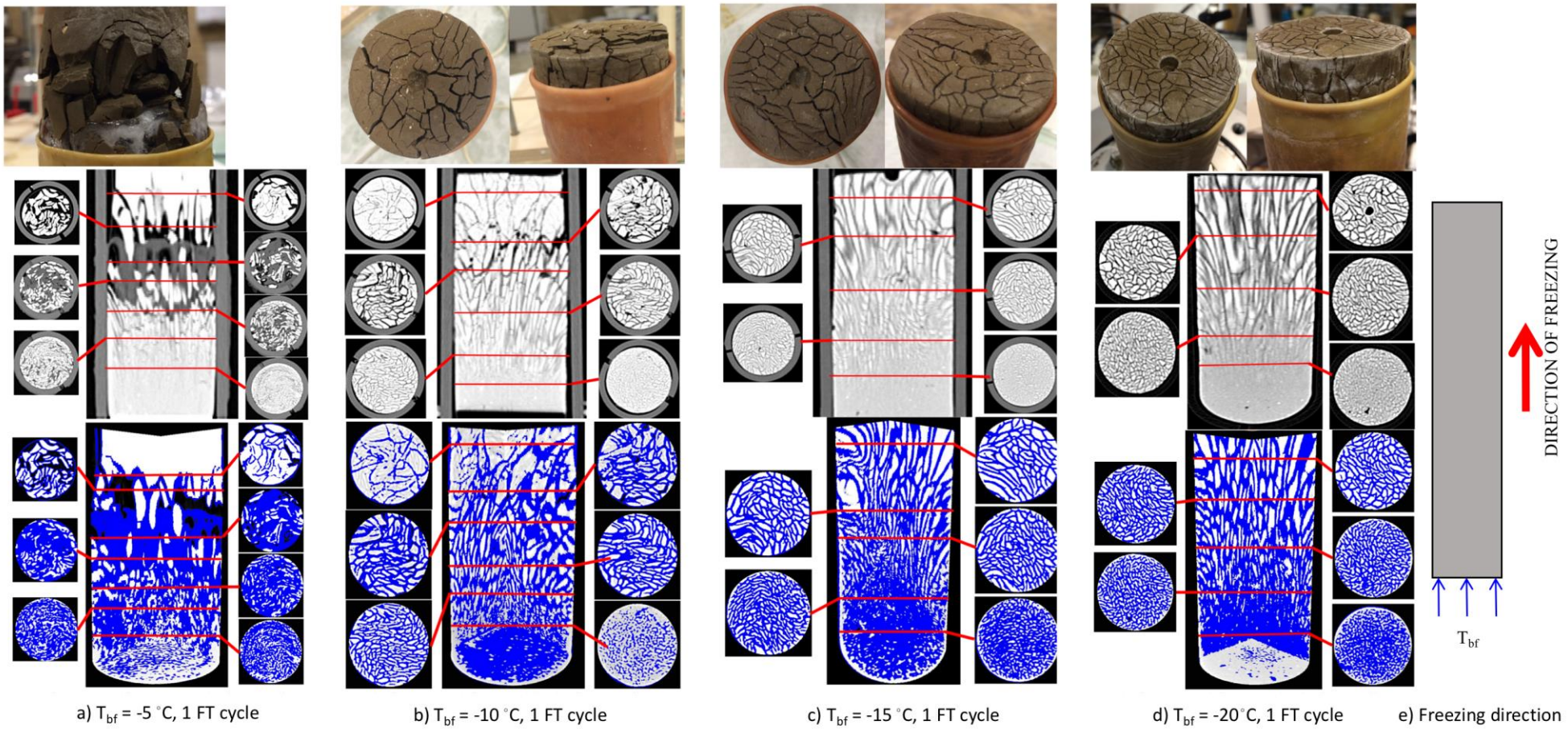

Figure 22: CT scans for different freezing rates at 1 FT cycle and T_{bf} = -20°C. TOP: Cracking on frozen sample before loading into triaxial cell; MIDDLE: CT scan of frozen sample. Pale grey is ice, white is soil, and black is voids; BOTTOM: Contrast CT showing ice distribution. White is solids, blue is ice, black is voids . (a) to (d) Different surface temperatures T_{bf} = -5, -10, -15, -20°C. (e) Schematic showing freezing direction

6.5. Relationship between soil structure and failure location

Samples subjected to faster freezing exhibited less bending than those subjected to slower freezing. Figure 23 shows the failure planes for samples at different freezing rates and 1 FT cycle, and for samples frozen at T_{bf} = -20°C with increasing FT cycles, relative to the plane of buckling and largest horizontal ice lens seen in the CT scans. After 1 FT cycle, the sample with T_{bf} = -20°C exhibited two clear bending planes, while the sample with T_{bf} = -5°C exhibited only one. The intermediate applied surface temperatures resulted in a primary failure plane, where most of the bending occurred, and a second failure plane with significantly less bending. The angle of internal friction appears to increase with increasing FT cycles, but because the samples exhibit significant bending, the actual failure location and angle could not be reliably determined.

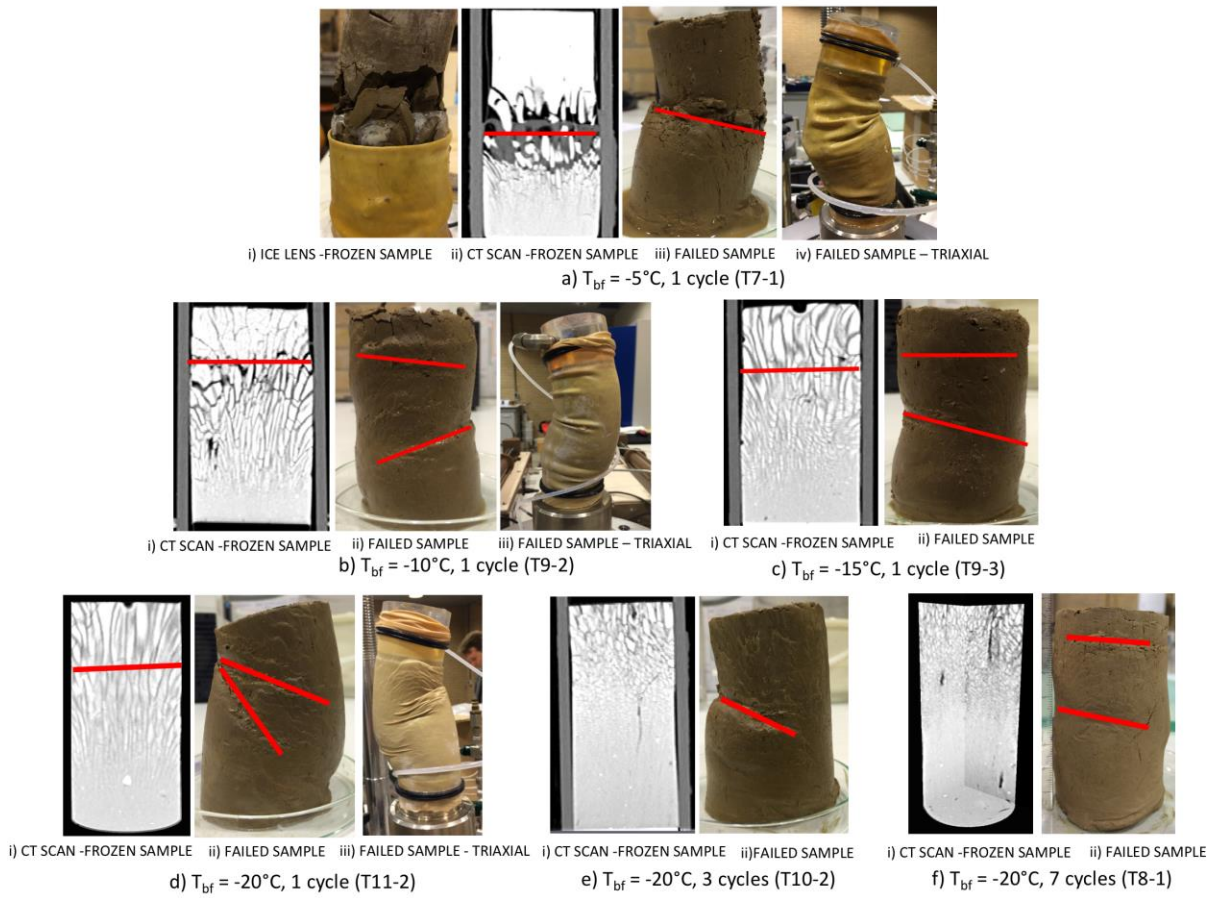

Figure 23: Location of largest horizontal ice lens from CT scans, failure location on thawed samples after triaxial test, and sample bending before removing from triaxial pedestal

The buckling in the failed samples increased as the freezing rate decreased. This is attributed to the thickness and location of a saturated zone created by thawing of the ice lenses, as discussed in 2.3. Changes in soil structure and ice lens formation. The largest continuous horizontal ice lens layer corresponded to a failure plane (Figure 23). When an ice lens formed parallel to the direction of freezing across the entire sample, both bending and shearing occurred along that plane. Larger copies of the CT scans with different freezing rates are located in A2.2. Macro-CT scans after 1 FT cycle with different freezing rates.

At T_{bf} = -20°C and 1 FT cycle, a thin horizontal ice lens was identified in the CT scans, corresponding to the location of the failure plane (Figure 23), as seen with lower freezing rates. After 1 FT cycle, no continuous horizontal ice layer was identified, although it is possible that a very thin lens that could not be identified on the CT scans was present. With increasing FT cycles at T_{bf} = -20°C, the failure plane location appeared to stabilise. This correlates to the occurrence of the equilibrium shear strength and lack of a continuous horizontal ice lens.

6.6. Change in stiffness

Changes in the slope of the failure plane were seen in the strength vs. strain plots (Figure 15, Figure 18). This suggests a relationship between the stiffness modulus and shear strength. This phenomenon was briefly investigated and is discussed in this section. 'Stiffness' refers to the tangent stiffness relating the initial shear strength development and axial strain. This was determined by calculating the slope of the tangent line from the origin of the strength vs. stress graphs, as illustrated in Figure 24.

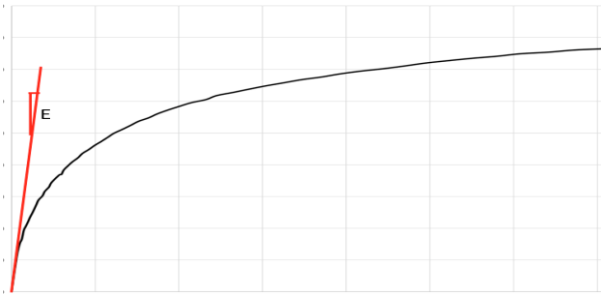

Figure 24: Schematic of stiffness calculation from strength vs. stress graphs

6.6.1. Change in stiffness with number of freeze-thaw cycles

Table 5 gives the tangent stiffness *E* of the samples as determined by the triaxial tests. These values are plotted in Figure 25 and Figure 26. After an initial increase at 1 FT cycle, the stiffness decreased with increasing FT cycles. An increase in stiffness occurred after 10 FT cycles at the same location the equilibrium shear strength (shown in Figure 16) was reached.

Table 5: Stiffness with number of freeze-thaw cycles and applied freezing temperatures

T_{bf} [°C]	# cycles	Sample name	Stiffness E [kPa]
Never frozen		average	1150.00
-20	1	T7-2	2308.33
-20	1	T11-2	2174.88
-20	1	T12-2	1838.89
-20	3	T6-1	417.72
-20	3	T10-2	229.46
-20	5	T6-4	143.73
-20	7	T5-1	125.85
-20	7	T6-2	152.87
-20	10	T4-3	458.33
-20	20	T1-2	642.31
-15	1	T9-3	527.66
-10	1	T5-2	144.70
-10	1	T9-2	369.23
-5	1	T7-1	41.41

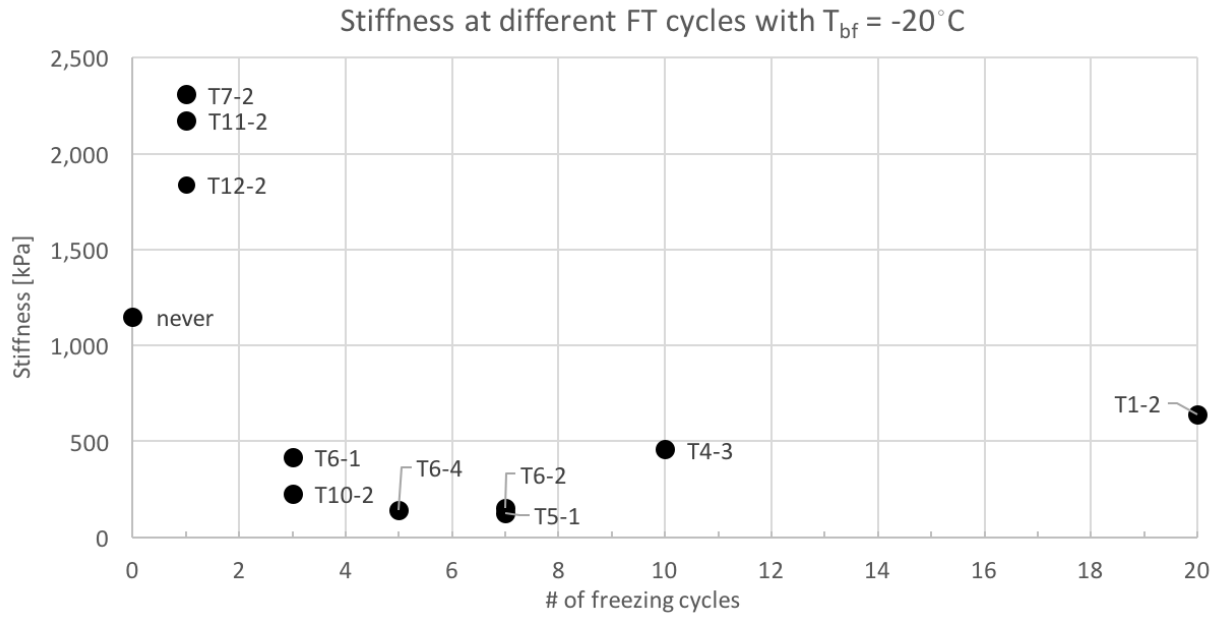

Figure 25: Soil stiffness with number of freeze-thaw cycles at T_{bf} = -20°C

Soil stiffness decreased over the period where most of the structural changes within the soil occurred. After 7 FT cycles, the ice lens distribution through the samples stabilized, and the stiffness increased. The data points for T_{bf} = -20°C after 1 FT cycle (samples T7-2, T11-2, and T12-2) have a much higher stiffness than never-frozen soil or samples subjected to more FT cycles, which agrees with the literature.

6.6.2. Change in stiffness at different freezing rates

Figure 26 shows the development of stiffness with applied freezing temperatures after 1 FT cycle. Faster freezing rates correspond to higher stiffness.

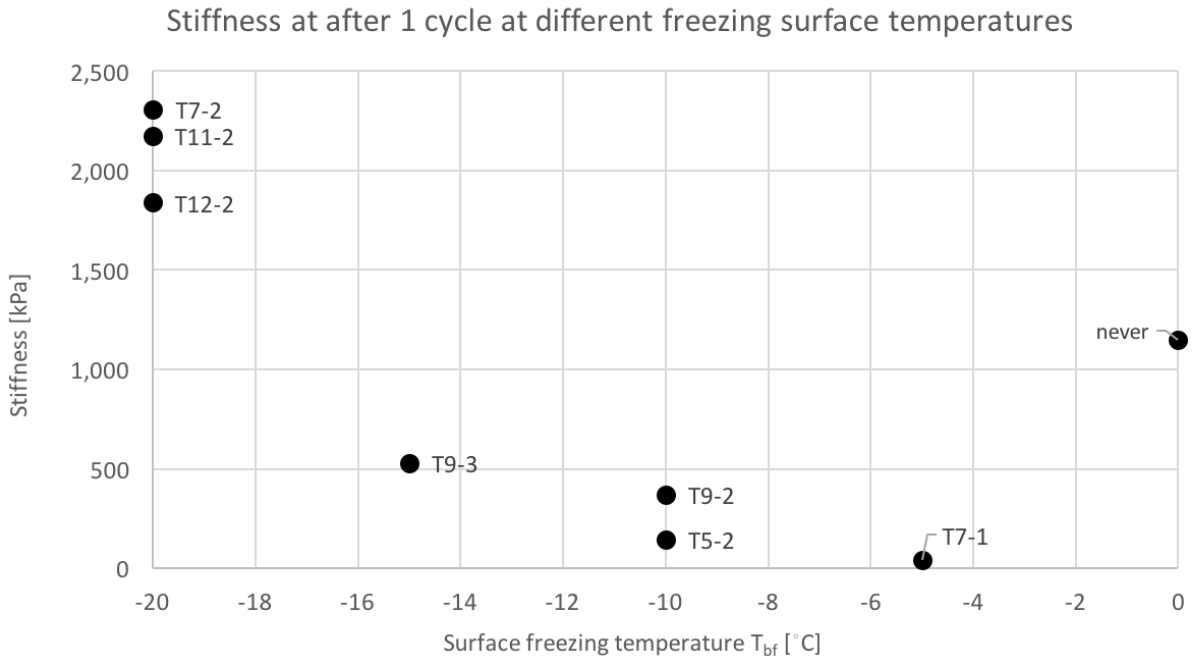

Figure 26: Soil stiffness for different applied freezing temperatures after 1 freeze-thaw cycle

Recall that samples with slower freezing rates had larger ice lenses and tended to fail along the plane of the thickest lenses in what was assumed to be a saturated layer. A slurry is less stiff than a soil with more uniform water distribution, such as what occurs at faster freezing rates. Thus, greater stiffness could be a reflection of the pore water and ice lens distribution within the soil, with more uniform distributions contributing to higher stiffness.

6.6.3. Relationship between stiffness and mobilised shear strength

The development of mobilised shear strength with increasing stiffness at different FT cycles is shown in Figure 27. It can be seen that the stiffness and shear strength decrease between 3 and 7 FT cycles. Between 10 and 20 cycles, the stiffness and the shear strength increase. At 1 FT cycle, the stiffness is larger than the never-frozen stiffness, and the shear strength is lower than 3 FT cycles. After 1 freezing cycle, the stiffness decreases, and between 3 and 7 FT cycles, the stiffness reduces with the shear strength. At 10 cycles, the stiffness increases, and the strength remains essentially the same. The mobilised shear strength after 1 and 10 FT cycles are approximately the same when the variability within the system is taken into account.

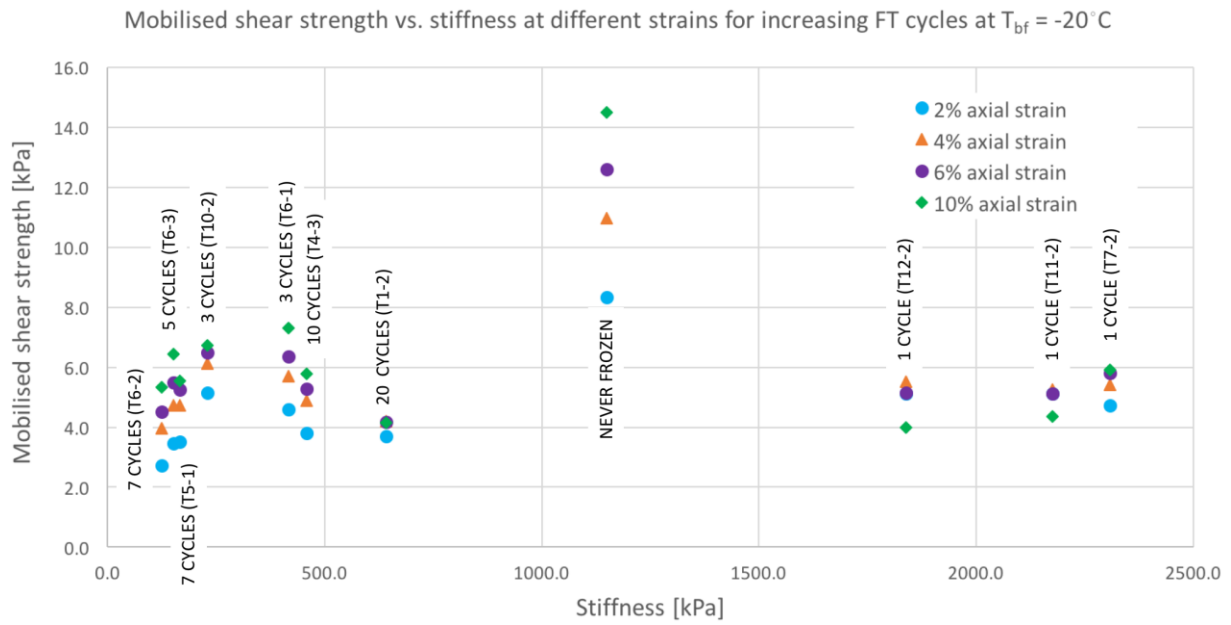

Figure 27: Mobilised shear strength vs. stiffness at different strains with increasing FT cycles at T_{bf} = -20°C

After 1 FT cycle, the stiffness and shear strength decreased as the thickness of the ice lenses increased. When no horizontal lensing was visible, the stiffness began to increase as the ice distribution became more uniform.

The development of stiffness and mobilised shear strength with different freezing rates after 1 FT cycle is shown in Figure 28. At applied surface temperatures warmer than -20°C, the stiffness was less than that of a never-frozen sample; only the samples with T_{bf} = -20°C were stiffer than the never-frozen material. The soil stiffness for all the freezing rates was expected to be larger than the never-frozen material. Instead, the lower shear strengths with increasing T_{bf} correspond to lower stiffness (with the exception of T_{bf} = -20°C) and larger ice lenses.

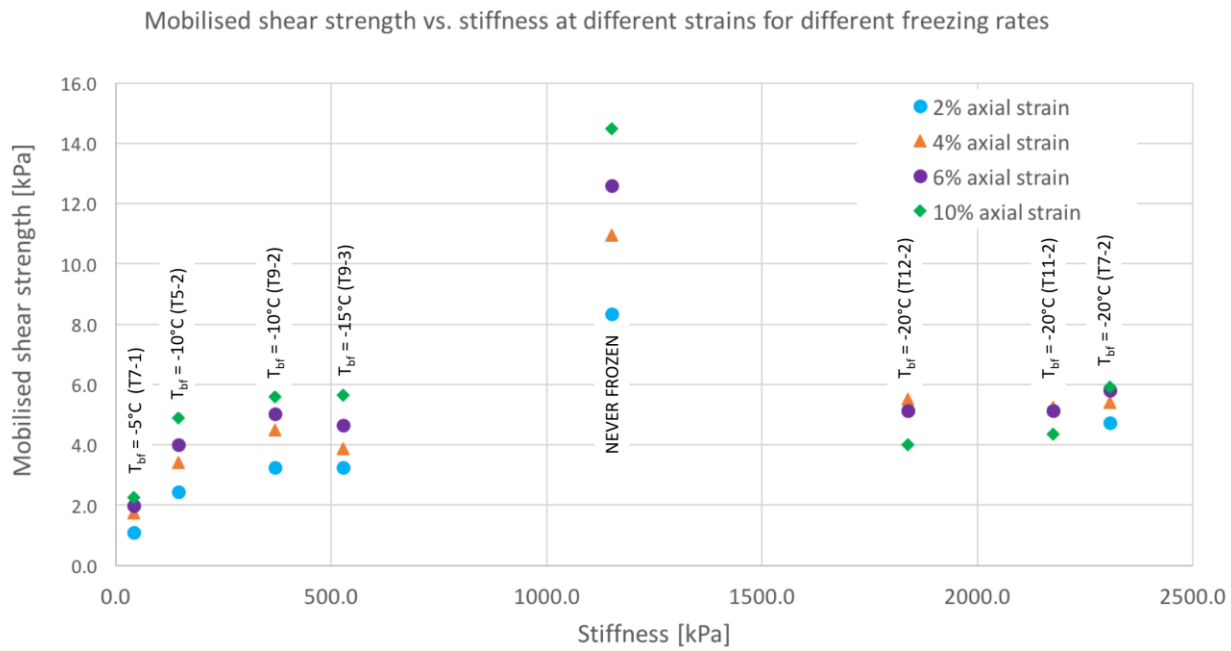

Figure 28: Mobilised shear strength vs. stiffness at different strains for 1 FT cycle at different freezing rates

6.7. Variability and reliability of results

Soil is inherently heterogeneous. Because of this, variation within the samples must be considered. Depending on the variation, the reliability of the results will be affected. Recognizing factors contributing to variability and error within the scope of this research allows for a better understanding of shear strength development of Illite clay.

6.7.1. Variability

An attempt was made to quantify the variability of the physical properties (water content, unit weights) and shear strength in the never-frozen samples. When samples were frozen, additional variability entered the system, as freezing is a non-homogenous process that is dependent on the void ratio and distribution of pore water in the soil. Variability was calculated as the variation from the mean of the soil property in question. Variations from the mean for different parameters are given in Table 6.

Table 6: Variation from the mean for different sample parameters

Parameter	Variation from the mean
Dry unit weight	4.2%
Water content	2.7%
Never-frozen shear strength	16.4%
Thawed sample shear strength	13.2%

The initial behaviour at 20 FT cycles, seen in Figure 15, matches that of 10 cycles, but a rapid transition to a residual shear strength (similar to that of 1 FT cycle) occurs. From this single 20 FT cycle test, the possible variation in residual shear strength cannot be reliability determined.

6.7.2. Reliability of results

Some inconsistency occurred in early tests due to the handling of the frozen samples prior to the triaxial tests. This was reduced in later tests as the handling procedure was improved, but these variations may have influenced the results. When possible, additional samples were prepared and tested at the same T_{bf} and number of cycles to confirm the results. Table 7 summarizes the samples where handling may have altered the results. A detailed description of all the samples can be found in A2.1. Summary of samples.

Table 7: Samples with conditions that may have resulted in unreliable results

Sample #	T_{bf} [°C]	# cycles	CT	Comments
T5-2	-10	1	X	Top ~ 15 mm not completely frozen.
T7-1	-5	1	X	While attempting to remove the top temperature probe, the sample separated at the plane between the frozen and unfrozen soil (where ice lens was visible). The structure of the sample was altered and the triaxial results should be disregarded. Top ~25 mm not frozen (from CT)
T7-2	-20	1		Some moisture loss from bottom of the sample during transfer to triaxial machine.
T8-1	-20	7	X	Peltier element/heat sink broke on 30/03/16. The sample was removed from unit #5 on 04/04/16 and wrapped in plastic in an attempt to keep water in the system. Sample was refrozen on 11/04 and placed in the freezer at 15:30 on 12/04. The sample was removed and tested at 19:15 on 14/04/15.
T9-2	-10	1		16/04/16: adjusted sample on copper plug to improve contact and get better cooling. Removed sample from box and completely took apart and reassembled. Process took ~5 min. Temperature control in the lab broke and appeared to be heating the top of the sample. Sample was placed into the freezer at 08:50 on 20/04/16 and removed on 22/04/16.
T12-2	-20	1		Peltier element broke ~1.5 hours after starting freezing cycle. Material not frozen, so left and moved from Unit 2 to Unit 1 and frozen the next day (stayed thawed in box for 17 hours).

As discussed in Section 5.2. Sample freeze and thaw time, the effectiveness of the insulation around the top and sides of the sample influenced the temperature readings at the top of the specimen. Temperature vs. time graphs were used to determine if a phase change occurred at the top of the sample.

Some samples were allowed to thaw overnight (up to 18 hours), while others were thawed for only 6.5 hours. It is possible that the difference in thawing time resulted in differences in the water distribution through the sample, with samples thawed overnight having a less pronounced slurry layer. However, the hydraulic conductivity of clay is fairly low, and the time required for the pore water to redistribute through the sample after thawing is not known. It is unlikely sufficient time was available for the water to drain back into the sample.

The true reliability of the results is difficult to determine, as there are insufficient data points to assess the error and develop a standard deviation. More tests are needed to draw conclusions about the reliability and variation within the samples, especially between 1 and 3 FT cycles, where the results were not as expected based on the literature review and models.

6.7.3. Problems with apparatus

Problems with the lab setup centred around inadequate cooling of the Peltier elements, resulting in overheating and loss of the elements. Maintaining good contact between the heat sink, Peltier element, and copper plug was critical for reaching low temperatures, and the silica heat transfer compound had to be applied evenly. For long-running tests, the heat transfer compound needed to be reapplied. The research described in this thesis required continuous operation of the elements, and thus placed more demand on the heat sinks than the work done by van den Bosch [9] using the same apparatus. At colder applied temperatures (T_{bf}), the heat sinks were required to remove more heat from the Peltier element, causing them to operate near capacity. It is thought that this high, continuous demand on the heat sinks accelerated the degradation of the circulation tubes, resulting in small leaks and diminished cooling capacity. Once the cooling fluid began leaking out of the system, the ability of the heat sinks to cool the Peltier elements rapidly decreased, ultimately resulting in failure of the heat sinks.

Numerous attempts were made to repair and/or upgrade the freezing units. The Nepton 280L extra-large 280 mm radiator, duel JetFlo 140 fans liquid CPU coolers used in the original setup are no longer available, and several alternative heat sinks were assembled. However, none were able to cool the Peltier elements enough that they could reach -20°C. Problems with the heat sinks persisted throughout the duration of the laboratory testing. By the end of testing, only one unit was capable of reaching -20°C. Attempts to replace the cooling fluid and repair the circulation tubes and Nepton heat sinks were unsuccessful.

6.9. Summary of results

This chapter described the results of the UU triaxial tests and macro-CT scans for samples with different number of FT cycles and freezing rates. The variation present in the results and the influence on the reliability were quantified by accounting for the non-homogenous nature of the soil and freezing process using the never-frozen samples and results from multiple tests with the same set of conditions. Problems encountered with the freezing apparatus were also discussed.

The results of this research are summarized below.

1. Illite clay exposed to freezing showed a significant reduction of shear strength compared to never frozen samples;

2. After 1 freezing cycle at T_{bf} = -20°C, the mobilised shear strength was reached at a low axial strain and was weaker than expected based on the literature. Strain softening occurred at 1 FT cycle, and residual strength was seen at 20 FT cycles. The intermediate cycles exhibited strain hardening;

3. Strength recovery was seen between 1 and 3 FT cycles. The peak mobilised shear strength after 1 freezing cycle was significantly smaller than after 3 cycles. Between 3 and 20 FT cycles, the shear strength decreased, and approached an equilibrium value after 7 cycles;

4. Slower freezing resulted in lower shear strengths. There was a significant difference between applied freezing temperatures of -5°C and -10°C, while the difference between -10°C and -15°C

was quite small. This suggests that the surface temperature influence on shear strength is most pronounced when T_{bf} is warmer than -10°C and large ice lenses are present;

5. Most of the changes in soil structure and ice lens formation occurred within the first 7 FT cycles. After 7 cycles, the ice distribution became more uniform, with many fine lenses forming over the height of the sample. The increase in uniform ice distribution contributed to the reduction in shear strength;

6. Slower freezing rates resulted in larger ice lenses. Fewer ice lenses formed with slower freezing rates, but were significantly larger than ice lenses formed at faster freezing rates;

7. After an initial increase in stiffness at 1 FT cycle when T_{bf} = -20°C, the stiffness and shear strength decreased as the size of the ice lenses increased. The stiffness increased when no continuous horizontal ice lens was visible;

8. The failure location of the thawed samples occurred at the plane with the largest horizontal ice lens. This was attributed to the formation of a weak, saturated layer when the sample is completely.

7. Discussion

The results of this research are discussed in this chapter. Findings that are inconsistent with the literature review are elaborated on and explanations are offered. Scale effects are also described.

7.1. Strength behaviour

While long-term strength recovery may occur after many FT cycles in drained conditions, sufficient consolidation to induce strength recovery was not expected due to the lack of overburden pressure and undrained conditions. In these experiments, the soil reached an equilibrium value with increasing FT cycles. Most of the strength and structural changes occurred during the first freezing cycle. After the first FT cycle, the space between the soil particles reduced during thawing, resulting in slight consolidation.

The presence of strain hardening and residual strength indicates that the material could carry a higher load before failing. The strain softening seen at 1 cycle (Figure 15) suggests that a significant amount of damage to the soil microstructure occurred after the first freezing cycle. This was attributed to the formation of clay blocks as cracks formed during freezing. These soil blocks sheared, then failed along a saturated (water-filled) slurry layer that formed between the blocks. This phenomenon was not identified in the existing literature, but construction practices in cold regions, such as Alaska, often involve re-levelling a foundation after its first winter.

Between 3 and 7 FT cycles, the shear strength development was in agreement with the assertion in the literature that most changes in frost susceptible soils occur within the first 7 FT cycles. The samples exhibited strain hardening until 20 FT cycles, where residual strength was observed. However, a significantly smaller than expected mobilised strength was seen after 1 FT cycle, which peaked at a low mobilised shear strength (approximately equal to the equilibrium shear strength after 7 FT cycles), low axial strain and exhibited strain softening. The strength recovery between 1 and 3 FT cycles was not identified in the existing literature.

The formation of large, continuous horizontal ice lenses with slower freezing rates coincided with a reduction in shear strength. Surface freezing temperatures approaching 0°C resulted in a weaker soil. Based on this trend, locally freezing clay as a stabilization measure in construction would best be done using colder temperatures to create more rapid freezing.

7.2. Ice lens formation

Samples failed along the plane of the largest continuous horizontal ice lens, with thicker lenses resulting in weaker, less stiff soil. This was attributed to the discontinuity within the soil structure at that plane and the presence of water that has not re-distributed through the sample. A weak slurry layer formed along the plane of the largest horizontal ice lens, resulting in a lower shear strength. Continuous horizontal lenses are either very small or not present with increasing FT cycles, and there is a significant change in soil structure between 1 and 3 cycles. After 1 FT cycle, an ice lens was visible and a slurry layer formed, while after 3 cycles, a higher shear strength occurred but no ice lens was seen. Samples with larger ice lenses had lower

shear strengths and stiffness, and the lack of a continuous ice lens after 3 FT cycles could explain the strength recovery.

Under in-situ conditions, described in 3.1. Model 1: Undisturbed conditions, water drains into the soil after the ice lenses melt, driven by pressures within the soil (overburden pressure) and gravity, which would reduce the thickness and time that a slurry layer would be present. While the pressure differential within the soil will redistribute the pore water under in-situ conditions, this process takes time. Because no overburden pressure was applied in this research, and the samples were thawed for a relatively short period of time, minimal re-distribution of pore water occurred.

The existing literature indicated that clay samples are prone to shearing at the interface between frozen and unfrozen material. This was supported by sample T7-1, with T_{bf} = -5°C. Although the surface freezing temperature was applied for 22 days, the top 25 mm did not exhibit any lensing. Whether or not the sample was completely frozen is uncertain, as the top temperature probe at the top of the sample became increasingly inaccurate over time, but appeared to be frozen into the sample. During attempts to remove the probe, the top (ice-free) part of the sample separated. The material was placed back on the sample to the best extent possible, but some material rearrangement occurred. The ice lenses and intact blocks of material could be clearly viewed with the naked eye (Figure 23). The lack of ice lensing in the upper portion of the sample (furthest from the freezing surface) can be explained by the movement of available water in the unfrozen part of the sample via cryogenic suction until the shrinkage limit of the soil was reached [3].

The equilibrium shear strength reached at T_{bf} < -10°C coincides with fewer changes in the soil structure. The difference in the ice lens formation between T_{bf} = -15°C and T_{bf} = -20°C is significantly less than the difference in ice lenses between T_{bf} = -5°C and -10°C (Figure 22). The increasingly uniform ice distribution through the sample with increasing FT cycles is in agreement with the findings of Ghazavi and Roustaei [32], Arenson [5], and Konrad [37].

7.2.1. Crack formation

Cracks formed in the horizontal and vertical directions in the frozen soil due to movement of pore water via cryogenic suction. Cracks are attributed to pressures from the volumetric expansion of ice overcoming the overburden pressure and separation strength of the soil. Differences in ice distribution can be attributed to the speed of the freezing front, as slower freezing allows more water to move through the soil. This explains the increasing size of the cracks moving away from the freezing side.

7.2.2. Failure planes

Failure occurred along the plane of the thickest continuous ice lens, as seen in samples with T_{bf} = -5°C (T7-2 and T10-1) (Figure 23). The relationship between ice lens thickness and failure plane location can be explained by the formation of a saturated zone in the thawed soil, as described in 2.4. Thaw weakening.

7.3. Stiffness

The stiffness after 1 FT cycle at T_{bf} = -20°C is almost double that of the never-frozen soil. This suggests significant rearrangement of the soil structure during the first FT cycle, so that it reaches its maximum mobilised strength before samples frozen at lower freezing rates. The increased stiffness after 1 FT cycle

may be due to soil fragments consolidating locally during the first freezing cycle at a high freezing rate. This phenomenon has been documented by Volokhov [24], Simonsen and Isacsson [16], Ghazavi and Roustaei [32], and Qi [19]. With increasing FT cycles, the microstructure is rapidly destroyed and the apparent cohesion of the entire sample decreased, resulting in lower stiffness and loss of shear strength.

As the freezing rate decreases, local consolidation is offset by the formation of large ice lenses that act as failure planes. The decreasing stiffness with increasing T_{bf}, seen in Figure 26, supports the design considerations suggested by GHSPA [38]. This change in stiffness can be attributed to a reduction in the void ratio as the soil consolidates due to cryogenic suction. The relationship between a softer (less stiff) soil and lower shear strength with decreasing freezing rates (Figure 26) is not in agreement with the findings of Ghazavi and Roustaei [32], who documented an increase in stiffness with T_{bf} approaching 0°C. This difference may be due in part to the very low confining pressures used in their research (between 30 and 90 kPa), as shear strength increases with confining pressures. Instead, lower shear strengths are seen with slower freezing rates, which result in lower stiffness. This is attributed to the influence of the slurry layer that forms along the plane of the largest horizontal ice lens.

7.4. Scale effects

The tests done for this research are not truly element tests and are subject to scale effects. As seen in the CT scans and existing literature, formation of ice lenses is highly depth dependent, and is a function of temperature gradient, soil properties, and availability of water. To capture changes in the soil structure and ice distribution, large samples are needed. The sample size used in this research was designed to be small enough that the freezing front would penetrate the entire sample and freeze all the pore water. The time required for the entire sample to freeze or temperature at the top of sample to stabilise varied with applied surface temperature. Colder temperatures have faster equilibrium times and deeper freezing front penetration. The lack of external water supply resulted in some parts of the soil exhibiting no ice lensing.

While the samples were saturated before the first freezing cycle, the movement of pore water during the freezing process resulted in a partially saturated material further from the freezing side. Triaxial tests were done on the samples within 12 hours of completely thawing, and it is thought that the pore water built up in the slurry layers did not redistribute through the sample.

Placing excess water on top of the sample would keep the material fully saturated and allow more extensive ice lens formation. The rate of freezing varies with depth, due to transience of the temperature boundary (in-situ) and heat losses from the sample edges (in the laboratory).

7.5. Summary of discussion

While the ice lens development seen in samples subjected to more than 3 FT cycles is in agreement with the literature, the strength recovery between 1 and 3 cycles was not identified in existing literature. This strength recovery can be attributed to the presence of a continuous horizontal ice lens across the width of the sample after 1 freezing cycle, which is no longer present at 3 cycles. Horizontal ice lenses created a weak, saturated failure plane. As ice distribution became increasingly uniform over the height of the samples, the mobilised shear strength decreased, in agreement with the literature review and models

developed in Chapter 3. With thicker ice lenses, the stiffness and shear strength decreased. This is attributed to the thickness of the slurry layer along the plane of the largest horizontal ice lens causing a local decrease in cohesion. The increase in soil stiffness after 1 FT cycle at a high freezing rate may be due to consolidation after the first cycle and lack of a slurry layer. The samples became partially saturated during freezing due to cryogenic suction pulling water towards the ice lenses, and are likely too short to be truly representative of in-situ conditions.

8. Conclusions and recommendations

The primary objective of this thesis was to evaluate the research question '*What is the influence of cyclic freezing and different ground temperatures on the shear strength of an Illite clay?'*. This was done by investigating the following sub-questions:

1. *What is the influence of repeated freeze-thaw (FT) cycles on shear strength?*

2. *What is the influence of surface temperature on shear strength after 1 FT cycle?*

3. *What is the influence of freezing rate and number of FT cycles on grain structure and ice lens formation?*

This section presents the final conclusions of this research, suggests improvements to the testing setup, and provides recommendations for future work.

8.1. Influence of freeze-thaw cycles on shear strength

It was predicted that the shear strength of the clay would decrease with increasing FT cycles, with most of the changes occurring within the first 7 cycles. The conclusions based on the results of this research are as follows:

1. The shear strength of Illite clay was significantly reduced after freezing;

2. Samples of clay exposed to 1 FT cycle reached their maximum mobilised shear strength at low axial strain and exhibited strain softening. Subsequent cycles exhibited strain hardening until reaching 20 cycles, which exhibited residual strength;

3. The mobilised shear strength at 3 FT cycles was larger than at 1 cycle. After the strength recovery between 1 and 3 cycles, the shear strength began to decrease, stabilising after 7 cycles (Figure 15). The strength recovery between 1 and 3 cycles was not identified in existing literature. This strength recovery was attributed to changes in the ice distribution through the sample and the formation of a slurry layer. More research is necessary to confirm this;

4. The soil stiffness after 1 freezing cycle was higher than for subsequent cycles. Soil stiffness decreased with increasing FT cycles until it reached 7 cycles. The dramatic reduction in stiffness between 1 and 3 FT cycles coincides with strength recovery and is attributed to local consolidation of soil blocks after 1 FT cycle and the presence of a slurry layer. The jump in stiffness between 7 and 10 cycles occurred at the equilibrium value of the shear strength and occurrence of uniform ice distribution.

8.2. Influence of freezing rate on shear strength

It was hypothesised that the shear strength would increase at colder applied surface temperatures and decrease at warmer temperatures. The influence of freezing rate on the soil is described below:

1. The applied freezing temperature at the surface of a sample had a significant impact on the shear strength. Slower freezing rates resulted in a lower shear strength, while faster freezing resulted in a higher shear strength (Figure 18);

2. The largest change in shear strength with different freezing rates occurred between T_{bf} = -5°C and T_{bf} = -10°C (Figure 18). At $T_{bf} \leq$ -10°C, the difference between the mobilised shear strengths reduced, suggesting that as freezing rates increase, the influence on the shear strength reduces as the ice distribution stabilises;

3. The stiffness of the soil increased with the freezing rate. Smaller mobilised shear strengths at lower freezing rates corresponded to less stiff soil. The decrease in stiffness was attributed to the influence of local consolidation being offset by the formation of large ice lenses.

8.3. Influence of FT cycles and freezing rate on soil structure and ice lens formation

It was predicted that the size of ice lenses would decrease as the freezing rate increased. Larger ice lenses were expected moving away from the freezing side, and lower shear strength was anticipated with larger ice lenses.

8.3.1. Influence of FT cycles on ice lens formation and shear strength

Freeze-thaw cycles result in significant structural rearrangement in the soil. Descriptions of the ice lens formation and their influence on the soil are as follows:

1. Smaller ice lenses formed as the freezing rate and number of FT cycles increased;

2. Smaller ice lenses formed near the freezing side. The horizontal ice lenses increased in size moving away from the surface and vertical cracks became larger. The presence of more, smaller ice lenses resulted in a lower shear strength;

3. Soil stiffness and mobilised shear strength decreased between 3 and 7 FT cycles. When a continuous horizontal ice lens was no longer visible, and ice distribution through the sample became uniform, the stiffness increased;

4. Strength recovery was seen between 1 and 3 FT cycles. This was attributed to the lack of continuous horizontal lensing as the ice distribution through the soil became more uniform with increasing FT cycles.

8.3.2. Influence of freezing rate on ice lens formation and shear strength

The freezing rate influenced the size and location of the ice lenses. The impacts of these changes are as follows:

1. The relative density of the clay is lower at slower freezing rates, and formation of ice lenses parallel to the direction of freezing results in planes that are weaker and fail more readily. Due to cryogenic suction, slower freezing resulted in larger ice lenses and increased cracking, which translated to lower shear strength;

2. The decreasing size of the ice lenses with increased freezing rate is in agreement with the findings of previous research. The slower freezing front progression allowed pore water to move across the 0° isotherm, resulting in larger ice lenses and cracks moving away from the freezing surface;

3. With increasing ice lens thickness, the stiffness of the soil decreased. This was due to the reduced stiffness along the slurry layer formed after thawing of horizontal ice lenses.

8.3.3. Relationship between ice lenses and failure location

The location of the failure planes was affected by the number of FT cycles and the freezing rate. The conclusions on the relationship between these factors and the failure location of the thawed soil are described below.

1. The samples failed along the plane of the largest continuous horizontal ice lens;

2. Faster freezing rates resulted in smaller horizontal ice lens layers; below T_{bf} = -15°C, very little horizontal lensing was visible. A small horizontal ice lens was seen at 1 FT cycle at T_{bf} = -20°C, and was no longer visible at 3 FT cycles. Samples with lower freezing rates exhibited increased cryogenic suction and movement of pore water towards the freezing front. This resulted in larger ice lenses which, upon thawing, created a saturated slurry layer that acted as the weakest plane within the sample.

8.4. Test equipment and methods

Conclusions regarding the implementation of the physical model described in Chapter 4 are discussed in this section. This has been broken into 3 components: sample preparation and handling, freezing units, and suggested improvements.

8.4.1. Sample preparation

The sample preparation in this research resulted in acceptably consistent samples. Variation in the water content was assumed to account for many of the variations in ice lensing and shear strength between samples tested under the same conditions. The density of the samples influenced the freezing and thawing time of the samples, as denser soils with lower permeability take longer to freeze.

8.4.2. Handling

The first 5 samples tested in this research may have been affected by the method of transferring the frozen sample from the freezing unit to the triaxial machine. Several samples exhibited melting at the base before being placed in the triaxial machine, resulting in some water and material loss. A consistent method of removing the samples from the copper plug and transferring to the triaxial machine without material loss or thawing at the bottom was developed after the first 5 tests. The revised process involved removing the sample from the sample box and carefully cutting at the base where it contacted the copper plug until it lifted off. The frozen sample was then quickly transferred to the triaxial pedestal and secured with gaskets to ensure no moisture loss from the bottom of the sample during thawing.

8.4.3. Freezing units

Inconsistencies and failure of the freezing units were a constant source of delay and loss of samples during this research. Problems arose from the inability of the heat sinks to prevent the hot side of the Peltier elements from overheating. This was likely caused by small leaks in the cooling fluid circulation tubes and diminishing cooling capacity. Some samples were compromised and discarded when the Peltier elements overheated and applied heating temperatures in excess of 80°C to the samples.

8.4.4. Improvements for future research

Suggested improvements for the freezing units and sample preparation are as follows:

1. Prepare the samples using a dry clay powder to better control the water content and unit weight;

2. Replace the liquid cooled heat sinks every 1.5 to 2 years, depending on usage, to ensure they can keep up with the demand from the Peltier elements. A heat sink with larger capacity should also be considered;

3. Improve the thermal envelope of the sample container by creating a continuous insulated box using insulation with a higher R-value. This would eliminate some of the seams/joints present in the current sample container. The thermal envelope of the insulation on the sides and top of sample is not perfect. There is some heat loss to the air, notably from the top of the sample;

4. Modify the freezing apparatus so temperature is applied at the top of the sample, rather than the bottom, to address the potential build-up of water above the bottom of the sample where vertical cracking is very small, and additional time needed for the pore water to drain into the sample. This may change the location of the failure planes and size of the ice lenses with increasing FT cycles.

8.5. Design applications

This research can be applied to engineering design in areas with seasonally frozen soils or where construction and implementation of thermo-active structures on frozen soils are planned. Based on the literature review and results of the tests described in this thesis, the following aspects are worthy of consideration:

1. The strength recovery between 1 and 3 FT cycles (attributed to formation of a slurry layer) suggests that foundation elements are best constructed and allowed to experience at least one complete FT cycle before applying loads;

2. The undrained shear strength after 1 FT cycle should be used as a conservative design value, as application of surface loads will accelerate consolidation and result in a stronger soil in the long-term;

3. Sufficient time should be allowed after the soil thaws for the pore water in the slurry layers to dissipate (drain) back in to the soil before applying a load. Alternatively, installing vertical drainage to accelerate water movement through the soil will reduce the influence of thaw weakening;

4. If ground is frozen for stabilization or construction purposes, a higher freezing rate will result in smaller ice lenses and fewer changes to the soil structure. This translates to a higher shear strength in soil frozen rapidly than a soil frozen with an applied surface temperature above -10°C.

7.6. Further research (recommendations)

The literature review and results of this thesis have identified several gaps in the current body of knowledge regarding the influence of freeze-thaw cycles and freezing rate on shear strength of clay. This section suggests further study based on this research.

1. The development of strength recovery between 1 and 3 FT cycles should be investigated under drained and undrained conditions. The influence of different thawing times and redistribution of pore water into the sample may change or eliminate the strength recovery seen in this research;

2. The influence of drained conditions on the shear strength of frost susceptible soil with different number of FT cycles and freezing rates should be investigated. Providing water on the free side of the sample to simulate groundwater will keep the material saturated and allow formation of ice lenses through the entire sample. Furthermore, drained tests can be used to determine physical properties, including the angle of internal friction and cohesion. The use of larger sample sizes will reduce the scale effects;

3. Because unconsolidated undrained (UU) triaxial tests are not truly representative of field conditions, samples should be tested after at least 1 consolidation step, representing construction of a foundation or structure, to obtain a more accurate view of the influence of overburden pressure. The author believes that the application of loads at the surface will result in smaller ice lenses, less deformation, and a more stable thermal envelope with fewer freezing cycles. Testing under confined, drained conditions with a surcharge load should accelerate the consolidation of the soil, resulting in a stronger soil and minimising froze heaving that could damage structures;

4. The influence of a structure on ice lens formation with increasing FT cycles should be investigated. The sample setup would need to be scaled to determine the area of influence of changes in soil structure.

8.8. Summary of conclusions

Freezing a clay results in a significant reduction of shear strength. Strength recovery seen between 1 and 3 FT cycles suggests significant damage to the soil microstructure occurs after 1 freezing cycle, but some immediate realignment of the soil particles causes a higher mobilised strength at 3 cycles. As the number of freezing cycles increases, the ice distribution through the soil becomes more uniform, and a distinct horizontal ice lens is not evident. The more uniform ice distribution through the sample after 1 cycle could account for the strength recovery, as a slurry layer will not form without a continuous horizontal ice lens. The behaviour of the soil after 3 FT cycles exhibited a reduction in shear strength approaching an equilibrium value. After 7 FT cycles, the ice lens development and shear strength stabilized. The presence of larger ice lenses at slower freezing rates resulted in weaker soil, attributed to the formation of a saturated slurry layer along the plane of the largest continuous horizontal ice lens after thawing. Soil stiffness decreased with increasing ice lens thickness. When no continuous horizontal ice lens was visible, the soil stiffness and mobilised shear strength stabilised. The shear strength development within the first 3 FT cycles should be further investigated under drained and undrained conditions, as different boundary conditions will yield different results.

Bibliography

[1] Chamberlain E.J. CRREL Monograph 81-2 Frost susceptibility of soils: USACE; 1981.
[2] Alley R.B. The Physical Science Basis: Changes in the Active Layer. In: Solomon S, et al., editors. Contribution of Working Group I to the Fourth Assessment Report of the Intergovernmental Panel on Climate Change. Cambridge, United Kingdom: IPCC; 2007.
[3] Andersland O.B., Ladanyi B. Introduction to Frozen Ground Engineering: Chapman & Hall; 1994.
[4] Chen W., Zhang Y., et al. Changes in soil temperature and active layer thickness during the twentieth century in a region in western Canada. Journal of Geophysical Research. 2003;108.
[5] Arenson L.U., Azmatch T.F., Sego D.C. A New Hypothesis on Ice Lens Formation in Frost-Susceptible Soils. In: Kane DL, Hinkel KM, editors. Ninth International Conference on Permafrost. Fairbanks, Alaska: Institute of Northern Engineering; 2008. p. 59-64.
[6] Talamucci F. Freezing processes in porous media: Formation of ice lenses, swelling of the soil. Mathematical and Computer Modelling. 2003;37:595-602.
[7] Ching J., Phoon K. Mobilized shear strength of spatial variable soils under simple stress. Structural Safety. 2013;41:20-8.
[8] Vardanega P.J., Bolton M.D. Strength mobilization in clays and silts. Canada Geotechnical Journal. 2011;48:1485-503.
[9] Bosch T.J.H.v.d. Influences of ice lens formation in silty soils. Delft, the Netherlands: Delft University of Technology; 2015.
[10] Wang D.-y., Ma W., et al. Effects of cyclic freezing and thawing on mechanical properties of Qinghai-Tibet clay. Cold Regions Science and Technology. 2007;48:34-43.
[11] Czurda K.A. Freezing Effects on Soils: Comprehensive Summary of the ISGF 82. Cold Regions Science and Technology. 1983;8:93-107.
[12] Liu J.-k., Peng L.-y. Experimental study on the unconfined compression of a thawing soil. Cold Regions Science and Technology. 2009;58:92-6.
[13] Kawaguchi T., Nakamura D., et al. Effects of Freeze-Thaw History on Deformation-Strength Properties and Permeability of Fine-Grained Soil. 18th International Conference on Soil Mechanics and Geotechnical Engineering. Paris2013. p. 357-60.
[14] Lai Y., Pei W., et al. Study on theory model of hydro-thermal-mechanical interaction process in saturated freezing silty soil. International Journal of Heat and Mass Transfer. 2014;78:805-19.
[15] Qi J., Vermeer P.A., CHeng G. A Review of the Influence of Freeze-thaw Cycles on Soil Geotechnical Properties. Permafrost and Periglacial Processes. 2006;17:245-52.
[16] Simonsen E., Isacsson U. Soil behavior during freezing and thawing using variable and constant confining pressure triaxial tests. Canadian Geotechnical Journal 2001;38:863-75.
[17] Georgiannou V.N., Burland J.B., Hight D.W. The undrained behaviour of clayey sands in triaxial compression and extension. Geotechnique. 1990;40:431-49.
[18] Wang T., Liu Y., et al. An experimental study on the mechanical properties of silty soils under repeated freeze–thaw cycles. Cold Regions Science and Technology. 2001;112:51-65.
[19] Qi J., Ma W., Song C. Influence of freeze-thaw on engineering properties of a silty soil. Cold Regions Science and Technology. 2008;53:397-404.
[20] Konrad J.M. A new concept of frost-heave characteristics of soils, by Otto J. Svec. Cold Regions Science and Technology. 1990;18:219-22.
[21] Chamberlain E.J., Gow A.J. Effect of Freezing and Thawing on the Permeability and Structure of Soils. Engineering Geology. 1979;13:73-92.
[22] Akagawa S., Nishisato K. Tensile strength of frozen soil in the temperature range of the frozen fringe. Cold Regions Science and Technology. 2009;57:13-22.
[23] Climate Adaption: Netherlands.

[24] Volokhov S.S. Effect of Freezing Conditions on the Shear Strength of Soils Frozen Together with Materials. Soil Mechanics and Foundation Engineering. 2003;40.
[25] Rempel A.W. Formation of ice lenses and frost have. Journal of Geophysical Research. 2007;112.
[26] Thomas H.R., Cleall P., et al. Modelling of cryogenic processes in permafrost and seasonally frozen soils. Geotechnique. 2009;59:173-84.
[27] Harris S.A., Heginbottom J.A., et al. Glossary of permafrost and related ground-ice termps. In: Research PsACoG, editor.1988.
[28] NSIDC. How Does Frozen Ground Form? In: Center NSID, editor. Physical Science and Frozen Ground. Boulder, Colorado, USA2016.
[29] Putkonen J. Soil thermal properties and heat transfer processes near Ny-Ålesund, northwestern Spitsbergen, Svalbard. Polar Research. 1998;17:165-79.
[30] Riseborough D.W. An Analytical Model of the Ground Surface Temperature Under Snowcover with Soil Freezing. 58th Eastern Snow Conference. Ottawa, Ontario, Canada2001.
[31] Wu Q., Hou Y., et al. Changes in active-layer thickness and near-surface permafrost between 2002 and 2012 in alpine ecosystems, Qinghai–Xizang (Tibet) Plateau, China. Global and Planetary Change. 2015;124:149-55.
[32] Ghazavi M., Roustaei M. Freeze-thaw performance of clayey soil reinforced with geotextile layer. Cold Regions Science and Technology. 2013;80:22-9.
[33] Briaud J.-L. Geotechnical Engineering: Unsaturated and Saturated Soils: Wiley; 2013.
[34] ASTM. Standard Test Methods for Liquid Limit, Plastic Limit, and Plasticity Index of Soils. ASTM Int'l; 2010.
[35] ASTM. Standard Test Methods for Laboratory Determination of Density (Unit Weight) of Soil Specimens. ASTM Int'l; 2009.
[36] ASTM. Standard Test Methods for Unconsolidated-Undrained Traixial Compression Test on Cohesive Soils. ASTM Int'l; 2015.
[37] Konrad J.M. Physical processes during freeze-thaw cycles in clayey silts. Cold Regions Science and Technology. 1998;16:291-308.
[38] GHSPA. Thermal pile design, installation and material standards. In: Center NE, editor. Davy Avenue, Knowlhill, Milton Keynes: National Energy Center; 2012.

Appendix 1: Macro-CT scans

A2.1. Macro-CT scans with different number of FT cycles at T_{bf} = -20°C

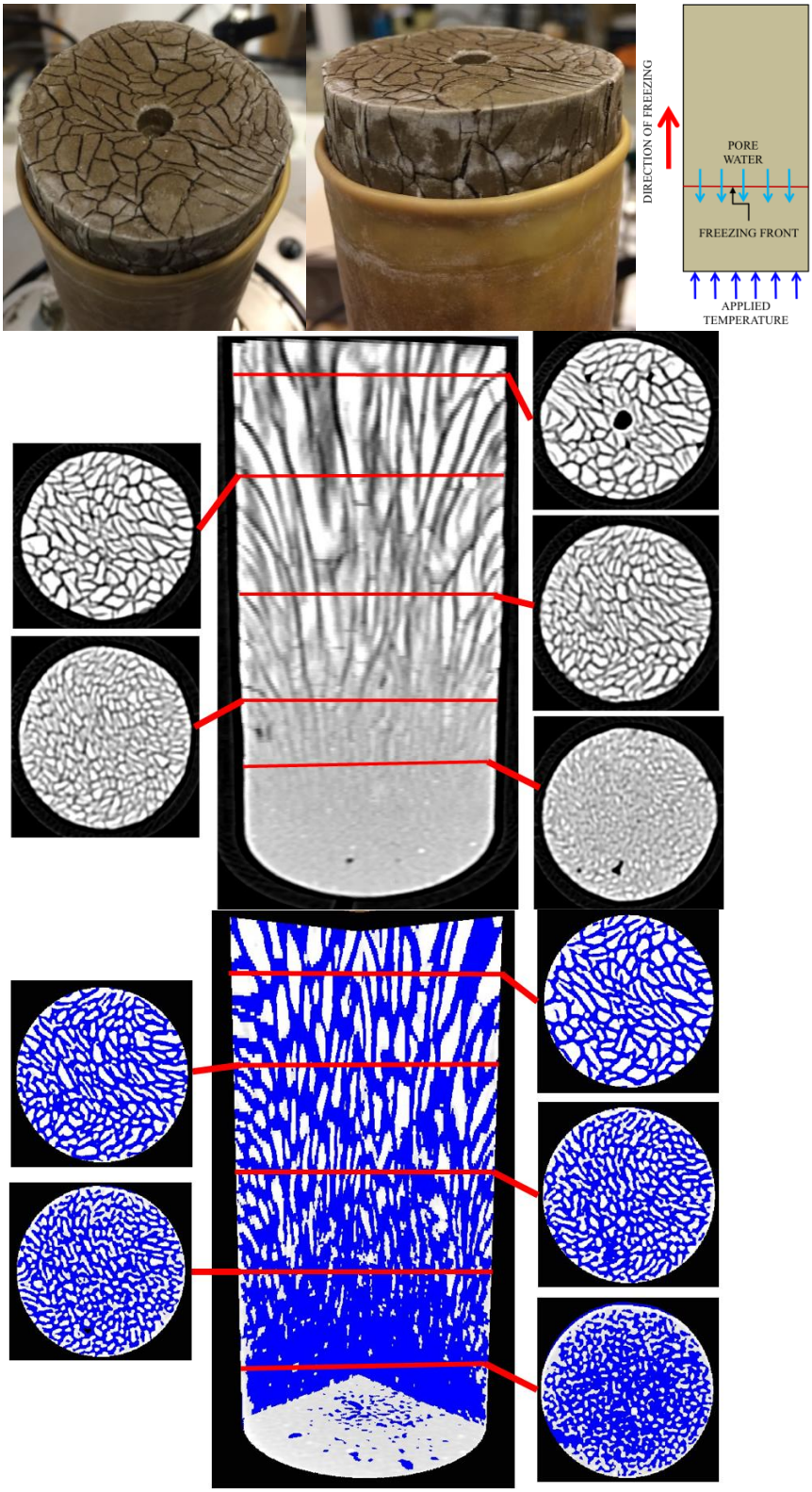

Figure 29: CT scan T_{bf} = -20°C after 1 FT cycle (sample T7-2). TOP: Cracking of frozen sample before loading into triaxial cell; MIDDLE: CT scan of frozen sample. Pale grey is ice, white is soil, and black is voids; BOTTOM: Contrast CT showing ice distribution. White is solids, blue is ice, black is voids

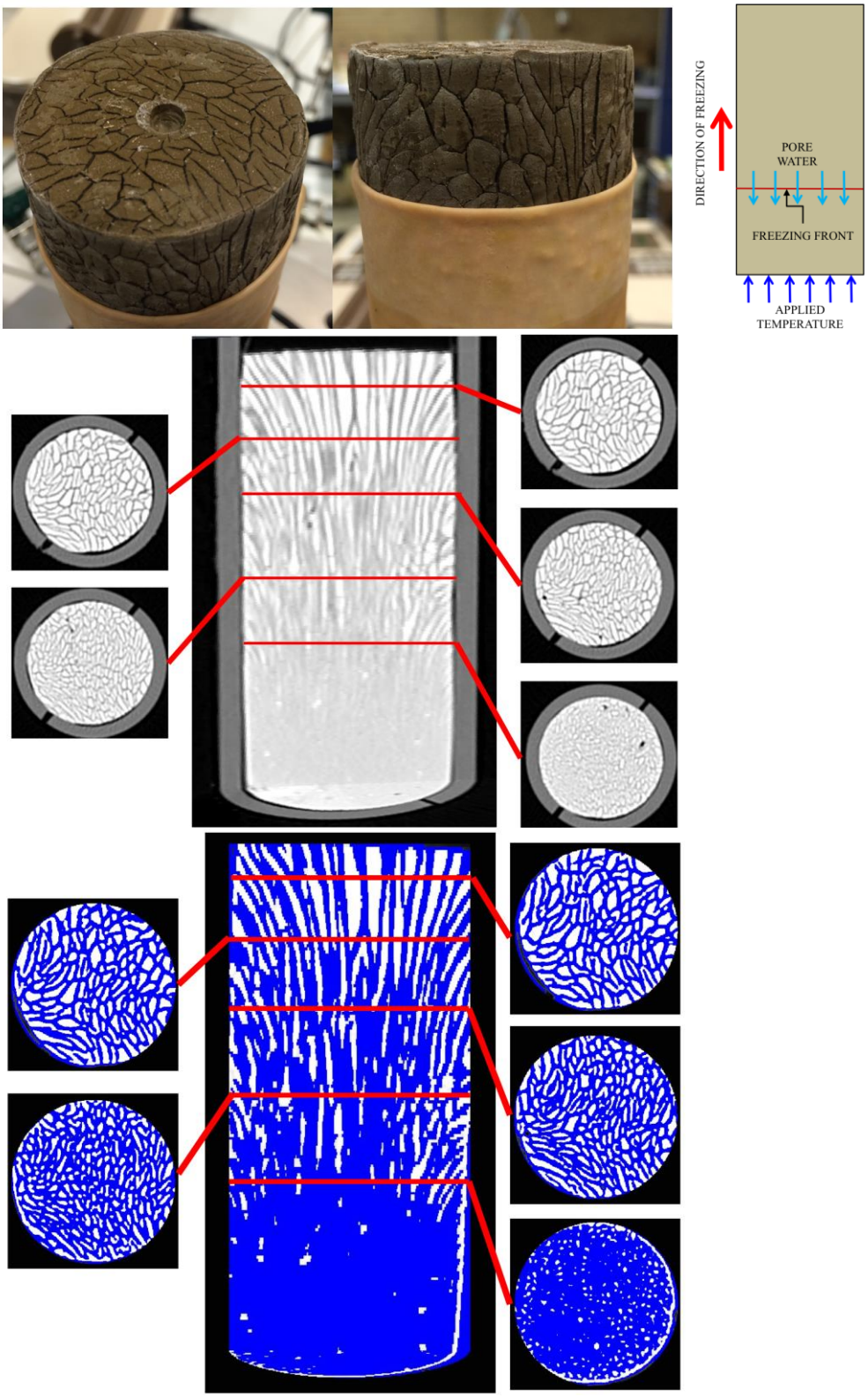

Figure 30: CT scan T_{bf} = -20°C after 1 FT cycle (sample T11-2). TOP: Cracking of frozen sample before loading into triaxial cell; MIDDLE: Freezing temperature applied at bottom of the sample. Pale grey is ice, white is soil, and black is voids; BOTTOM: Contrast CT showing ice location. White is solids, blue is ice, black is voids.

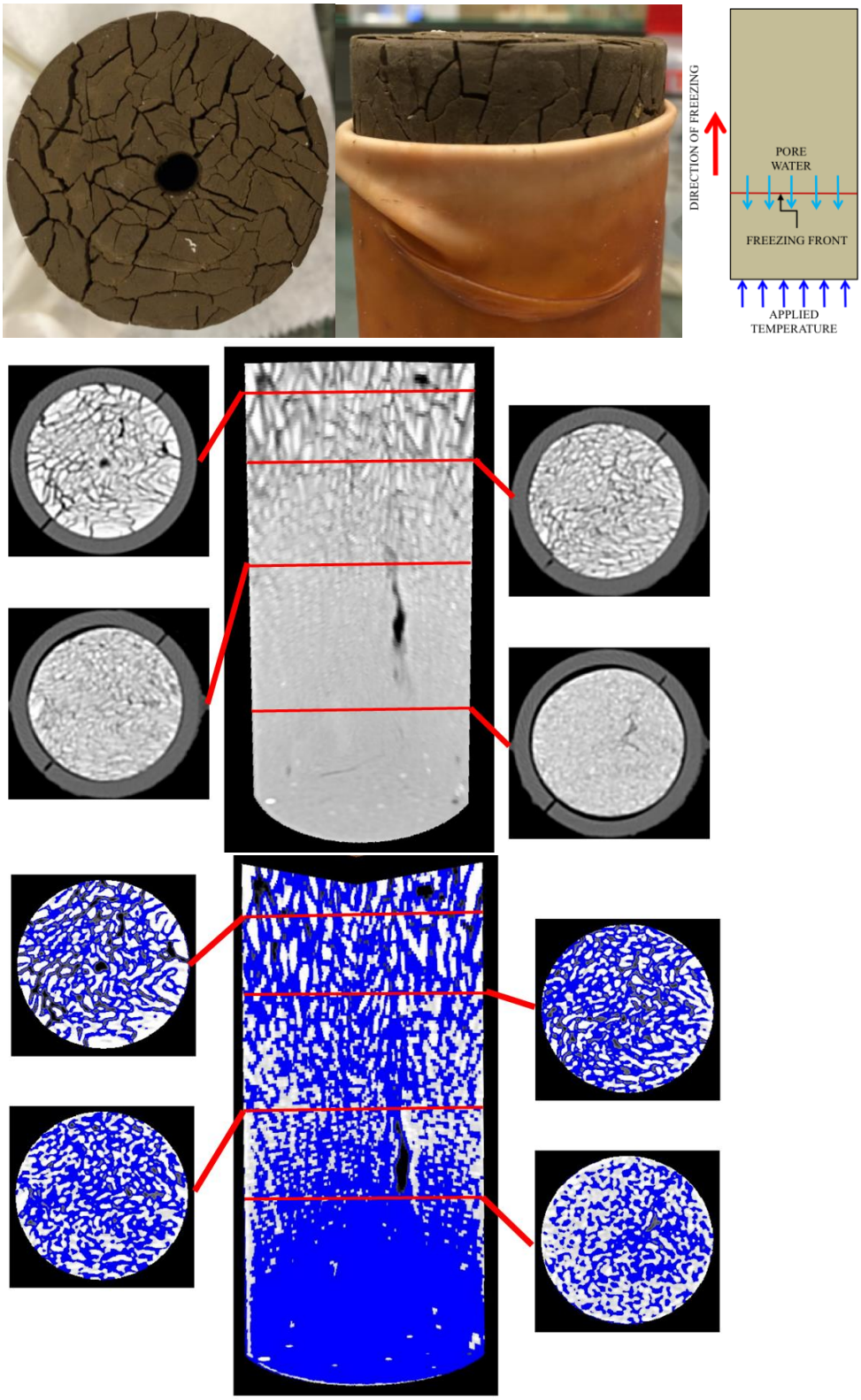

Figure 31: CT scan T_{bf} = -20°C after 3 FT cycles (sample T10-2). TOP: Cracking of frozen sample before loading into triaxial cell; MIDDLE: Freezing temperature applied at bottom of the sample. Pale grey is ice, white is soil, and black is voids; BOTTOM: Contrast CT showing ice location. White is solids, blue is ice, black is voids.

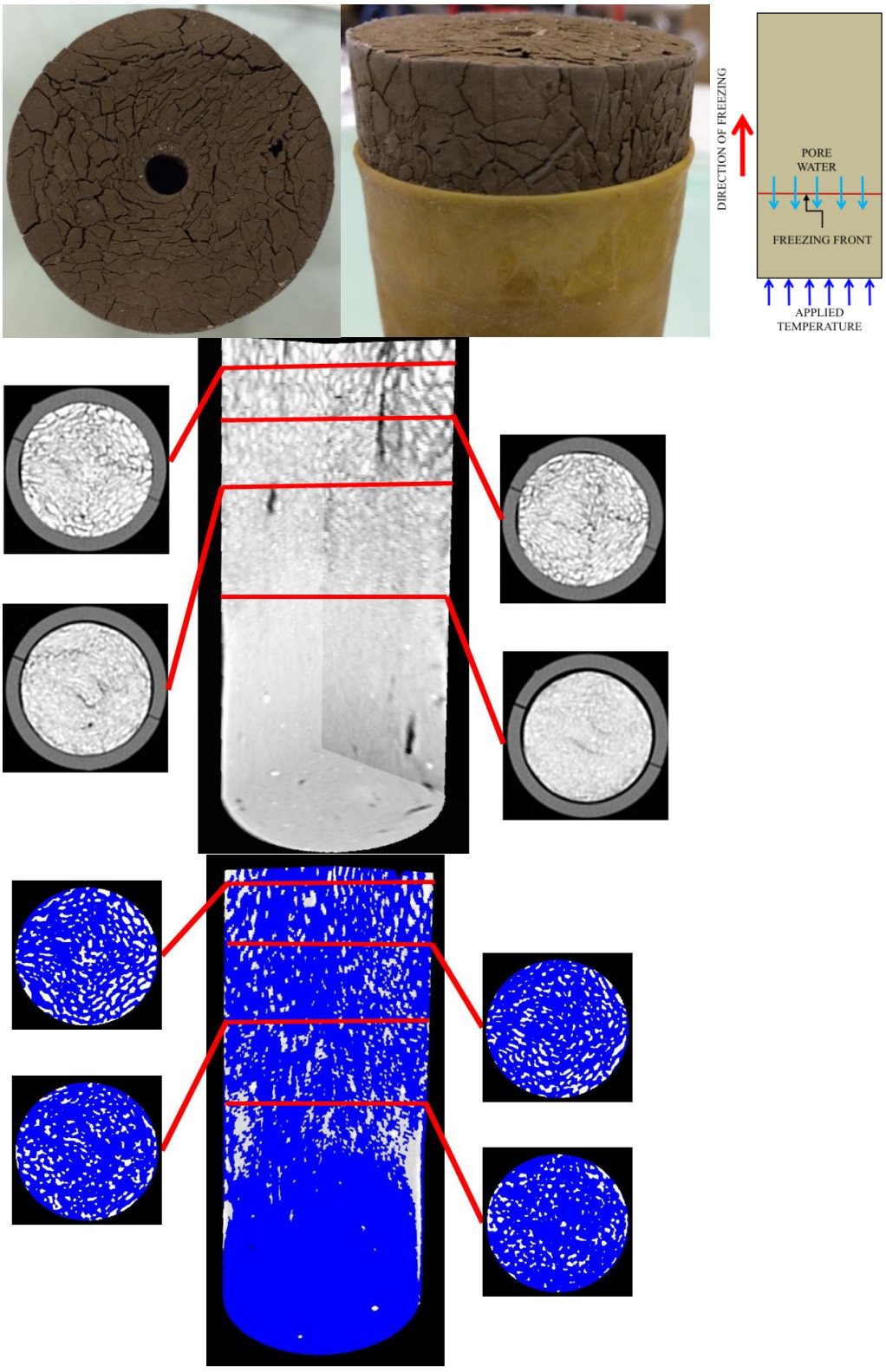

Figure 32: CT scan T_{bf} = -20°C after 7 FT cycles (sample T8-1). TOP: Cracking of frozen sample before loading into triaxial cell; MIDDLE: Freezing temperature applied at bottom of the sample. Pale grey is ice, white is soil, and black is voids; BOTTOM: Contrast CT showing ice location. White is solids, blue is ice, black is voids.

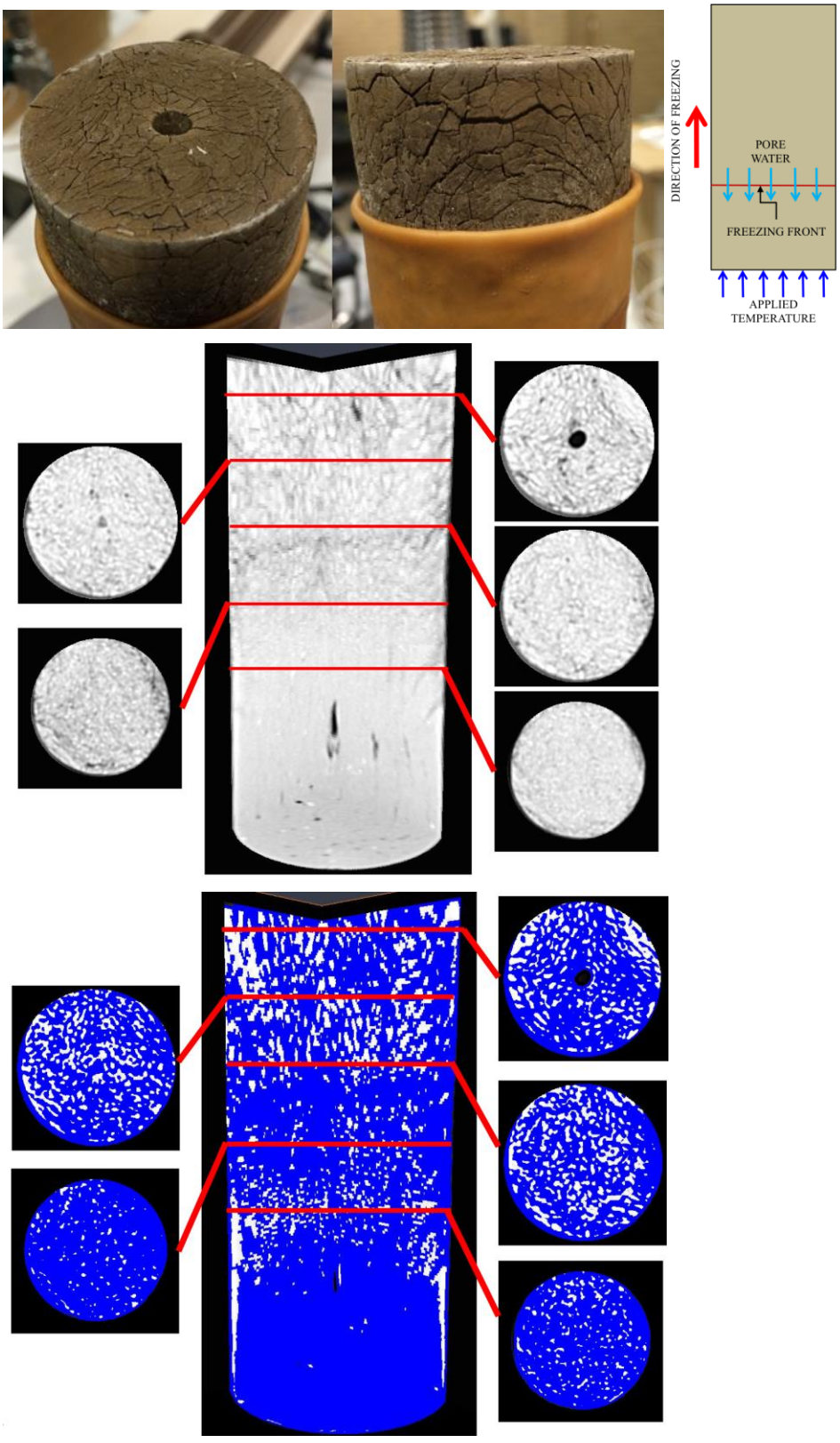

Figure 33: CT scan T_{bf} = -20°C after 10 FT cycles (sample T9-1). TOP: Cracking of frozen sample before loading into triaxial cell; MIDDLE: Freezing temperature applied at bottom of the sample. Pale grey is ice, white is soil, and black is voids; BOTTOM: Contrast CT showing ice location. White is solids, blue is ice, black is voids

A2.2. Macro-CT scans after 1 FT cycle with different freezing rates

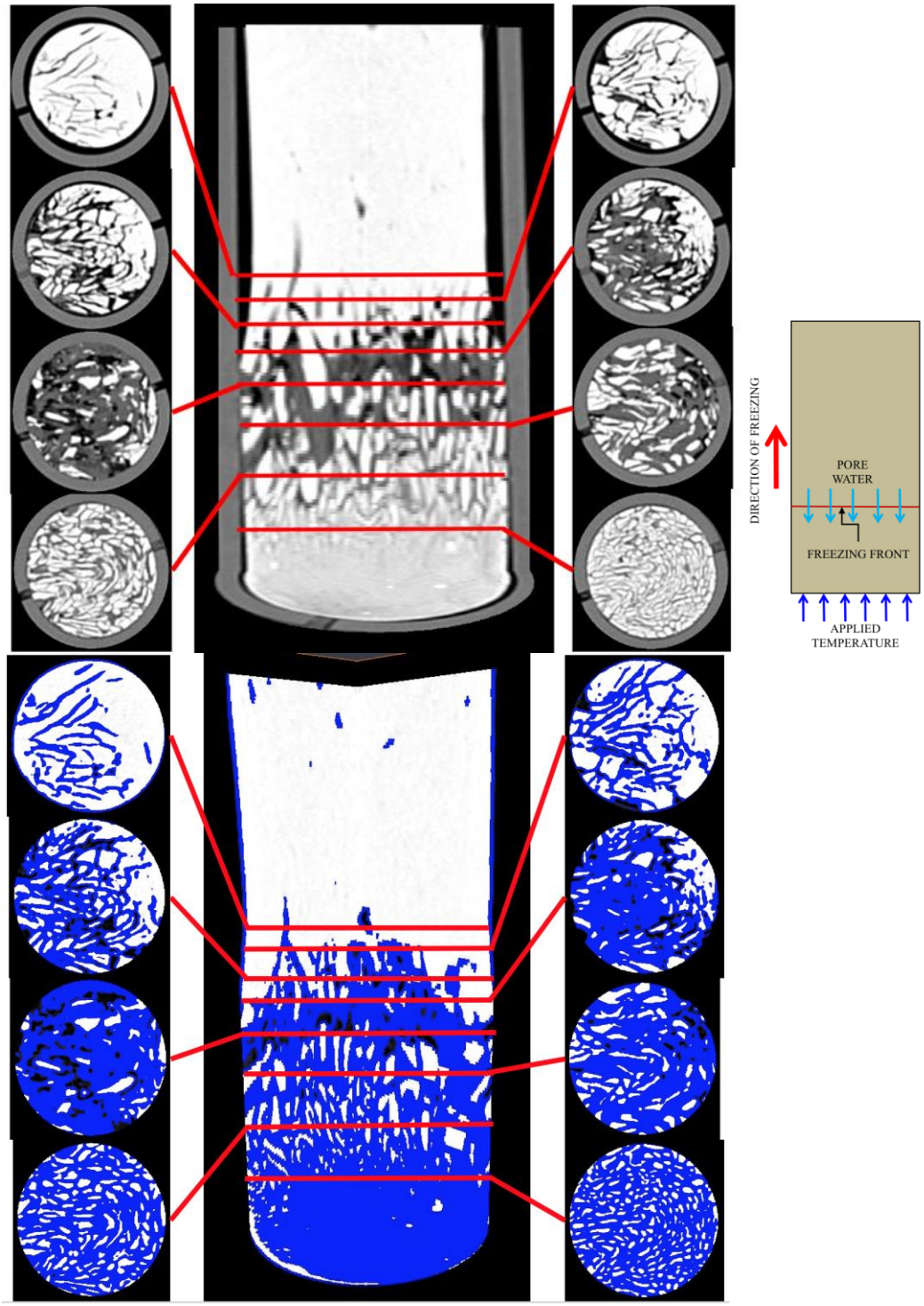

Figure 34: CT scan T_{bf} = -5°C (sample T10-1). TOP: Freezing temperature applied at bottom of the sample. Pale grey is ice, white is soil, and black is voids. BOTTOM: Contrast CT showing ice location. White is solids, blue is ice, black is voids. The top 50 mm is frozen but has minimal ice lensing

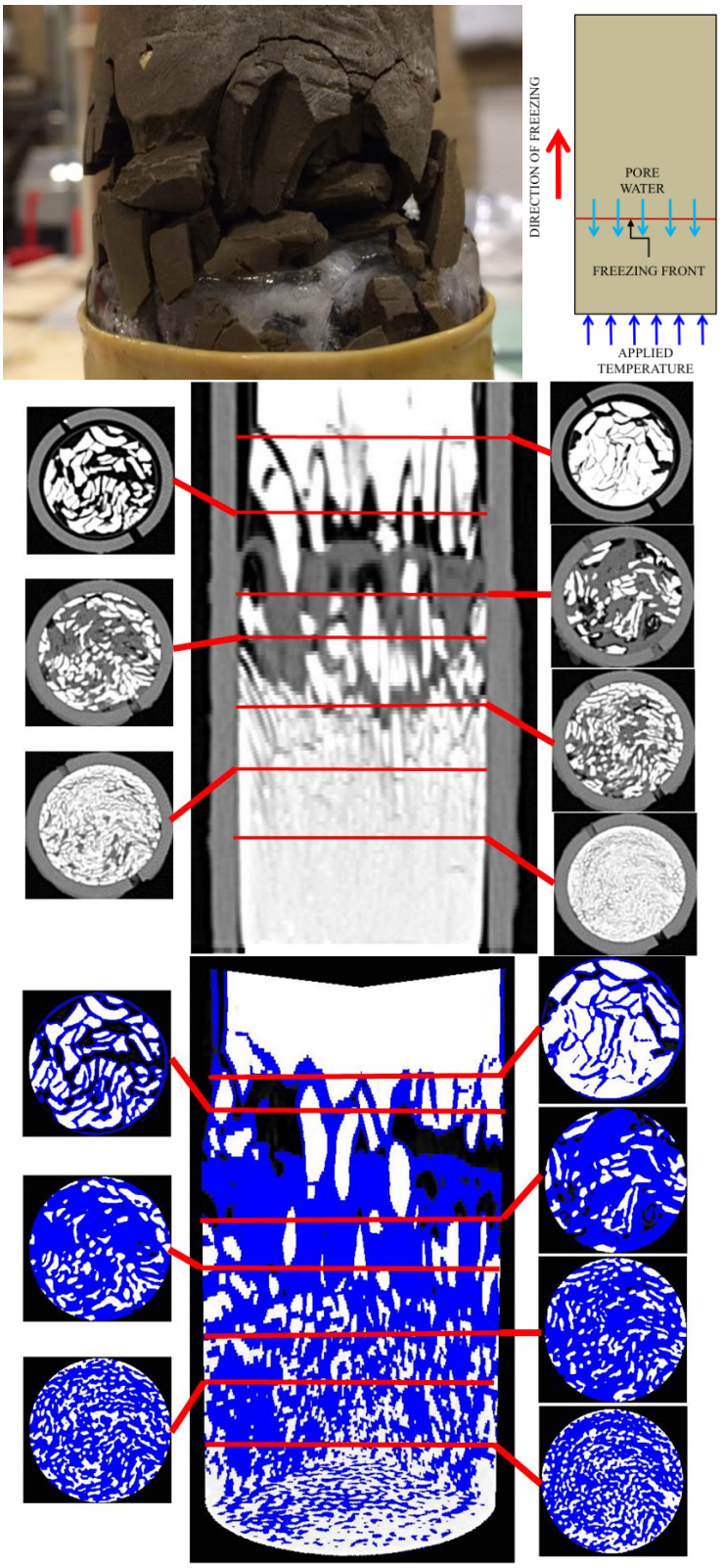

Figure 35: CT scan T_{bf} = -5°C (sample T7-1). TOP: Cracking on frozen sample before loading into triaxial cell; MIDDLE: Freezing temperature applied at bottom of the sample. Pale grey is ice, white is soil, and black is voids. BOTTOM: Contrast CT showing ice location. White is solids, blue is ice, black is voids. The top 25 mm is frozen but exhibits minimal lensing

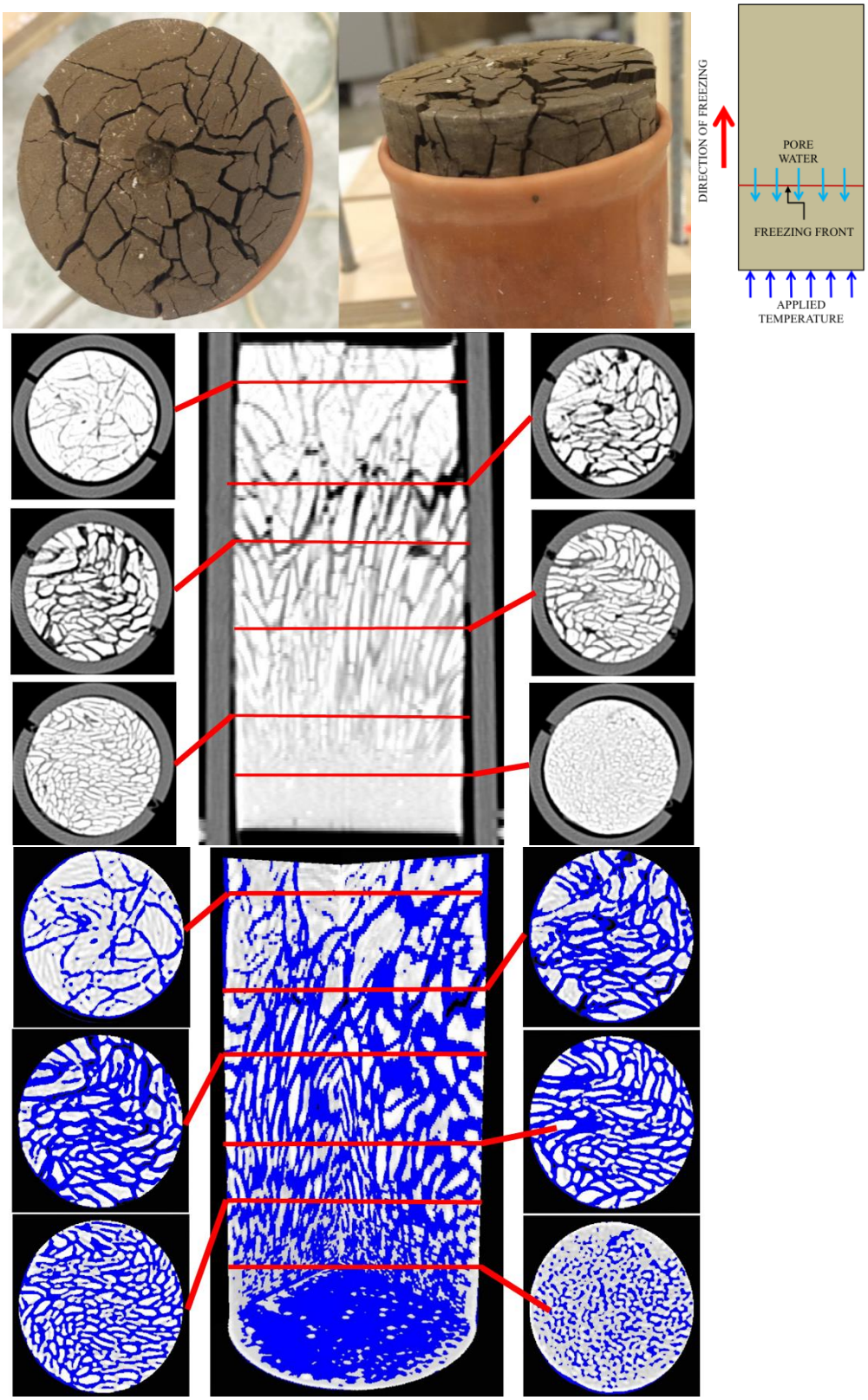

Figure 36: CT scan T_{bf} = -10°C (sample T9-2). TOP: Cracking on frozen sample before loading into triaxial cell; MIDDLE: CT scan of frozen sample. Pale grey is ice, white is soil, and black is voids; BOTTOM: Contrast CT showing ice distribution. White is solids, blue is ice, black is voids

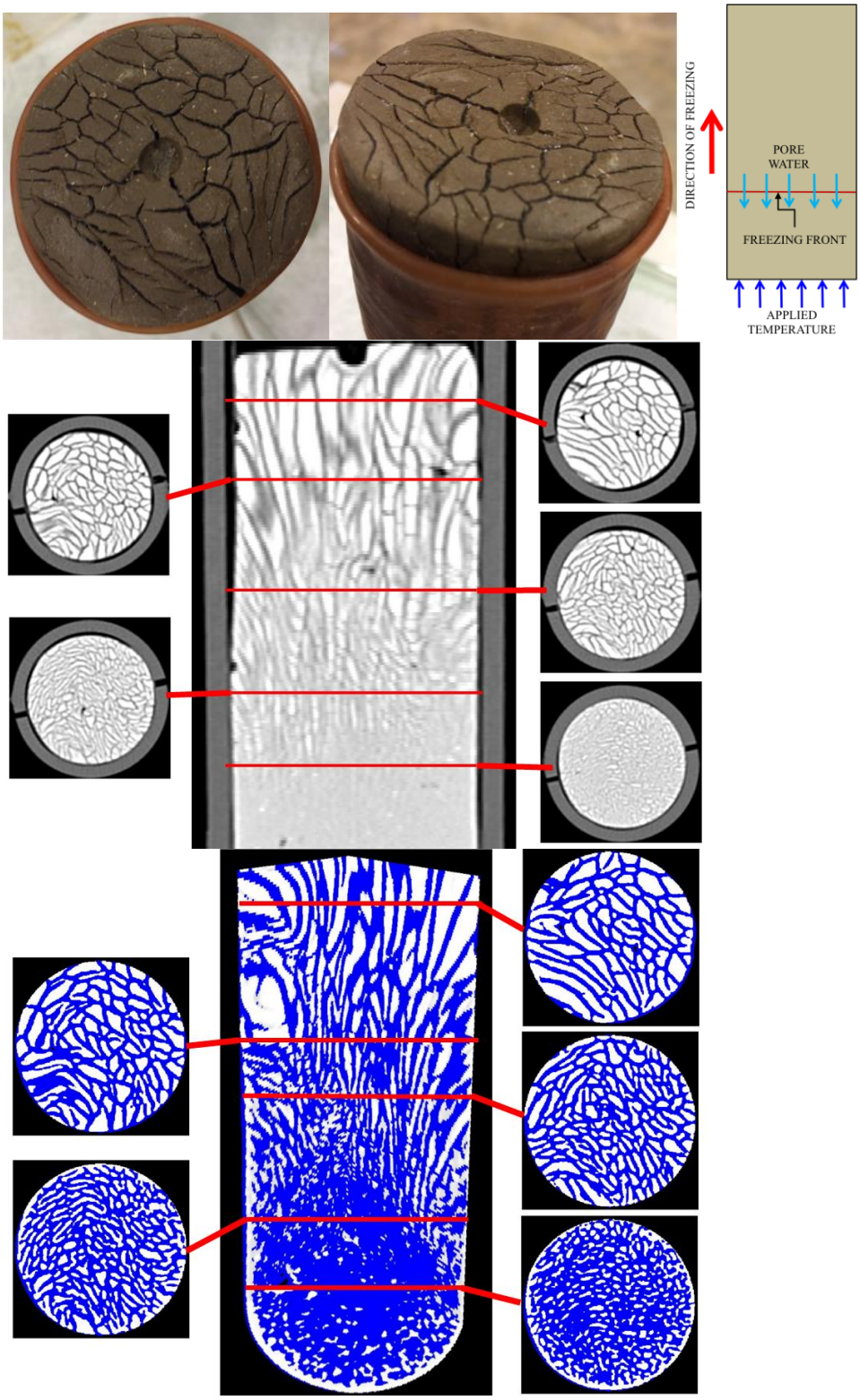

Figure 37: CT scan T_{bf} = -15°C (sample T9-3). TOP: Cracking of frozen sample before loading into triaxial cell; MIDDLE: Freezing temperature applied at bottom of the sample. Pale grey is ice, white is soil, and black is voids; BOTTOM: Contrast CT showing ice location. White is solids, blue is ice, black is voids.

Appendix 2: Lab results

A2.1. Summary of samples

Table 8: Summary of samples and comments on handling/testing

Sample #	T_{bf} [˚C]	# cycles	γ_{dry} [kN/m^3]	w [%]	CT	Comments
T1-2	-20	20	18.46	16.3		Let sample sit on Peltier element after turning unit off to make easier to remove from copper plug. The bottom thawed a bit and there was some material & moisture loss when transferring to the triaxial machine
T3-1	-20	5	22.36	17.2		
T3-2	-15	3	22.36	17.2		Freezing unit (#3) broke on 12/04d. Sample was placed in plastic bag and moved to freezer at -20C at 13:45. Removed and tested at 16:00 on 15/04/16
T3-9	-15	1	22.36	17.2	X	
T4-2	-20	10	21.70	19.5		
T5-1	-20	7	21.76	18.9		
T5-2	-10	1	21.76	18.9	X	Top ~ 20 mm not completely frozen.
T6-1	-20	3	23.82	18.2		
T6-2	-20	7	23.82	18.2		
T6-3	-20	5	23.82	18.2		
T7-1	-5	1	21.67	19.0	X	While attempting to remove the top temperature probe, the sample separated at the plane between the frozen and unfrozen soil (where ice lens was visible). The structure of the sample was altered and the triaxial results should be disregarded. Top ~50 mm not frozen (from CT)
T8-1	-20	7	21.65	20.3	X	Peltier element/heat sink broke on 30/03/16. The sample was removed from unit #5 on 04/04/16 and wrapped in plastic in an attempt to keep water in the system. Sample was refrozen on 11/04 and placed in the freezer at 15:30 on 12/04. The sample was removed and tested at 19:15 on 14/04/15.
T8-2	-20	15	21.65	20.3		There was a small amount of thawing at the base of the sample while loading into the triaxial test loading rate was entered as 0.01 mm/min (should have been 0.1 mm/min).
T9-2	-10	1	21.95	18.3		16/04/16: adjusted sample on copper plug to improve contact and get better cooling. Removed sample from box and completely took apart and reassembled. Process took ~5 min. Temperature control in the lab broke and appeared to be heating the top of the sample. Sample was placed into the freezer at 08:50 on 20/04/16 and removed on 22/04/16.
T9-3	-15	1	21.95	18.3	X	

T10-1	-5	1	23.46	16.0	X	Some material left on copper plug when sample placed in triaxial machine. This was pretty minimal, and shouldn't influence the results much. Top 50 mm of sample not frozen (from CT scan). DISREGARD triaxial results since much of sample was unfrozen, so it's stronger than it would be otherwise
T10-2	-20	3	23.46	16.0	X	Placed in freezer at 09:00 on 18/04/16. Removed and placed in triaxial cell at 16:15 on 18/04/16
T12-2	-20	1	19.65	17.1		Peltier element broke ~1.5 hours after starting freezing cycle. Material not frozen, so left and moved from Unit 2 to Unit 1 and frozen the next day (thawed in box for 17 hours).

A2.2. Unit weights

	A	B	C	D	E	F	G	H	I	J	K	L	M	N	O	P
1	Prep date	18/02/16		23/02/2016		01/03/16			05/04/2016				08/03/2016			
2	Sample #	T1-aa	T1-bb	T2-aa	T-bb	T3-aa	T3-bb	T3-cc	T4-aa	T4-bb	T4-cc	T4-dd	T5-aa	T5-bb	T5-cc	T5-dd
3	tare	49.48	46.67	46.65	49.48	46.68	46.68	44.55	42.59	41.3	43.68	44.55	43.71	49.48	49.51	44.54
4	m_{wet} [g]	99.14	113.66	101.79	97.35	100.22	90.11	131.02	127.12	115.95	134.75	100.93	113.74	117.49	129.63	133.34
5	m_{dry} [g]	86.31	96.53	87.59	85.02	86.42	78.36	108.67	105.44	96.77	111.34	86.42	95.7	100.02	109.01	110.76
6	w	14.87%	17.75%	16.21%	14.50%	15.97%	14.99%	20.57%	20.56%	19.82%	21.03%	16.79%	18.85%	17.47%	18.92%	20.39%
7	h_1	12.10	17.10	13.80	12.00	13.2	10.4	22.6	21.9	19.1	23.1	13.8	17.3	16.5	20	22.1
8	h_2	12.00	17.00	13.90	11.90	13.5	10.9	22.2	21	18.9	23	13.9	17	16.9	20	22.6
9	h_3	13.00	17.10	14.00	11.10	13.6	11	22.6	21.6	18.9	23	13.9	17.5	17	20.4	22.9
10	h [mm]	12.37	17.07	13.90	11.67	13.43	10.77	22.47	21.50	18.97	23.03	13.87	17.27	16.80	20.13	22.53
11	d_1	48.10	48.20	47.90	47.80	48.1	48.2	47.2	48	48	47.3	47.3	47.8	47.9	47.9	47.9
12	d_2	47.90	48.00	47.80	48.00	48.1	48	47.9	48	48	47.9	47.9	48	48	48	47.9
13	d_3	48.90	48.10	47.90	48.00	48	40	48.1	47.9	47.7	47.8	47.9	47.9	47.9	48	48.2
14	d [mm]	48.30	48.10	47.87	47.93	48.07	45.40	47.73	47.97	47.90	47.67	47.70	47.90	47.93	47.97	48.00
15	V [cm^3]	22.66	31.01	25.01	21.05	24.38	17.43	40.20	38.85	34.18	41.10	24.78	31.11	30.32	36.38	40.78
16	ρ [g/cm3]	2.19	2.16	2.20	2.27	2.20	2.49	2.15	2.18	2.18	2.22	2.28	2.25	2.24	2.20	2.18
17	ρ_d	1.91	1.83	1.90	1.99	1.89	2.17	1.78	1.80	1.82	1.83	1.95	1.89	1.91	1.85	1.81
18	γ [kN/m3]	21.49	21.18	21.62	22.30	21.54	24.44	21.09	21.34	21.42	21.73	22.31	22.07	22.00	21.60	21.36
19	γ_d	18.83	18.10	18.72	19.59	18.69	21.38	17.60	17.81	17.99	18.06	19.22	18.68	18.84	18.27	17.85
20	γ_{avg}	21.34		21.96		22.36			21.70				21.76			
21	$\gamma_{avg,dry}$	18.46		19.15		19.22			18.27				18.41			
22	average w	16.3%		15.4%		17.2%			19.5%				18.9%			
23	average ρ_d	1.87		1.94		1.95			1.85				1.90			
24	Variation:															
25	γ	-3.10%		-0.29%		1.52%			-1.47%				-1.21%			
26	γ_{dry}	-1.60%		2.08%		2.44%			-2.64%				-1.88%			
27	ρ_d	-1.81%		1.87%		2.23%			-2.84%				-0.21%			
28	w	-10.04%		-15.28%		-5.24%			7.85%				4.30%			

	A	Q	R	S	T	U	V	W	X	Y	Z	AA	AB	AC	AD
1	**Prep date**	14/03/16				21/03/2016			23/03/2016			11/04/2016			
2	**Sample #**	**T6-aa**	**T6-bb**	**T6-cc**	**T6-dd**	**T7-aa**	**T7-bb**	**T7-cc**	**T8-aa**	**T8-bb**	**T8-cc**	**T9-aa**	**T9-bb**	**T9-cc**	**T9-bb**
3	**tare**	44.55	42.61	44.99	43.71	49.47	43.81	41.32	41.33	44.54	45.49	50.89	47.6	47.8	44.54
4	**m_{wet} [g]**	95.98	111.12	124.92	139.35	109.59	133.12	124.78	134.84	127.34	134.91	125.93	125.78	125.66	128.67
5	**m_{dry} [g]**	82.89	93.67	104.62	115.21	94.3	110.47	103.68	111.18	106.4	112.42	107.18	106.12	106.16	107.64
6	**w**	15.79%	18.63%	19.40%	20.95%	16.21%	20.50%	20.35%	21.28%	19.68%	20.01%	18.00%	18.53%	18.37%	19.54%
7	**h_1**	12	17.1	19.9	24	15	23.8	22.1	23.1	20.7	22.1	18	19	19	20.9
8	**h_2**	12	16.9	19.4	4.6	15	22.9	21.2	23.9	20.9	22	18.8	19	19	20.1
9	**h_3**	12.8	16.9	19.8	24.1	14.9	23	21	23.9	20.6	22		19.1	19	20.6
10	**h [mm]**	12.27	16.97	19.70	17.57	14.97	23.23	21.43	23.63	20.73	22.03	18.40	19.03	19.00	20.53
11	**d_1**	47.9	47.9	47.9	47.9	47.2	47	48.1	47.9	48.2	48	48.9	48.1	48.1	47.9
12	**d_2**	47.1	48	48	47.9	47.1	47.1	48	48	48.1	48.1	48.7	48	48	48
13	**d_3**	48	47.2	48.1	48	47.9	47.1	48.2	48	48	48.1	48.6	47.9	48.1	48
14	**d [mm]**	47.67	47.70	48.00	47.93	47.40	47.07	48.10	47.97	48.10	48.07	48.73	48.00	48.07	47.97
15	**V [cm^3]**	21.89	30.32	35.65	31.70	26.41	40.42	38.95	42.71	37.67	39.98	34.32	34.44	34.48	37.10
16	**ρ [g/cm3]**	2.35	2.26	2.24	3.02	2.28	2.21	2.14	2.19	2.20	2.24	2.19	2.27	2.26	2.27
17	**ρ_d**	2.03	1.90	1.88	2.49	1.96	1.83	1.78	1.81	1.84	1.86	1.85	1.92	1.91	1.90
18	**γ [kN/m3]**	23.04	22.16	21.99	29.59	22.32	21.67	21.01	21.47	21.55	21.93	21.44	22.26	22.15	22.24
19	**γ_d**	20.02	18.79	18.53	24.61	19.33	18.09	17.57	17.81	18.12	18.39	18.28	18.90	18.82	18.71
20	**γ_{avg}**	23.82				21.67			21.65			21.95			
21	**$\gamma_{avg,dry}$**	20.26				18.33			18.11			18.67			
22	**average w**	18.2%				19.0%			20.3%			18.3%			
23	**average ρ_d**	2.05				1.86			1.84			1.89			
24	**Variation:**														
25	**γ**	8.16%				-1.61%			-1.68%			-0.33%			
26	**γ_{dry}**	7.95%				-2.32%			-3.50%			-0.52%			
27	**ρ_d**	7.72%				-2.53%			-3.71%			-0.72%			
28	**w**	0.40%				4.95%			12.12%			0.95%			

	A	AE	AF	AG	AH	AI	AJ	AK	AL
1	**Prep date**	14/04/2016			17/05/2016		20/05/2016		
2	**Sample #**	**T10-aa**	**T10-bb**	**T10-cc**	**T11-aa**	**T11-bb**	**T12-aa**	**T12-bb**	**T12-cc**
3	**tare**	47.58	50.89	47.61	46.08	49.47	46.46	41.33	49.47
4	**m_{wet} [g]**	142.29	101.03	96.26	143.13	144.66	139.19	89.18	120.3
5	**m_{dry} [g]**	118.56	88.52	84.51	119.07	121.04	116.96	77.36	102.87
6	**w**	20.02%	14.13%	13.90%	20.21%	19.51%	19.01%	15.28%	16.94%
7	**h_1**	23.1	11.1	11.3	24.7	23.8	22.9	11	17
8	**h_2**	23.1	11.1	10.9	24.9	23.2	22.9	10.9	17
9	**h_3**	23.2	10.9	11.3	24.9	23.5	22.1	11	17
10	**h [mm]**	23.13	11.03	11.17	24.83	23.50	22.63	10.97	17.00
11	**d_1**	48	48.1	47.9	47.1	48	48.1	48.1	48
12	**d_2**	48	48	47.9	47.9	48	48.1	47.9	48
13	**d_3**	48.1	48.1	48	48.1	48.1	48.2	48	48
14	**d [mm]**	48.03	48.07	47.93	47.70	48.03	48.13	48.00	48.00
15	**V [cm^3]**	41.92	20.02	20.15	44.38	42.58	41.18	19.84	30.76
16	**ρ [g/cm3]**	2.26	2.50	2.41	2.19	2.24	2.25	2.41	2.30
17	**ρ_d**	1.88	2.19	2.12	1.82	1.87	1.89	2.09	1.97
18	**γ [kN/m3]**	22.16	24.56	23.68	21.45	21.92	22.08	23.65	22.58
19	**γ_d**	18.57	21.65	20.91	17.95	18.45	18.67	20.64	19.43
20	**γ_{avg}**	23.46			21.68		22.77		
21	**$\gamma_{avg,dry}$**	20.38			18.11		19.58		
22	**average w**	16.0%			20.3%		17.1%		
23	**average ρ_d**	2.07			1.84		1.98		
24	**Variation:**								
25	**γ**	5.81%			-2.22%		2.67%		
26	**γ_{dry}**	7.76%			4.26%		3.52%		
27	**ρ_d**	7.59%			-4.41%		3.36%		
28	**w**	11.24%			12.61%		5.37%		

A2.3. Triaxial Results

Never-frozen (base-line) samples:

Table 9: Triaxial test results for never-frozen samples with variation from the average value

Sample #	T1-0	T2-0	T3-0	T4-0	T5-0	T6-0	T7-0	T8-0	T9-0	T11-0	average
Batch	T1	T2	T3	T4	T5	T6	T7	T8	T9	T11	
T_{bf}	never frozen										
Max. mobilised str [kPa]	14.69	14.84	14.34	15.39	14.96	13.75	17.51	18.97	15.50	21.31	16.12
variation	8.9%	7.9%	11.1%	4.6%	7.2%	14.7%	8.6%	17.6%	3.9%	32.2%	17.6%
shear str @ axial strain = 2%	7.01	7.97	6.91	9.19	9.24	7.76	8.80	8.88	8.27	9.39	8.34
variation	16.0 %	4.5%	17.2%	10.2%	10.8%	7.0%	5.5%	6.5%	0.8%	12.6%	17.2%
shear str @ axial strain = 4%	9.50	10.40	9.09	11.90	11.67	9.67	11.82	12.36	10.37	12.84	10.96
variation	13.3 %	5.1%	17.1%	8.5%	6.5%	11.8%	7.8%	12.8%	5.4%	17.1%	17.1%
shear str @ axial strain = 6%	11.11	12.40	10.64	13.18	12.73	11.01	13.67	14.16	11.86	15.20	12.60
variation	11.8 %	1.6%	15.5%	4.6%	1.1%	12.6%	8.5%	12.4%	5.8%	20.7%	15.5%
shear str @ axial strain = 10%	13.06	13.60	12.36	14.83	14.38	12.71	15.80	16.49	13.45	18.18	14.49
variation	9.8%	6.1%	14.7%	2.4%	0.7%	12.3%	9.1%	13.8%	7.1%	25.5%	14.7%

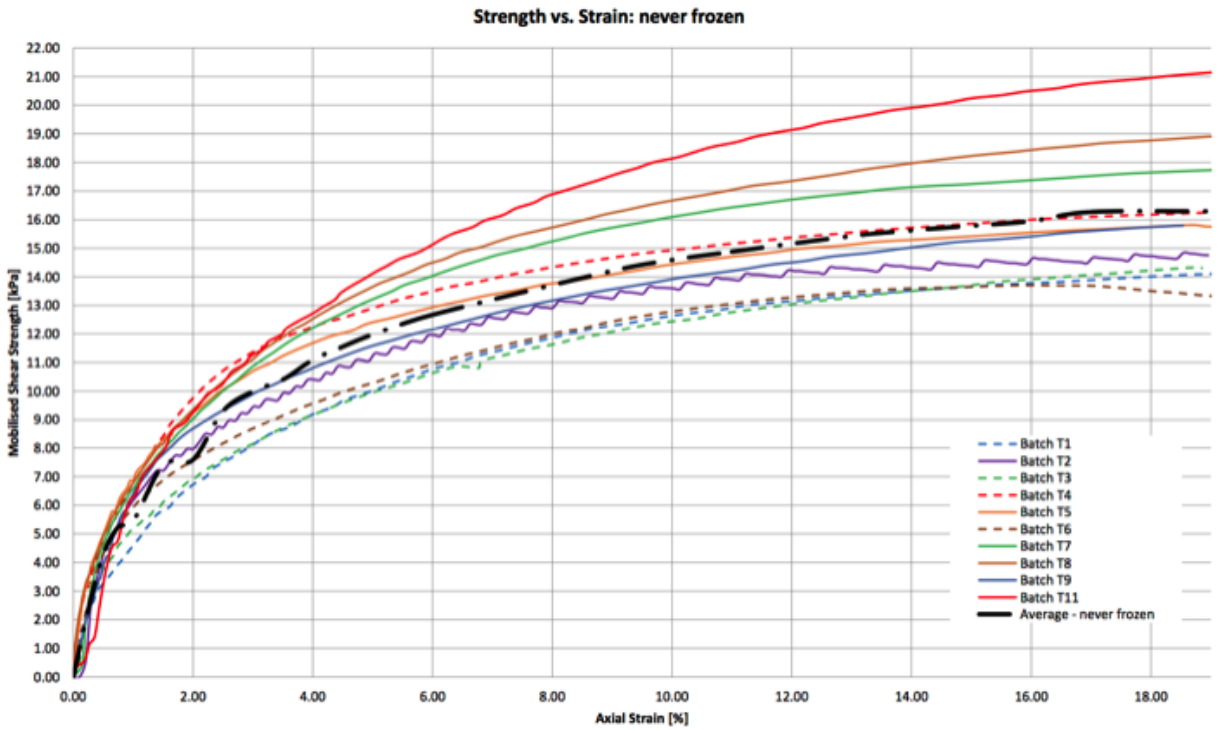

Figure 38: Shear strength vs. axial strain for never-frozen samples

Thawed samples:

Table 10: UU triaxial results: thawed samples

Sample #	T_{bf} [°C]	# FT cycles	Mobilised shear strength [kPa]			
			axial strain = 2%	axial strain = 4%	axial strain = 6%	axial strain = 10%
T7-2	-20	1^{CT}	4.73	5.40	5.81	5.91
T11-2	-20	1^{CT}	5.13	5.24	5.13	4.35
T12-2	-20	1	5.13	5.51	5.14	4.00
T6-1	-20	3	4.59	5.70	6.35	7.30
T10-2	-20	3	5.14	6.11	6.48	6.72
T3-1	-20	5	4.08	5.84	6.64	7.44
T6-3	-20	5	3.50	4.72	5.25	5.55
T5-1	-20	7	2.71	3.96	4.52	5.32
T6-2	-20	7	3.46	4.72	5.50	6.45
T4-3	-20	10	3.79	4.89	5.29	5.78
T1-2	-20	20	3.71	4.20	4.18	4.15
T9-3	-15	1^{CT}	3.26	3.87	4.64	5.64
T5-2	-10	1^{CT}	2.43	3.42	4.00	4.88
T9-2	-10	1^{CT}	3.25	4.50	5.04	5.59
T7-1	-5	1^{CT}	1.10	1.75	1.98	2.25